MODELING OF A GENERIC LASER GUIDED WEAPON WITH VELOCITY PURSUIT GUIDANCE AND ITS PERFORMANCE ANALYSIS USING VARIOUS CONTROL STRATEGIES

A THESIS SUBMITTED TO
THE GRADUATE SCHOOL OF NATURAL AND APPLIED SCIENCES
OF
MIDDLE EAST TECHNICAL UNIVERSITY

BY

DÜNYA RAUF LEVENT GÜNER

IN PARTIAL FULFILLMENT OF THE REQUIREMENTS
FOR
THE DEGREE OF MASTER OF SCIENCE
IN
MECHANICAL ENGINEERING

AUGUST 2004

Approval of the Graduate School of Natural and Applied Sciences

Prof. Dr. Canan Özgen
Director

I certify that this thesis satisfies all the requirements as a thesis for the degree of Master of Science

Prof. Dr. S. Kemal İder
Head of Department

This is to certify that we have read this thesis and that in our opinion it is fully adequate, in scope and quality, as a thesis for the degree of Master of Science.

Prof. Dr. M. Kemal Özgören
Co-Supervisor

Prof. Dr. Bülent E. Platin
Supervisor

Examining Committee Members

Prof. Dr. Y. Samim Ünlüsoy (METU-ME)

Prof. Dr. Bülent E. Platin (METU-ME)

Prof. Dr. M. Kemal Özgören (METU-ME)

Prof. Dr. Mehmet Çalışkan (METU-ME)

Prof. Dr. Yavuz Yaman (METU-AEE)

I hereby declare that all information in this document has been obtained and presented in accordance with academic rules and ethical conduct. I also declare that, as required by these rules and conduct, I have fully cited and referenced all material and results that are not original to this work.

Dünya Rauf Levent Güner

ABSTRACT

MODELING OF A GENERIC LASER GUIDED WEAPON WITH VELOCITY PURSUIT GUIDANCE AND ITS PERFORMANCE ANALYSIS USING VARIOUS CONTROL STRATEGIES

Güner, Dünya Rauf Levent

M.S., Department of Mechanical Engineering

Supervisor: Prof. Dr. Bülent E. Platin

Co-supervisor: Prof. Dr. M. Kemal Özgören

August 2004, 175 Pages

In this thesis, a base for the modeling and analysis of laser guided weapons is constituted. In particular, the effects of several control schemes on the performance of a generic laser guided weapon system are investigated. In this generic model, it is assumed that the velocity pursuit guidance is employed via a velocity aligning seeker as the sole sensor.

The laser seeker is modeled experimentally, based on data obtained by conducting a series of tests. The laser reflection is also modeled. Aerodynamic coefficients of the generic geometry are generated by the software Missile Datcom. A nonlinear, six degree of freedom simulation is constructed incorporating 10 Hz laser sensing, velocity pursuit guidance, seeker model, and multiple control schemes.

The effects of bang-bang, bang-trail-bang, multiposition and continuous control techniques on weapon performance are investigated for stationary and moving targets under ideal and noisy conditions. Flight characteristics like miss distance,

range envelope, impact speed, and time of flight are monitored. Weapon's maneuverability is investigated and the effect of employing a theoretical down sensor on the performance is demonstrated.

In the light of simulation results, comparisons between various schemes are carried out, improvements on them and their flight envelopes are emphasized. It is concluded that the multiposition scheme provides a significant performance increase in most delivery types and can be an alternative to the continuous scheme. It is shown that the continuous scheme can achieve longer ranges only if backed up by a down sensor.

Keywords: Bang-bang, laser seeker, multiposition control, nonlinear simulation, velocity pursuit

ÖZ

HIZ TAKİP GÜDÜMÜ KULLANAN LAZER GÜDÜMLÜ SİLAH SİSTEMİNİN MODELLENMESİ VE ÇEŞİTLİ DENETİM STRATEJİLERİNİN PERFORMANSINA ETKİSİNİN İNCELENMESİ

Güner, Dünya Rauf Levent

Yüksek Lisans, Makina Mühendisliği Bölümü

Tez Yöneticisi: Prof. Dr. Bülent E. Platin

Ortak Tez Yöneticisi: Prof. Dr. M. Kemal Özgören

Ağustos 2004, 175 Sayfa

Bu tezde lazer güdümlü silah sistemlerinin modelleme ve analizine yönelik bir temel oluşturulmuştur. Çeşitli güdüm/denetim tekniklerinin, algılayıcı olarak sadece kendini hız vektörü yönüne çevirebilen bir arayıcı vasıtasıyla hız takip güdüm tekniği kullanan hayali bir lazer güdümlü silahın performansına etkileri araştırılmıştır.

Lazer arayıcı, bir dizi test yapılarak deneysel olarak modellenmiştir. Lazer ışınının yansıması modellenmiş, sisteme ait aerodinamik katsayılar Missile Datcom yazılımı ile bulunmuştur. 10 Hz'de alınan açı hatası bilgilerini kullanarak çalışan, hız takip güdümlü, çeşitli güdüm/denetim modülleri ve arayıcı modeline sahip doğrusal olmayan bir benzetim oluşturulmuştur.

Bang-bang, 3 konumlu, çok konumlu ve orantısal denetim tekniklerinin silahın performansına etkisi, gürültüsüz ve gürültülü ortamlarda, sabit ve hareketli hedeflere karşı yapılan atışlar ile araştırılmıştır. Uçuş karakteristikleri, kaçırma

mesafesi, atış zarfı, çarpma hızı, uçuş zamanı gibi parametreler aracılığıyla gözlenmiştir. Silahın manevra yeteneği incelenmiş, aşağı yönünü belirleyen kuramsal bir algılayıcının silah performansına etkileri gösterilmiştir.

Benzetim sonuçlarının ışığında değişik denetim teknikleri karşılaştırılmış, sistemlerin başarımları ve uçuş zarfları vurgulanmıştır. Çok konumlu denetimin çoğu atış koşulunda kayda değer iyileştirme sağladığı ve orantısal denetime bir seçenek olarak kullanılabileceği, orantısal denetim kullanılması durumunda ise, sistemin aşağı yönü saptayan bir algılayıcı ile desteklenmesinin faydalı olacağı anlaşılmıştır.

Anahtar Kelimeler: Bang-bang, lazer arayıcı, çok konumlu denetim, doğrusal olmayan benzetim, hız takip güdümü

To my father, Remzi Güner...

ACKNOWLEDGMENTS

I would like to express my sincere thanks to my supervisor Prof Dr Bülent Platin who re-ignited the flame of academic work enthusiasm in my heart, for having the spirit of an excellent teacher rather than just a supervisor, for his humanity, support and understanding throughout the study. Special thanks go to my co-supervisor Prof Dr. Kemal Özgören for his continuous support, key suggestions, and morale motivation with his never disappearing smile in his hard times.

I would like mention Dr. Murat EREN, my manager at ASELSAN-MGEO Navigation and Guidance Systems Design Department, for his understanding and patience during the study.

Dr. Gökmen Mahmutyazıcıoğlu is greatly acknowledged for his technical support during aerodynamic modeling.

My colleagues, especially Elzem Akkal, Özgür Ateşoğlu, Volkan Nalbantoğlu are greatly acknowledged for their technical assistance.

I would like to thank to all people in METU Registrar's Office, for being the closest ally of students in university, by solving our problems as soon as possible.

And my Family... My mother Saadet, father Remzi, and my little brother Can Güner deserve endless thanks, for their love, support and endurance to me.

TABLE OF CONTENTS

LIST OF TABLES

LIST OF FIGURES

LIST OF SYMBOLS

Symbols

C_n^b	transformation matrix from navigation to body frame
C_i	rotation matrix about i^{th} axis
C_x	axial force coefficient
C_y	side force coefficient
C_z	normal force coefficient
C_L	rolling moment coefficient
C_M	pitching moment coefficient
C_N	yawing moment coefficient
$C_{z\delta e}$	normal force coefficient derivative with elevator deflection
$C_{m\delta e}$	pitching moment derivative with elevator deflection
$C_{M\alpha}$	pitching moment coefficient derivative with angle of attack
$C_{y\beta}$	side force coefficient derivative with sideslip angle
$C_{z\alpha}$	normal force coefficient derivative with angle of attack
C_{Mq}	pitching moment coefficient due to pitch rate
C_{zq}	normal force coefficient derivative with pitch rate
C_{Lp}	roll moment derivative with roll rate, roll stiffness
D	distance between missile's center of mass, and detector's center
$\vec{F}$	force vector
F_{Ai}	i^{th} component of aerodynamic force
g	gravity vector magnitude
$\vec{H}$	angular momentum vector
I	radiant intensity

I_k	mass moment of inertia about k'th axis
Iij	product of inertia
m	mass
$\bar{M}$	moment vector
P	power
$\vec{p}$	linear momentum vector
q	size distribution of scattering particles
r	radius
R	range
$\vec{R}_{gT}\big\|_i$	range between detector center and target expressed in frame i
T	transmission
V	visibility
$x\big\|_I$	x vector with respect to inertial frame
$x\big\|_F$	x vector with respect to fixed frame
y_c	distance from the rolling body axis to the area center of fin panel

Greek letters

α	angle of attack
α	lead angle
β	sideslip angle
γ	reflectivity
δ	control surface deflection
θ	divergence angle
θ	incidence angle
Θ	test set roll angle
λ	wavelength
φ	yaw angle
θ	pitch angle

ϕ	roll angle
σ	atmospheric attenuation coefficient

Abbreviations

ADATS	air-defense anti-tank system
AGM	U.S. designation for air to ground (surface) missile class
AIM	U.S. designation for air interceptor missile class
AMRAAM	advanced medium range air-to-air missile
BB	bang-bang
BTB	bang-trail-bang
C	continuous
CAS	control actuation system
CCW	counter clockwise
CEP	circular error probable
CM	center of mass
CW	clockwise
DSP	digital signal processing
DZ	deadzone
ECCM	electronic counter counter measure
EO	electro-optic
ERA	explosive reactive armor
FO	forward observer
FOV	field of view
HARM	high speed anti-radiation missile
Hz	hertz
(I)IR	(imaging) infrared
IMU	inertial measurement unit
INS/GPS	inertial navigation system / global positioning system
JASSM	joint air to surface standoff missile
JDAM	joint direct attack munition

JSOW	joint standoff weapon
LOAL	lock on after launch
LOCAAS	low cost autonomous attack system
LOBL	lock on before launch
LOS	line of sight
MBT	main battle tank
MP	multiposition
NED	north east down
NTS	night targeting system
NVG	night vision goggle
PRF	pulse repetition frequency
RAM	rolling airframe missile
RF	radio frequency (radar guided)
RGM	U.S. designation for surface ship launched anti-surface missile class
RPG	rocket propelled grenade (i.e. RPG-7)
SLAM	standoff land attack missile
TERCOM	terrain contour matching
TOW	tube launched-optically tracked-wire guided
TVM	track via missile
UAV	unmanned aerial vehicle
UV	ultraviolet
WCMD	wind corrected munition dispenser

CHAPTER I

INTRODUCTION

The purpose of this chapter is to define the aim and scope of this study, constitute a general understanding of laser guidance and its principles, introduce the primary characteristics of a generic laser guided weapon subject to study, comment about its drawbacks, and decide an approach to improve its performance.

A general informative background about guidance systems is given and the place of laser guidance among those methods is described. The history of laser guided weapons is briefly explained along with the current state of laser guided weapons and their employment areas with various examples. The tendency of armed forces in designing and fielding precision weapons is also explained in the light of the statistical knowledge about recent conflicts.

The working principle of laser guidance is briefly explained, laser designators and guided weapon employment are narrated. The literature about the subject matter is also overviewed.

This chapter is concluded with the expected original contributions to the subject and scope of the thesis describing the contents of following chapters.

1.1 GUIDANCE METHODS

It will be helpful to describe the methods of control and guidance before proceeding with laser guided weapon systems. One classification of precision guided weapons is according to their guidance and control methods as control

guidance and homing guidance. The navigation equipment also provides a self contained navigation capability to attack fixed targets.

Control guidance: This guidance methodology relies on a highly capable control station at the ground. It includes systems in which the missile is dumb and the control station is smart. Command guidance and beam rider guidance are the examples for the control guidance. Both the missile and target are tracked by the control station. Guidance commands are sent to the missile by radio waves or by any other means. This approach lets a cost reduction by the placement of many sensors and guidance components on the ground station, thus reducing the cost per missile. Capabilities of these missile systems depend on the control station's technology level. The number of targets that can be engaged simultaneously is a matter of control system capabilities. The control guidance backed with various terminal homing seekers, is used at high altitude, long range air defense systems. Some examples include MIM-14 Nike Hercules (1950's), MIM-104 Patriot (PAC-1/PAC-2), Crotale low altitude air defense system. Wire guidance is also a type of command guidance where the guidance commands are sent to the missile by the control unit via wire. An example to the wire guided weapons is the BGM-71 TOW anti-tank missile system. Some torpedoes are also directed to their targets by utilizing wire at the early stages of their trajectory until the target is within the acoustic sensor range of the torpedo.

Homing guidance: Active, semi active and passive guidance are subcomponents of homing guidance. In homing guidance, the missile is equipped with necessary sensors and guidance algorithms to engage enemy assets.

Active guidance: In active guidance, the target is illuminated by emissions generated by the missile. For example, active radar guided missiles send radar waves to a large conical area and regain radar signals reflected from the target. These returning signals are then used to compute the necessary information to track and intercept the target. Active systems have the capability to detect and track targets by themselves without requiring any external aid. Active radar guided missiles are mostly used at long range tactical missiles where platform dependency

becomes a negative effect in survivability and the number of targets to be engaged simultaneously is the difference between life and death.

Active radar guided missiles are used in anti-ship missiles (RGM-84 Harpoon, SS-N-19 Shipwreck, Exocet), medium / long range air to air missiles (AIM-120 AMRAAM, METEOR), and high capacity air defense systems (ASTER-15/30). Some anti-tank missiles, such as AGM-114 Hellfire Brimstone version, use active MMW seekers. An example of these types of missiles is the RGM-84 Harpoon anti-ship missile utilizing active radar homing at the terminal phase of flight. The launching platform is free to engage the next target or maneuver once the missile is fired. There is no need to track the missile until it hits.

Semi active guidance: In semi active guidance, it is necessary to illuminate the target by an external source. The missile has necessary sensors in its seeker to detect the reflected form of energy (laser, radar, etc.) from the target. Semi active radar guidance is widely employed medium range ship / air defense systems such as RIM-7 Sea Sparrow. Sea Sparrow missile can engage targets that are constantly illuminated by a target illumination radar. The ability to engage multiple targets is limited with the number of target illuminating radars.

Passive Homing: In passive homing, the weapon seeker detects the target's emissions in the form of acoustic (torpedo), thermal, UV, RF, magnetic (mine), etc. Since the weapon emits no energy, it is harder to detect. Passive homing is used at torpedoes and short range air/missile defense weapons. Passive homing missiles are mostly fire and forget type. Some examples are FIM-92 Stinger (IR/UV), RIM-116 RAM (RF/IR), AGM-119 Penguin (IR), Javelin (IIR), AGM-88 HARM (RF, anti-radiation missile)

Navigation equipment: Navigation equipment is used widely in guidance of missiles against fixed targets and to plan routes during midcourse phase. Missiles equipped with inertial navigation systems can be programmed to attack fixed targets without any other sensor. Other methods such as TERCOM (terrain contour matching), sun or star sensors are also widely used in order to navigate and attack

at fixed targets. These equipments are very useful in planning attack routes, control of missile position and attitude, etc.

Since weapons have initial, midcourse and terminal phases of their flights, it is often necessary to combine one or more of these guidance methods. Actually, it is necessary to employ various sources of information in different phases of flight. Some of the dictating factors are the range, ECCM (electronic counter counter measure) capability, flight altitude, engagement requirements. Some missiles especially utilize command guidance to be more immune to decoys. This permits the system to analyze target information in a more capable computer system to eliminate jamming effects. On the other hand, active systems are required to engage multiple targets at a time where time is critical, which is very important in ship defense against anti-ship missiles. A frigate can be engaged with multiple sea skimming anti-ship missiles that are programmed to hit at the same time. The ship defense system must be capable of handling these threats, classify, track, intercept within a limited time. Long range anti-ship or anti-aircraft missiles require inertial guidance in order to maintain their trajectory accurately at the midcourse phase. When the missile comes at the detection range of its seeker, terminal homing guidance takes over to cope with the evading targets.

Among those guidance systems, the laser guidance is one of the preferred methods used against both stationary and moving targets due to its pinpoint accuracy. Currently there are two types of laser guidance. Semi active laser guidance and laser beam riding which is a type of command guidance. There are also attempts to use laser radar technology to design active homing missiles with scanning (and imaging) laser like LOCAAS (low cost autonomous attack system) to engage enemy armored vehicles.

In a laser beam riding guidance, the system consists of a missile control/launch unit equipped with electro-optical means to track and illuminate targets with laser, and a missile equipped with a detector or receiver at the back of the missile to detect the incoming laser energy form the launcher. The laser designator always sends the laser beam on the target or the proper intercept point till impact. The

detector is used to sense the difference between the laser energy coming on its quadrants and the corrective action is taken to align the missile with the laser beam.

This type of guidance is widely seen in anti-tank weapons of Russian origin. Some examples include AT-10 Stabber, AT-12 Swinger, AT-14 Kornet, AT-15 Khrizantema (a combination of radar and laser beam riding is used.) Trigat MR (Europe). There are some examples in SHORAD (short range air defense) systems like Canadian ADATS (air-defense/anti-tank) laser beam riding system and the English Starstreak air defense missile.

The other and most widely used laser guidance method is the semi active laser guidance. Unlike laser beam riding guidance, the target can be designated by the launcher platform or any other external source such as a forward observer team, UAV (unmanned aerial vehicle), helicopter, or any other front line asset. These weapons have a laser sensing detector located at the front of the weapon. Since these systems see the laser reflection from the target, they do not have to fly on the line of sight between the launcher and the target. This allows the target to be illuminated by other sources and a more flexible flight profile can be achieved.

1.2 LASER GUIDED WEAPONS

Studies to develop laser guided weapons were started in the early 1960's. [1] The primary motivation in the development of laser guided weapons was to find a way to employ missiles against ground targets such as tanks. Attempts were made to develop acoustic, radar and IR seekers to identify and engage tanks, but all failed at that period. The thought of using laser technology to mark targets was also considered, with the advances in laser technology. The main problem was that, the target had to be illuminated by a forward observer in the field who had to carry the laser illuminator. It was believed that the beam should illuminate the target continuously. The power required to generate the beam continuously to the required distances was tremendous and power sources were so big to use in the field by the forward observer. Later, engineers figured out that it was possible to

use a pulsed laser instead of a continuous one, which could create very high power and short duration pulses to illuminate the target. This approach made the development of laser designators possible. Further advances in laser technology led to the fielding of first generation laser guided weapons which entered service in late 1960's and in 1970's. The results were impressive. The first real conflict was the Vietnam War in which Thanh Hoa Bridge near Hanoi in North Vietnam was heavily damaged in one attack with laser guided weapons. This bridge had been bombed in various previous attempts with classical ballistic weapons, resulting 800 sorties and 10 aircraft losses. [1] One of the famous laser guided missiles was and still is the AGM-65E laser Maverick (versions with EO, IIR, IR guidance also exist.).

The laser guidance is employed at several air to surface missiles from heavy assault weapons to anti-tank missiles, since it does not require a very sophisticated seeker technology and also due to its high accuracy. Most medium to long range anti-tank missiles use laser guidance, too. A typical example is the AGM-114 (A/B/C/K) Hellfire. It is equipped with a laser seeker, a precursor charge, a main shaped charge warhead and a solid rocket motor.

There are various examples of cannon launched laser guided projectiles, whose main purpose is to provide effective fire support to infantry against moving enemy targets such as tank columns, where friendly direct fire weapons can not engage due to tactical situation and range problems. Typical examples are the US. M-712 Copperhead (155 mm), the Russian Kitolov (122 mm), Krasnopol (152 mm), Santimetr (152 mm) guided artillery rounds and the Smelchak (240 mm) mortar round.

Although laser guided weapons are widely used at the inventories of many countries, they earned their reputation during the First Gulf War in 1991. The success of precision guided munitions in this war led to the research and development of new weapons, and the armed forces decided to employ more precision guided munitions in their inventory. The percentage of precision guided munitions including laser guided ones, are dramatically increasing. In Operation

Desert Storm, the total percentage of precision munitions to the overall expenditure was as low as 5 %. [2] But high hit rates led to the increased use of precision guided munitions at incoming conflicts.

In Operation Deliberate Force performed in Bosnia, NATO forces launched 1026 weapons from aircrafts, of which nearly 63 % were laser guided precision munitions. [3], [4] In operation Iraqi Freedom, the ratio of guided munitions to the overall usage was almost 68 %. The share of laser guided weapons among guided munitions was as high as 50 %. [5]

The development of new laser guided weapons is continuing. Lessons learned from recent conflicts showed that most future conflicts will take place in urban areas where a high risk of civilian casualties exists. This “civilian casualties” fact is a very important factor that can degrade the international support of a country in war, even in peace keeping operations. Most weapons utilized in NATO countries today were designed in the cold war era, with the only thought to destroy the outnumbering Russian and Warsaw Pact weapons. Today’s low intensity conflicts in urban areas dictate the development of new precision weapons with a pinpoint accuracy and low collateral damage. In order to overcome adverse effects, new precision guided weapons with smaller warheads are being designed. The United States is planning to employ a new generation small laser guided missile using the bodies of unguided 2.75“ rockets in her inventory, to use in attack helicopters, starting from 2007 (APKWS Program).

The current tendency in weapon technology is, to increase the number of precision guided munitions in inventories of armed forces of most countries. There are many precision guided weapons under development and in service (WCMD, JASSM, JSOW, JDAM, new generations of Tomahawk missiles, SLAM, etc.) precision guided weapons utilize one or more of the guidance and navigation equipments such as INS/GPS (all weather stationary target engagement), laser guidance (pinpoint accuracy and moving target intercept), IIR terminal seekers (terminal phase, moving target intercept, no illumination required.), etc.

1.3 WORKING PRINCIPLES OF LASER GUIDED WEAPONS

The components of a laser guided missile are not much different than any missile. The missile consists of a strapdown or a gimbaled laser seeker section which is equipped with generally a 4-quadrant laser detector and suitable optics, an electronic card to decode the laser code, a guidance system to analyze target's relative direction, a control section which converts guidance system commands to physical control surface deflections, a warhead, a fuze, and an engine if any.

In order to employ laser guided weapons, two main components are necessary. A designator and a laser guided weapon. Laser designators are special equipments which are used in both aerial designation pods and forward observer posts. A laser designator creates a very high power but short duration pulses of laser. Ground laser designators consist of a laser source and suitable binocular optics for the operator to aim and track the target easily. Aerial target designator pods are more complicated, often have sophisticated laser spot trackers, stabilized thermal and day cameras for the pilot, and longer range laser sources.

The designator is aimed at the target by means of operator optics. The laser beam strikes the target surface and reflected. The reflection can usually be detected in a large volume of space as a function of range, weather conditions, etc. A laser guided weapon is launched by the platform when the pilot or the weapon operator assures that he/she is in the launch envelope of the weapon and a correct approach bearing is followed.

The weapon may be launched according to its type in LOBL (lock on before launch) or LOAL (lock on after launch) mode. LOBL requires that the weapon seeker locks on the laser energy reflected from target and starts following it by its seeker head before being fired. When the seeker locks on target at the pylon, it is launched by the pilot. In LOAL deliveries, the weapon is released when the pilot or weapon operator satisfies that the weapon will see the reflected laser energy sometime after release. In those cases, the weapon may perform midcourse guidance or flies ballistic according to the type of weapon.

The acquisition starts when the reflected laser energy starts falling on the seeker. The reflected light enters the seeker as a collimated large beam due to the small aperture of the seeker and the large volume of reflected energy in space. Optics collects the incoming laser beam and directs it on the surface of the detector where the falling energy causes a voltage or current formation on the detector. Since there is a line of sight angle between the weapon and the target, when refracted by the lenses most of the energy will fall into one region of the detector, giving information about the line of sight angle between the target and weapon. This is a necessary knowledge for the guidance system to operate. Depending on the sensitivity and structure of the seeker it is possible to extract the LOS (line of sight) angle, lead angle, or LOS rate from the seeker. This information may be employed at various guidance methods, along with some additional sensors. For example, a gimbaled seeker which can accurately determine the LOS rate when backed up by gyros and accelerometers, can be used at proportional navigation.

Laser designators and seekers use a pulse coding system to ensure that a specific seeker and designator combination work in harmony. By setting the same code in both the designator and the seeker, the seeker will track only the target illuminated by the designator. The pulse coding is based on PRF (pulse repetition frequency). Coding allows simultaneous or nearly simultaneous attacks on multiple targets by a single aircraft, or groups of aircraft, launching laser guided weapons set on different codes. [5],[6]

The effects of smoke, dust, and debris can limit the use of laser-guided weapons. The reflective scattering of laser light by smoke particles or other obscurants may present false targets. Rain, snow, fog, and low clouds can prevent effective use of laser-guided munitions. Snow on the ground can produce a negative effect on laser-guided munitions accuracy with its high reflectance. Fog and low clouds block the field of view of laser-guided munition’s seeker, which reduces the guidance time. This reduction may affect the probability of hit. [5], [7]

1.4 SYSTEM DEFINITION AND MAJOR ASSUMPTIONS

Among the wide range of laser guided weapon arsenal ranging from guided projectiles to heavy assault weapons, only the air to ground glide weapon class will be the main subject of investigation in this thesis.

Regarding the common properties of similar weapons, the following characteristics of the generic weapon system are to be used.

- The system is assumed without any propulsion.
- The weapon is assumed to have a velocity aligning probe mounted seeker (like the Russian KAB-500 and 1500L laser guided weapons).
- The laser seeker is assumed to have a 4-quadrant detector, as used in most laser guided weapons.
- The guidance system is assumed to be a velocity pursuit type without any additional sensor onboard.

In the operation of laser guided weapons, there are some factors that are effective on the delivery accuracy. Some of them can be stated as podium effect, spot motion, jitter, spillover, etc. Since these adverse effects are present in all laser guided weapon employments, they can be regarded as external effects independent of weapon. In this thesis, these effects are not considered in the analysis. Only the factors that are directly related with the weapon's unique properties are taken into account.

1.5 LITERATURE SURVEY

The literature survey is divided into two areas, the first is to assess the specific characteristics of similar weapons and the second is to review previous research done about the subject matter.

The open literature is surveyed in order to obtain information about the selected type of weapon system and ongoing work about laser guided weapons. Since

technical information open to public is limited for defense systems, some reports and articles have to be used to determine the general performance characteristics of these types of weapons.

In order to understand the general behavior of laser guided, velocity pursuit, air to ground glide weapons, several reports are investigated. [6][7] give general information about laser guided weapons. [2][3][5] analyze the usage of precision guided munitions on recent conflicts along with their usage techniques, numbers, shortfalls, etc.

Most sources [6][7][8][9] report that, the accuracy is heavily dependent on many factors such as release altitude, dive angle, release speed for these types of weapons. It is reported that, best results are obtained by high to medium altitude fast dive attacks, which provide an extra energy to weapon. It is also understood that the total energy at the release point is a very effective element of weapon's success. For weapons that use full control surface deflections, the energy is dissipated rapidly due to a high drag. If the release energy is low, the weapon can not maintain its maneuvering ability for a long time, and can not perform necessary sudden maneuvers required at the last seconds of terminal phase of the flight and may fall short of the target.

Some conclusions obtained from the literature survey about weapon performance can be summarized as follows,

- Weapon oscillates about the instantaneous line of sight due to its guidance logic and control system, when it has enough energy and thus, maneuvering potential.
- Various sources claim that, in high dive angle deliveries, the weapon has high energy which provides maneuverability at end game phase. This results in accurate hits.
- Maneuverability decreases as the target is approached.

- Gravity is always an important factor which dominates and pulls the weapon below the LOS as velocity decreases. This causes the weapon to fall short of the target especially at low altitude, low speed launches.
- Gravity and bang-bang guidance causes sag below original boresight LOS which means short fall.
- Full canard deflection logic causes loss of energy.

The amount of technical data that is available to public focusing on laser guided weapons of selected kind or on guidance and control of probe mounted seekers with velocity pursuit guidance is limited. There are some works on missiles, but they are mostly related with INS/GPS use and utilizing proportional navigation. Some examples are narrated below.

Perkgöz [10] investigated the guidance and control of a tail controlled bomb. In his work, the bomb's primary sensor system is the INS/GPS hybrid navigation system, from which, an accurate position and attitude information can be obtained. The study implemented a fuzzy logic guidance system along with proportional navigation to a tail controlled bomb. This study can be performed for weapon systems with sophisticated INS/GPS systems backed up with or without high accuracy terminal seekers like the GBU-29/30/31 JDAM weapon system. Unfortunately it is not possible to implement the proportional navigation with existing sensors onboard, to the class of laser guided weapons in this study.

Akkal [11] investigated the use of PWM (pulse width modulation) control system for a generic ASGM (air to surface guided munition). In her study, there is a theoretical seeker model which was constructed by using several assumptions such as fully linear angle-voltage relationship, which was obtained by an assumed spot size and geometric interpretation.

Ralph and Edwards [12] analyzed the effect of aircraft delivery system errors on enhanced laser guided weapons. The study was based on three versions of last generation laser guided air to surface weapons having autonomous INS and INS/GPS. They examined the conditions for optimal weapon guidance as well as

their dependence on systematic errors. Also, effects of error sources on the ability of weapon to obtain a valid guidance solution were analyzed. The study was based on a 6-DOF (six degrees of freedom) simulation for three generic types of weapons, utilizing predictive proportional navigation which navigates to the estimated target location until a laser acquisition starts. Their laser seeker model assumes that, if the signal power received by the laser seeker is higher than a specified value, acquisition starts. They examined the effects of transfer alignment errors on the weapon performance for two different delivery scenarios and concluded that an INS/GPS hybrid weapon navigation system was less sensitive to delivery errors and transfer alignment errors than the only INS and three gyro cases. The seeker model was used to determine the LOS angle error. Their study was performed for laser guided weapons having some additional sensors. On the contrary, the current work in this thesis is primarily based on the analysis of a laser guided weapon without any additional sensors.

It is possible to state the following works in the area of laser behavior, which helped in constituting a laser reflection pattern. Baba [13] proposed a shape measurement system by a novel laser range finder, for objects having both Lambertian and specular reflectance properties. Kim [14] offered a modified laser attenuation formula to be used in laser power attenuation calculations in laser communication systems. Akbulut and Efe [15] examined the use of laser and RF communication links and analyzed these links in various weather conditions.

1.6 OBJECTIVE OF THESIS

During the literature survey, it is seen that the majority of studies on laser guided weapon systems with velocity pursuit guidance and velocity aligning seeker as the only sensor, are either limited or unavailable. Most of such studies focus on the research of proportional navigation guidance using inertial sensors. There is no open information about how these systems can be improved without making major modifications in guidance and control units. There is a gap between weapons

employing bang-bang control with velocity pursuit guidance and IMU (inertial measurement unit) equipped proportional navigation employing systems.

This thesis aims both

- to constitute a base that can be used for the analysis of laser guided weapons and
- to investigate the effects of several control methodologies on the performance of a generic laser guided air to surface weapon system having common properties of such kind of weapons.

The results of literature survey show that, there exist several drawbacks of laser guided weapons of this kind. The major drawbacks of the system can be classified as

- excess maneuvers due to bang-bang control,
- rapid turn down in toss deliveries, and
- gravity sag.

The performance of this type of weapon systems can be further improved in the following areas:

- Increasing range
- Decreasing or maintaining miss distance while increasing range
- Increasing moving target intercept efficiency
- Gravity compensation and saving energy

Although several improvements can be suggested such as adding inertial sensors, gimbaled seeker, INS/GPS, etc, each of them suffer from the cost parameter and additional complications introduced to the launching platform such as requirements for MIL-STD-1553/1760 databus, etc.

In this thesis, it is aimed to increase the performance of the weapon without requiring significant modifications to the system

- by the effective use of the detector lead angle information, and
- by the use of different control techniques ranging from bang-bang to continuous schemes.

1.7 SCOPE

After general information about air to surface guided weapons and guidance techniques are given and the objectives of the thesis are stated in the current chapter, the modeling phase starts.

Chapter 2 gives a brief information about the laser reflection mechanisms. Laser designators, the attenuation of laser energy in the atmosphere, target types, reflection patterns such as diffuse and specular reflection are defined. The laser model that will be used in simulations is described.

Chapter 3 deals with the laser seeker modeling. Some background information about the laser seekers are described, such as laser detection techniques, focusing methods, and lead angle value determination from 4-quadrant detectors. The work done in the laser seeker modeling phase constitutes an experimental study with a 4-quadrant laser detector to obtain the relationship between the lead angle and the voltage of the detector, the analysis of the results and the determination of some parameters of the test setup such as boresighting error. The results obtained helped in forming a laser seeker behavior pattern with a linear and a saturated region.

Chapter 4 is about the derivation of equations of motion for a rigid missile. Dynamic equations that are necessary to define the motion of a missile in 6-DOF simulation are derived. These equations come out to be nonlinear coupled first order differential equations that are solved numerically in the simulation studies using initial flight conditions. Aerodynamic coefficients in these equations are

derived as function of angle of attack and Mach number by using the Missile Datcom software.

In Chapter 5, the guidance and control system is introduced. Important angles in the guidance system are defined, and the velocity pursuit guidance method is narrated. Bang-bang, bang-trail-bang, multiposition and continuous control methodologies and their usage are introduced.

Chapter 6 gives information about the 6-DOF simulation model created in Matlab 6.5. Implementations of several models into Simulink are briefly described.

Chapter 7 is dedicated to the nonlinear flight simulations. Primary launch scenarios against moving and stationary targets are determined and performances of control methods are investigated. Results of bang-bang, bang-trail-bang, multiposition and continuous canard deflection schemes are compared for multiple scenarios.

Chapter 8, the conclusion chapter, summarizes the work done, and results obtained. Recommendations for future work are also mentioned.

CHAPTER II

LASER REFLECTION MODELING

2.1 INTRODUCTION

Since, the main purpose of this thesis is to constitute a base for the modeling of laser guided weapons, it is necessary to include the effects of laser behavior in the analysis. The laser designation process and the reflection characteristics from the targets must be understood to see if some additional important factors due to relative attitude of weapon and target are introduced or not.

In order to obtain some logical conclusions, the laser reflection is taken into account in the modeling phase. Several laser designators are investigated and some key elements of their specifications are found. The laser beam and its behavior at the atmosphere, along with the weather conditions are investigated; target types and their response to incoming laser are also analyzed briefly. A laser model which is based on minimum detectable power constraint is formed in the light of all this information.

2.2 LASER GUIDED WEAPON EMPLOYMENT

Laser guided weapons are employed by the use of laser designators located either on the ground or on airborne units. Cannon launched laser guided munitions such as M-712 Copperhead are mostly directed to targets by a combat observation and lasing teams equipped with laser designators, NVG's (night vision goggle), and necessary communication equipment. Helicopter mounted laser designators like NTS on AH-1W's or ground vehicles guide laser guided anti-tank missiles. For heavy laser guided weapons, both aircraft (LANTIRN, Pave Tack, etc.) and

forward observer laser designators are used. Airborne laser designators have both advantages and disadvantages over ground designators. They can have more output power and capable optics, providing longer range, the LOS obscuration is not a very serious problem, and they are more immune to any counter fire. On the other hand, ground designators can distinguish targets better. The line of sight problem and the chance of being hit are main disadvantages of ground designator teams.

It is possible to designate a target by the same aircraft or by utilizing wingmen. Attack helicopters and aircraft use these “scout-killer” tactics widely. The concept relies on the “buddy lasing” where one aircraft designates the target and the other shoots.

On the other hand, since it is very hard for a high speed aircraft pilot to detect camouflaged and concealed targets from long ranges, most combat air support missions are performed by a coordination with the FO (forward observer) team on the ground and ordnance deploying aircraft. The FO team can show the location of the target to the aircraft by designating it with a laser beam. The laser spot tracker on the aircraft is automatically slewed to the incoming laser reflection and the pilot can understand the location of target. Further communications regarding the laser code, attack bearing, correct “laser on” time, etc., between the ground and airborne units lead to the ordnance delivery at the correct bearing and time.

2.3 LASER DESIGNATORS

In laser aided weapon delivery systems, a laser designator is used to illuminate the target. The designator produces a train of very short duration, high peak power pulses of light which are collimated in a very narrow beam and directed to the target. These laser pulses are reflected off the target and are detected by a laser receiver [16].

Typical ground laser designators use 1064 nm wavelength with pulsed laser designation having 10-20 ns pulse width and divergence angles of less than 1 mil.

A laser beam has a very small diameter but it has the tendency to diverge rapidly. In order to prevent a high divergence, laser designators mostly have suitable optics to expand the beam. By the use of special beam expanders, the laser beam is sent from the designator in the form of collimated light. Beam expanders consist of two lenses with one small and one large focal length lens. They can be grouped as Keplerian and Galilean expanders according to the lens types. By this way, laser beam is expanded and turned into a higher radius collimated beam. This beam has a larger radius but in turn it has a very low tendency to diverge. Unfortunately, the divergence can not be thoroughly eliminated, so every designator has some unique beam divergence characteristics. The beam is sent to the target as a small circular portion at the designator exit, which is constant all throughout the way, and the expanding circle grows with the distance. [17]

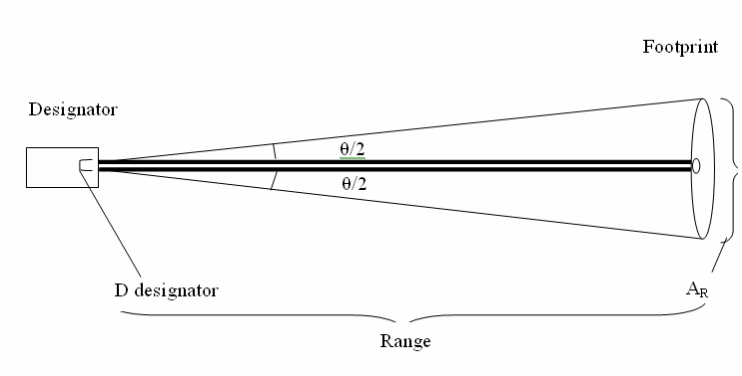

Figure 2-1 Laser beam footprint

Assuming that the target and the designator are at the same height as shown in Figure 2-1, the laser footprint on the target can be found as,

$$A_R = \frac{\pi(\theta R + d_{designator})^2}{4} \tag{2.1}$$

where R is the range between the designator and the target, θ is the divergence angle, and $d_{designator}$ is the designator aperture diameter.

At long ranges, the beam divergence angle dominates and the laser spot can be assumed to be the base of a cone whose apex angle is the divergence angle. In this case, $d_{designator}$ can be eliminated from the equation.

If the beam cross section is bigger than the target or if there exist some misalignment in the laser designator and observation optics, or if the operator illumination is poor, the beam footprint may fall on both the target and the background terrain behind the target. In this case, laser reflections from both the target and the terrain are sensed by the detector. This is called spillover. [18]

The spillover causes a wrong lead angle sensing. There are some logics used such as the last or first pulse logics to overcome this difficulty. One other adverse effect of spillover is the loss of laser energy that is to be reflected from target.

2.4 LASER ATTENUATION IN THE ATMOSPHERE

A laser beam is attenuated as it propagates through the atmosphere. In addition, laser beams are often broadened, defocused, and may even be deflected from their original directions. These atmospheric effects have far reaching consequences for the use of lasers in optical communication, weaponry, ranging, remote sensing, and other applications that require the transmission of beam in the atmosphere. [19]

The attenuation and amount of beam alteration depend on the wavelength, output power, makeup of the atmosphere, and day to day atmospheric conditions. The attenuation increases as the visibility decreases. Clouds, smoke, dust, snow, rain, laser wavelength, height are effective in atmospheric attenuation.

Laser beams travel in the atmosphere according to Beer's law, which states that [19]

$$T = e^{-\sigma R} \tag{2.2}$$

where T is the transmission which takes a value between 0 and 1, σ is the atmospheric attenuation coefficient (1/km), and R is the range (km).

There are tabulated values for the attenuation coefficient of atmosphere for various meteorological conditions and wavelengths. There are also normalization graphics that can provide altitude corrections. By using these two types of graphics, it is possible to calculate atmospheric attenuation coefficients. But for each visibility value it is necessary to find a different point on these graphs.

In order to overcome this difficulty, there is another formula which introduces some small error but is practical to use. This formula also relates the visibility to the atmospheric attenuation coefficient as [19]

$$\sigma = \frac{3.91}{V} \cdot \left(\frac{550}{\lambda} \right)^{q} \tag{2.3}$$

where V is visibility (km), λ is wavelength (nm), and q is the size distribution of the scattering particles (1.6 for high visibility for V>50 km, 1.3 for average visibility for 6 km<V< 50 km).

If the visual range is less then 6 km due to haze, the exponent q is related to the visual range by the following empirical formula, [19]

$$q = 0.585V^{1/3} \tag{2.4}$$

where, V is expressed in kilometers.

Figure 2-2 and Table 2-1 show the behavior of atmospheric attenuation coefficient as function of visibility which is calculated by using Equation (2.3). it is seen that the attenuation increases drastically as the visibility decreases.

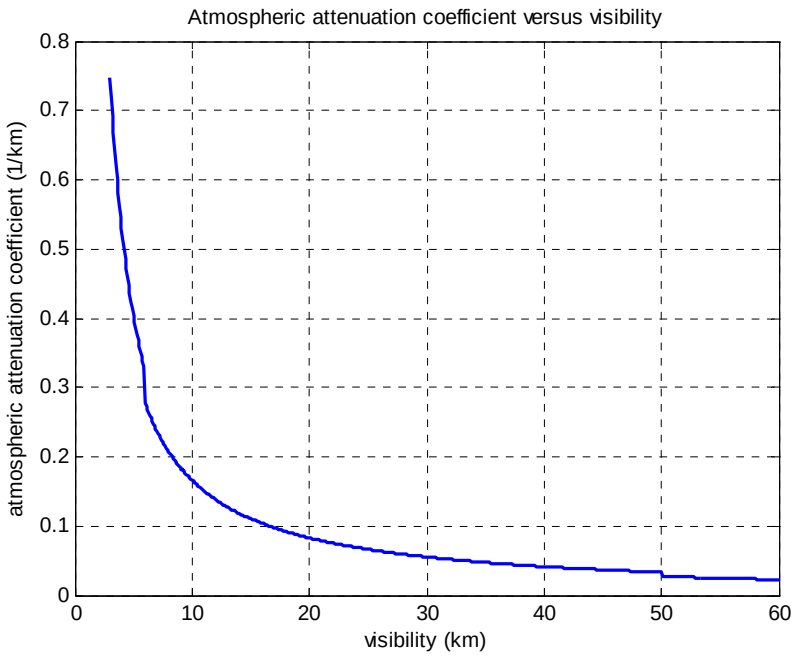

Figure 2-2 Atmospheric attenuation coefficient for 1064 nm as function of visibility

Table 2-1 Atmospheric attenuation coefficient (approximation) for various visibility values

Conditions	1064 nm (1/km)	Sea level visibility (km)
Exceptionally clear	0.0226	60
Very clear	0.0414	40
Standard clear	0.07	23.5
Clear	0.111	15
Clear	0.138	12
Light haze	0.207	8
Medium Haze	0.404	5
Light Rain (4mm/hr)	0.62	3.5
Haze	0.75	3

2.5 TARGET TYPES

Targets can be classified into two groups as cooperating and noncooperating targets.

A cooperating target is specifically designed to enhance the laser return signal. Special reflectors such as 90 degree prism-like surfaces are used to reflect the laser in the incoming direction. By this way, the laser return is easily detected and tasks like distance measurement can be performed.

Noncooperating targets are generally regarded as diffusely reflecting objects (like rocks, trees, buildings, or tanks). The term "noncooperative" is used because the target has not been prepared in advance to enhance the reflected return of the transmitted beam. [20]

Another important factor in laser reflection is the target reflectivity. Each target has a different reflectivity at a certain wavelength, depending on its material properties. The reflectivity, γ, at the laser wavelength of different targets can vary from less than 1 % to almost 100 %. When the reflectivity is not known and cannot be estimated, a value of 20 % or 0.2 (absolute number) is generally used. [18]

2.6 REFLECTION PATTERNS

The reflection of a laser beam from a target is a function of the laser wavelength as well as mechanical and material properties of the surface. Some surfaces that act as diffuse reflectors at one wavelength can behave totally different at other wavelengths.

There are three reflection types from surfaces. Diffuse reflection, specular reflection, retroreflection. The resultant reflection can be composed of diffuse, specular or both. [21][22]

The retroreflection is an artificial form of reflection that occurs due to the placement of retroreflectors or cats eyes on the surface. These retroreflectors can directly send the incoming beam back to the designator as seen in Figure 2-3.

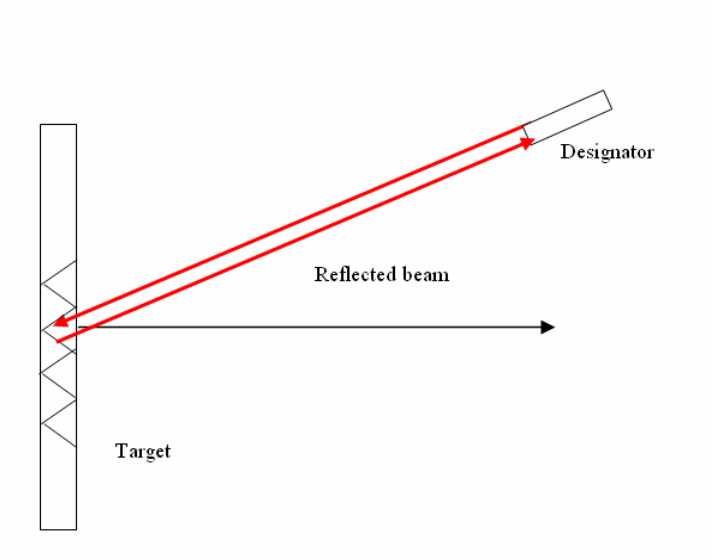

Figure 2-3 Retroreflection

The specular reflection is the reflection of light from a mirror-like surface, and occurs when the surface is smooth with respect to the laser wavelength. The incoming beam is reflected with an angle equal to the incidence angle as seen in Figure 2-4.

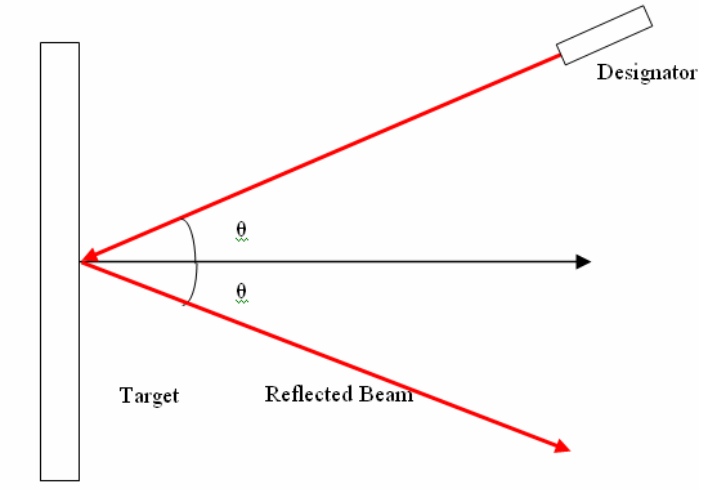

Figure 2-4 Specular reflection

The diffuse reflection is defined as the reflection from a surface in which the beam is scattered in all directions, like reflection from a rough surface. An ideal diffuse surface in which the reflected brightness is independent of the viewing angle is called a Lambertian surface. [18]

If the wavelength of the light beam is much smaller than the surface roughness of the target, the diffuse reflection occurs. The surface behaves like having many small surfaces with different normal directions.

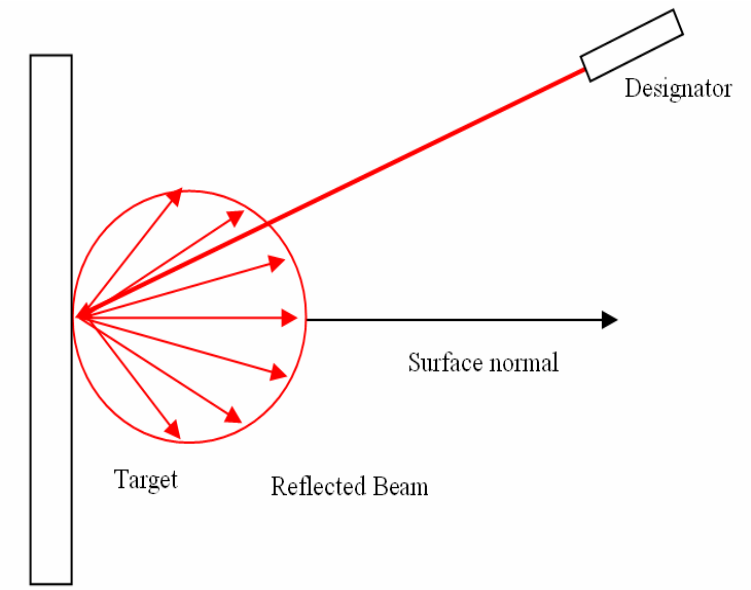

Figure 2-5 Diffuse reflection in Lambertian scheme

An ideal diffuse reflection is characterized by the Lambertian scattering (Figure 2-5). A rough surface acts as a plane of infinitesimal scattering sites which reflect the beam in a radially symmetric manner. The reflected radiant intensity, I(Φ), representing the power per unit solid angle, is dependent upon the cosine of the angle Φ between the surface normal and the viewing direction as

$$I(\Phi) = I_0 \cos(\Phi) \tag{2.5}$$

where I_0 is the radiant intensity reflected along the normal of the surface.

In most surfaces, both specular and diffuse components occur and the reflection pattern turns out to be the combination of specular spike, specular lobe and diffuse region as depicted in Figure 2-6.

The three components have the following characteristics; the diffuse lobe represents both an internal scattering mechanism and multiple reflections on the surface in a random manner. As a result, the light reflected from the surface of the object diffuses hemispherically in all directions. The specular lobe spreads at a certain range around the specular direction which is the angle at which the incident angle equals the reflected angle. It was shown that this component has some off-specular peaks for sufficiently high degrees of surface roughness, and that it then shows the characteristics of an asymmetric distribution with respect to specular direction. [13]

The specular spike represents a mirror-like reflection, and it is nearly zero in all directions except for a very narrow range around the specular direction. For a very smooth surface, the specular spike component is dominant, however, as the roughness of the surface increases, the specular spike component shrinks rapidly and the specular lobe component begins to dominate.

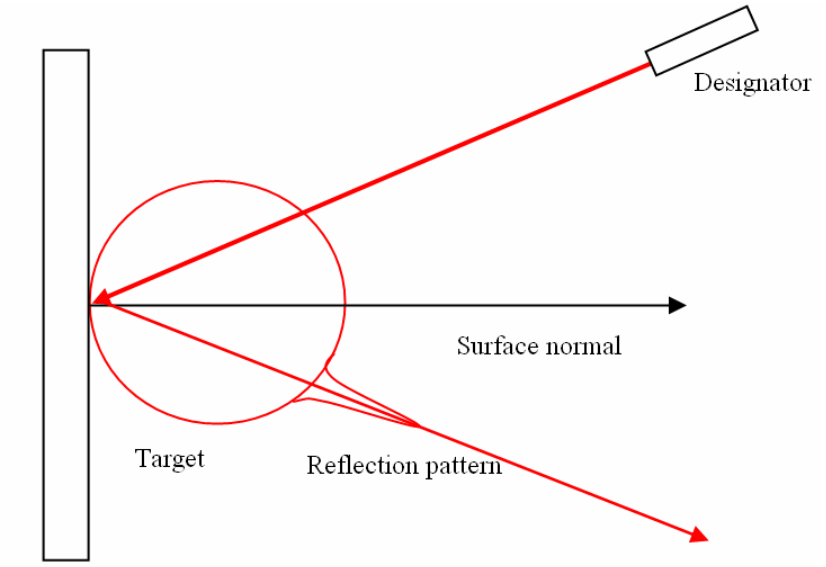

Figure 2-6 Combined reflection pattern

2.7 LASER MODEL

In order to develop a laser model, several assumptions and decisions should be made. It is necessary to decide on the reflection pattern from the target, target reflectivity value, output power of designator, weapon target geometry, and use these parameters with the effect of atmospheric attenuation, in order to find the laser detection range.

The shape of main battle tanks must be taken into account to decide on the proper reflection scheme. The literature for the laser reflection scheme of tank type targets is either limited or classified. It is necessary to make some assumptions about the laser reflection scheme.

Target armor plates are painted metal and have a high roughness. As a result, the diffuse reflection component dominates and target planes can be assumed as diffuse reflectors. There is also a specular component which reflects in a very narrow direction. This component is not taken into account due to its very narrow reflection direction. A seeker will not probably detect that reflection unless it is at the corresponding reflection direction.

Considering only one target armor plane, which is assumed to be diffusely reflective instead of specular, the reflected beam is scattered in all directions into a hemispherical pattern, with a maximum intensity reflected normal to the target plane.

However; regarding the target completely, which is a main battle tank having various armor plating with very different normal lines that are specifically designed to deflect incoming rounds, it is not possible to determine a general normal direction for the tank. Each armor plate will contribute to the overall reflection and Lambertian scatterings from armor plates with different normal directions can be assumed to form a hemisphere of uniform reflected power. Figure 2-7 is a photo of Russian T-72 MBT (Main Battle Tank) equipped with ERA (explosive reactive armor) packages on turret, hull front and skirt sides. [23]

Using this assumption, it is possible to create a hemispherical region of reflected rays, and to obtain a minimum detectable power region for the weapon. By this way, the laser reflection will affect the target acquisition range of the weapon and the limits of weapon acquisition can be created. Beyond these limits, the weapon will not acquire the target and fly ballistic.

Figure 2-7 Russian T-72S MBT equipped with ERA packages, with different surface normal directions [23]

Footprint: It is assumed that the target is illuminated by a ground laser designator, approximately having the same altitude with target.

With a beam divergence of 0.5 mils, the footprint diameter on the target at a range of 4 km will be around 2 meters. So the footprint will be a circle with a radius of 1 meter. The target is said to be a main battle tank, having dimensions about 8 x 3 x 3.5 meters The NATO standard target dimensions are 2.3 x 2.3 meters. Considering the dimensions of a main battle tank and the standard target dimensions, it is possible to assume that all the incoming laser energy falls and is reflected from the target, without any spillover.

Detection Range: The output power of the laser designator is taken as 5 mW, considering the specifications of ground designators. Since the entire laser beam is assumed to be reflected from the target's projected area (no spillover), the power reflected from the target will be attenuated only by the atmospheric attenuation and target reflectance parameters.

The power at the target P_{target}, can be found by multiplying the designator output power $P_{designator}$ with the transmission coefficient. T,

$$P_{target} = P_{designator} T \tag{2.6}$$

The transmission coefficient can be calculated by using Beer's law in Equation (2.2). The atmospheric attenuation coefficient is found by the help of Equation (2.3).

The target reflectivity, γ, for a military vehicle with olive drab paint is 0.118 and light brown surface is 0.257 [24]. Other sources [8] report that the reflectivity of dirty olive drab metal (tank surface) can change between 0.02 and 0.3. Although the precise amount of laser reflected from target is difficult to determine, an average reflectivity between 0.2 and 0.5 can be used.

Assuming that there is no spillover, the reflected power $P_{reflected}$ can be found by considering the target reflectivity as

$$P_{reflected} = P_{target} \gamma \tag{2.7}$$

Assuming a dominant diffuse reflection from all target surfaces, the reflected power is radiated uniformly into a hemisphere and a fraction of this power is sensed by the seeker as depicted in Figure 2-8. The power collected by the seeker $P_{received}$, is equal to $P_{reflected}$ multiplied by the atmospheric transmission, and the ratio of the seeker optics to the area of a hemisphere with a radius equal to range as seen in Equation (2.8).

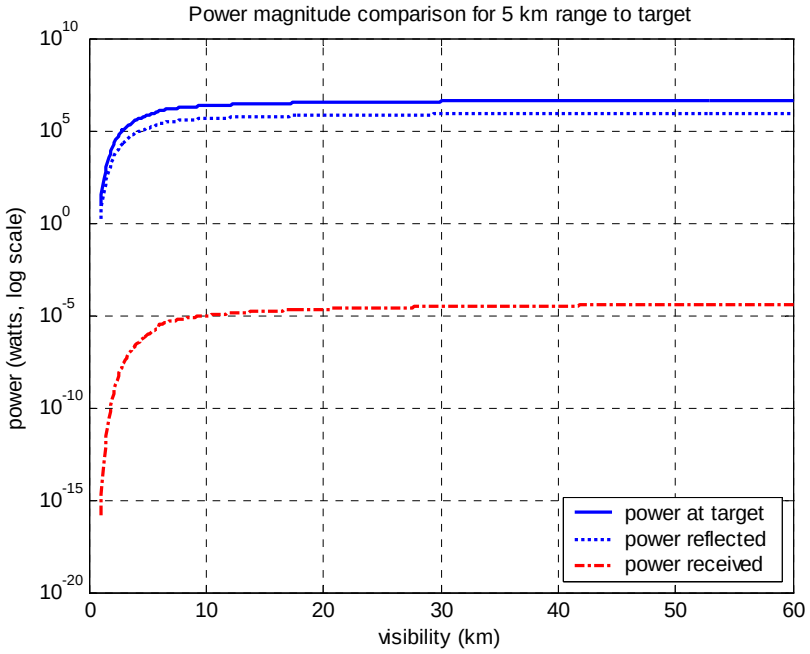

Figure 2-8 Power decrease due to attenuation and reflectivity

$$P_{received} = P_{reflected} T \frac{A_{seeker}}{A_{hemisphere}} = P_{reflected} T \frac{\pi r^2_{seeker}}{2\pi R^2} \tag{2.8}$$

False Targets: The laser reflection model given above does not include the effects caused by screening aerosols, snow, etc. or countermeasure systems like creation of false targets (decoy) by laser replicators since such kind of countermeasure effects are beyond the scope of this thesis. These countermeasures are dealt with the ECCM logics of the signal processing unit of the weapon to discriminate the false and real target, and are present in each laser guided weapon regardless of its guidance system.

All scenarios are performed with a ground designator at a range of 3000 meters from the target in high visibility conditions and aircraft attack bearing is assumed same with the designator-target line at the time of firing.

Figure 2-9 shows the effect of target reflectivity coefficient on seeker acquisition range for designator target range of three kilometers as function of visibility. The target acquisition range is heavily dependent on the target reflectivity and

minimum detectable power value of the weapon seeker. The designator range to target is less effective on detection range as seen in Figure 2-10.

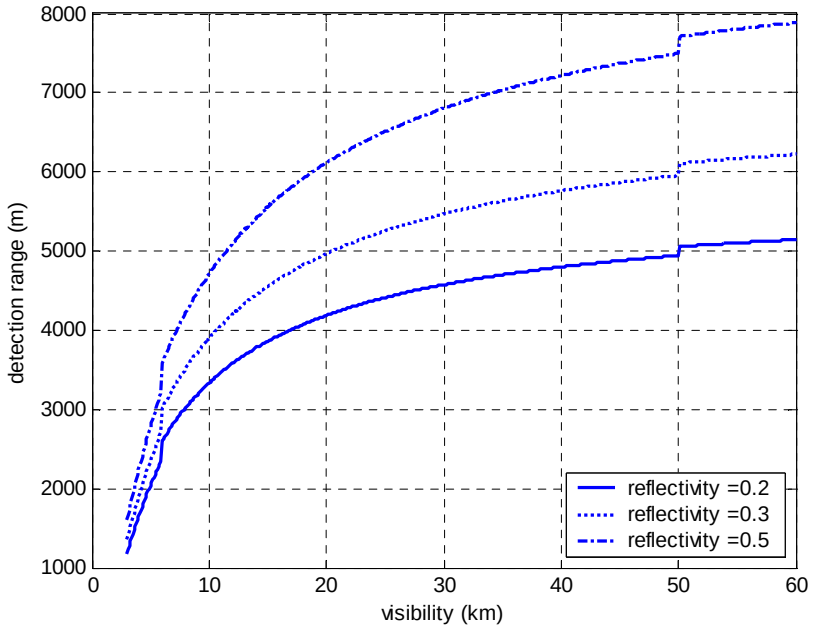

Figure 2-9 Effect of target reflectivity on detection range

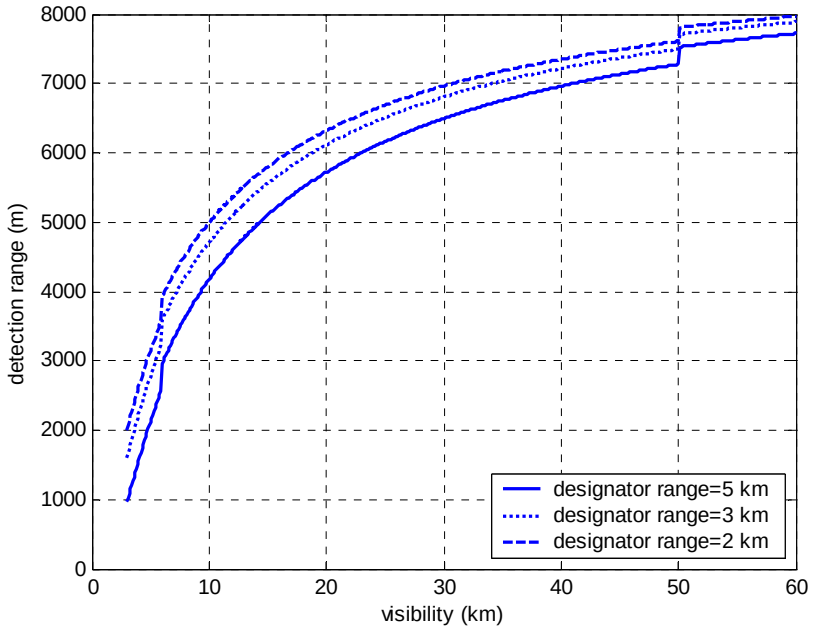

Figure 2-10 Effect of designator location on detection range

The detection range graph for a specific minimum detectable power and target reflectivity of 0.5 is shown in Figure 2-11. In this case the designator to target location is 3 km. For a designator having same output capacity, the power of the laser beam can be doubled by producing 10 nanosecond pulses. This allows the laser beam reflection to be detected several kilometers away.

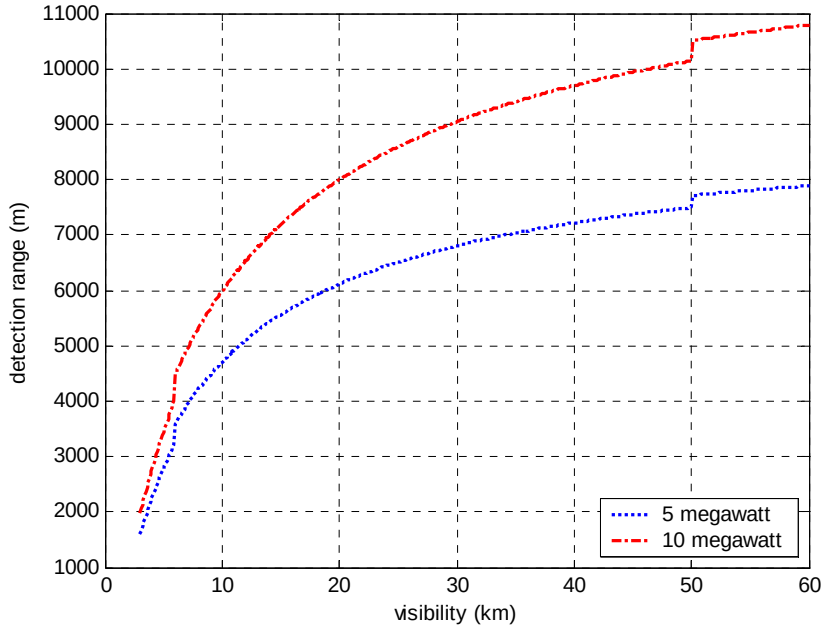

Figure 2-11 Output power difference of short duration pulses

The detection range calculations show that the acquisition range is heavily dependent on several factors such as atmospheric attenuation coefficient, visibility, output power, and target reflectivity. For adverse weather conditions the detection range is heavily degraded.

It is a known and accepted fact that laser guided weapons performances are dependent on weather conditions. In this thesis the simulations are be based on good weather conditions. Fog and heavy adverse weather conditions are not taken into account, since their effects would be the extreme cases of weapon employment.

2.8 DISCUSSION

In this chapter, the laser reflection from a target is modeled basically. Mainly the reflection scheme of the laser is used to determine the envelope at which the seeker of the laser guided weapon will acquire target. This is achieved by the use of minimum detectable power by the laser seeker and the corresponding range at which, power reaches to the seeker at a given designator-target geometry, within specified atmospheric conditions. The minimum power detectable by the weapon seeker determines the range at which the reflected energy can be sensed and guidance command generation starts.

In an attempt to use several available control methods, it is necessary to understand if the laser seeker can give the necessary information that the control strategy requires. The following chapter is dedicated to model the laser seeker, and understand if it can be used in harmony with the candidate control system logics.

CHAPTER III

LASER SEEKER MODEL

3.1 INTRODUCTION

It is essential and critical to model the seeker of a laser guided weapon precisely in order to obtain its realistic model and to design a guidance system which has a good performance and applicable to a real system. In this respect, it is necessary to know the behavior of the laser detector and to understand if it has a truly linear region or not. Depending on the optics design, it may or may not be possible to extract a linear lead angle-voltage relationship even in a small range of lead angle. If the detector has a linear region, its characteristics must be determined for the use in further studies. In order to achieve this goal, all components and working logic of the seeker system must be known. Seeker is the most important part of a weapon since it is the eye and only means of target detection capability of the weapon. All commands are generated relying on the knowledge coming from the seeker. In order to increase performance of a weapon; it is essential to extract an accurate data from the seeker.

In this chapter, a general structure of laser seekers and their working logic is introduced and a brief information about laser detector types is given. Laser sensing techniques and focusing methods will be explained.

Since the detector type used in most second generation laser guided weapons from anti-tank munitions to heavy air to surface weapons are 4-quadrant diode type, the seeker modeling in this study is based on this type of detectors.

As an original contribution, the lead angle-voltage relationship of a 4-quadrant detector is found by performing a series of tests on a special test setup. Details of

these tests along with the results obtained are discussed. The detector is mainly used as a source of experimental data to be used in 6-DOF simulations. By this way, the data obtained is believed to contain several noise and error sources within itself. The data is assumed to be the final form of information to be used by the guidance system.

3.2 GENERAL DESCRIPTION OF LASER SEEKERS

In the well known laser guidance method, the target is illuminated by either a ground or airborne designator and the laser guided weapon is fired. Since the weapon homes on the reflected laser energy from the target, the laser seeker is located at the front end of the weapon. Some laser guided weapons use gimbaled seekers which align themselves rapidly and accurately to the incoming laser reflection by gyros. This kind of seekers can extract an accurate LOS rate data, to be used with proportional navigation, etc. Some laser guided weapons such as the Russian KAB-500L/1500L series utilize probe mounted detectors to employ velocity pursuit guidance. The structure, which is like a hat on the nose of the weapon, aligns itself to the velocity vector by aerodynamic means. The laser detector is mounted on this structure and it directly senses the yaw and pitch lead angles according to the seeker coordinate system. This is a cheap and effective solution to deal with fixed targets.

Laser signals are not continuous; they have a pulse repetition frequency. Hence, laser seekers can obtain information in 10 to 20 Hz frequency range. This is also an important issue which must be taken into account in their modeling.

3.2.1 GENERAL LASER SEEKER LAYOUT

Laser seekers mainly consist of the following parts:

Dome: It is the frontal part of the seeker. Its primary objective is to protect the seeker from external environmental effects. It must also stand to high temperatures when the weapon is subjected to the plume of other weapons that are fired before.

For most optical seekers, the dome is preferred to be hemispherical. The design of the dome is important since any impurity on the surface may cause a wrong information about target. Some domes are coated by screening materials to act as a filter to eliminate unwanted wavelengths.

IR Filter: It is a special filter that is permeable to a small wavelength band mainly at 1064 nm. It prevents unwanted noise signals from sun and other sources from reaching the detector's sensitive area.

The background noise is reduced by a band pass optical filter. The filter is centered at the laser wavelength. The bandwidth is normally set as narrow as possible and allows for tolerances and shifts caused by temperature changes and ageing. [25]

Lenses and mirrors: Lenses and mirrors are used to make the laser spot fall on the detector. Various simple and complicated seeker optic designs exist.

Detector: Various detector types are used in laser guided weapons. Most second generation laser guided weapons use a 4-quadrant silicon diode type detector. In these type detectors, the active region is divided into 4 equal quadrants by several separator bands. The energy falling on the detector's sensitive area creates either a voltage or a current on the detector's surface which is sent to electronic cards for further processing.

Electronic Cards: The laser energy that falls on the detector's active regions produce current or voltage. This signal is sent to the electronic circuitry. For current producing detectors; these currents enter into an electronic card where they are converted to voltage. Some additional operations are also performed at electronic cards depending on the weapon system.

3.2.2 LASER SENSING TECHNIQUES

There are various types of laser sensing techniques such as bang-bang, defocused spot, and fully proportional sensing. [26]

Bang-bang sensing determines only the direction along which the laser pulse energy is sensed. The output is always either a positive or a negative constant with an equal size. This output causes a continuous oscillation around desired value and there is always an error between the exact quantity which is to be measured, and the sensed value.

Defocused spot sensing determines which quadrant the laser pulse is mostly sensed within the seeker FOV (field of view). When the spot falls on the central region, a signal that is proportional to the angular offset can be generated. This kind of sensors are mostly used in gimbaled seekers, where a highly sensitive detector and an accurate gimbal mechanism work to hold the laser spot within a linear region.

Fully proportional sensors produce a signal that is proportional to the angular offset within the total FOV of the seeker. Such kind of sensors are best for systems employing strapdown (body fixed) proportional navigation guidance. It is also possible to obtain a proportional sensor by using cross plates in front of the detector to shadow the incoming laser energy and create a fully proportional signal.

3.2.3 FOCUSING METHODS

There are different focusing methods for the incoming laser energy. With a proper design of seeker optics, the laser energy can be spotted on the detector as a point or a circle. Spotting as a point is achieved by placing the detector on the focal length of lens. Defocusing is achieved by a proper placement of the detector before or after the focal length of lens. In the case of 4-quadrant detectors, a defocused spot sensing provides a linear region which eliminates the LOS error. Increasing the size of the defocused spot may provide an increased size of the linear region but causes some noise problems.

3.2.4 DETECTOR TYPES

If the focal length of the lens and the linear displacement of the image from the optical axis are known, the angle between the optical axis and the target can be calculated. Devices that allow this measurement usually produce an output voltage that corresponds to the position of the image on the detector. [20]

There are various types of photodetectors. Only two of these detector types are mentioned here, which are quadrant photodiodes and silicon position sensors. Silicon position sensors are given as an example to mention other detector types.

A quadrant photodiode is an imaging surface that is physically divided into 4 equal area segments. Each segment has separate cables for signal output. When the detector axis is boresighted with the target, all quadrants receive an equal amount of energy. When there is an angle of incidence, some quadrants experience more energy. If the laser spot is very small, it may fall on the finite width of the separation between quadrants and produce an erroneous information. Another problem is that the position information is saturated when all the incoming energy falls onto one quadrant. These problems are solved either by defocusing the image or by using a long focal length optics design that results in larger image size and displacement. When a position information is obtained from a pulsed laser source, it is necessary to add an electronic circuitry that freezes the peak value of pulses coming from each quadrant.

Silicon position sensors consist of a segment of photo-detective silicon with four terminals for signal output and a terminal for the application of a back-bias voltage. There is no separation into segments as in a quadrant photodiode.

The position information is deduced by comparing the signal outputs from each terminal. The laser spot on the sensitive area causes a current to flow, but because of the construction of the diode, the current flows only by traveling through the silicon to each of the four output terminals. Because the silicon has a given resistance per unit length, more current flows to the closest terminals and less to the terminals that are farthest from the focused image. [20]

Silicon position sensors of this type have several advantages over the quadrant devices. Since there is no gap in the active region, there is no constraint on the minimum diameter of the spot, also linear position information data is available anywhere on the active region. [20]

Since most laser guided weapons use 4-quadrant photodiodes, the analysis here is performed on this type of detectors.

3.2.5 ERROR SIGNAL GENERATION IN 4-QUADRANT DETECTORS

In 4-quadrant photodiodes, an error signal in the form of voltage is generated when the laser spot is not centered on the detector. This signal is a measure of the angle of arrival. Error signals are formed by sum and difference logics and a normalization of the signal intensity. The error signal is proportional to the angle of arrival and also to the intensity of the signals. To make it just proportional to angle of arrival, the error signal is divided by the sum of energy in all four quadrants. The angle of arrival in pitch (yaw) plane can be determined by looking at the difference between up (right) and down (left) halves of the detector.

$$pitcherror = \frac{(upleft + upright) - (downleft + downright)}{upleft + upright + downleft + downright} \tag{3.1}$$

$$yawerror = \frac{(upright + downright) - (upleft + downleft)}{(upleft + upright + downleft + downright)} \tag{3.2}$$

3.3 LASER GUIDED WEAPON SEEKER ANALYSIS

For the analysis of 4-quadrant type seekers, an old, out of inventory, laser guided weapon seeker is obtained, and used for the modeling of seeker section.

Current guidance system of second generation laser guided weapons works as follows.

The target is illuminated by a ground or airborne laser designator. Laser signals are reflected from the target and reach the nose of the seeker; the optical dome. The

laser beam and other waves from different light sources such as sun also enter the seeker. IR filters used at domes eliminate those beams that are not at the 1064 nm wavelength. A special lens which has almost the same diameter with the detector focuses the incoming laser energy onto the detector. A 4-quadrant detector senses the energy and currents are produced at all quadrants of the detector. These currents enter into an electronic card called "preamplifier" where they are converted to voltages. These voltages arrive to a circuit where they are added to obtain up, down right, left half circle voltages. Then each half circle voltage is compared with the others to determine pairs of commands like up-right; up-left; down-right; down-left or just left/right or up/down.

In the light of the above explanations it can be stated that, the system is not designed to measure the lead angle accurately. It just relies on the switching of quadrants and giving commands to orient the weapon in such a way that the weapon oscillates on an apparent line of sight. Only commands are up-down and left-right with full deflection according to the detector axes. The system can not detect the true down direction. Down information produced is with respect to detector axes; it does not show the gravity direction.

Performance of the weapon is degraded due to high energy use because of bang-trail-bang logic. In order to prevent the excessive and unnecessary kinetic energy use and overloaded maneuvers; accurate determination of the target lead angle is crucial in all phases of flight. Decreasing the lead angle may be accomplished with smaller canard deflections in most phases of flight if the seeker has potential in outputting linear angle of arrival information. If the lead angle can be accurately determined; a proper canard deflection to boresight the weapon with LOS direction can be given. This leads to less kinetic energy loss and less system resource allocation.

In order to model the seeker, it is necessary to establish the lead angle – voltage relationship. It is also necessary to investigate if the seeker can produce an information that can be used by control schemes that utilize multiposition or continuous canard deflections. These control schemes require an unsaturated

region of lead angle – voltage function where proportional canard commands can be generated. For this purpose a series of experiments are performed. The results that are obtained from the experiments provide data about the behavior of the seeker and information which is necessary to decide if a seeker modification is necessary or not.

3.3.1 SEEKER TESTS

The purpose of seeker tests is to establish a clear relationship between the lead angle and the voltages generated by the seeker.

The equipments used in tests are,

- laser test equipment,
- laser detector and optics,
- oscilloscope and probes.

A sketch of test setup is seen in Figure 3-1.

There are some important difficulties that are to be handled in order to have a complete and effective analysis.

- The exact positioning of the seeker quadrants (X or +) on the test mount is not known. This must be determined by examining output voltages at certain yaw – pitch positions.
- Laser source could not be aligned exactly to point directly to the center of the detector. This means that there is a boresight angle whose effect must be determined.
- The numbering of quadrants and their locations up/left, etc. are not known. By using test results, an appropriate convention which is to be used throughout the study must be established.

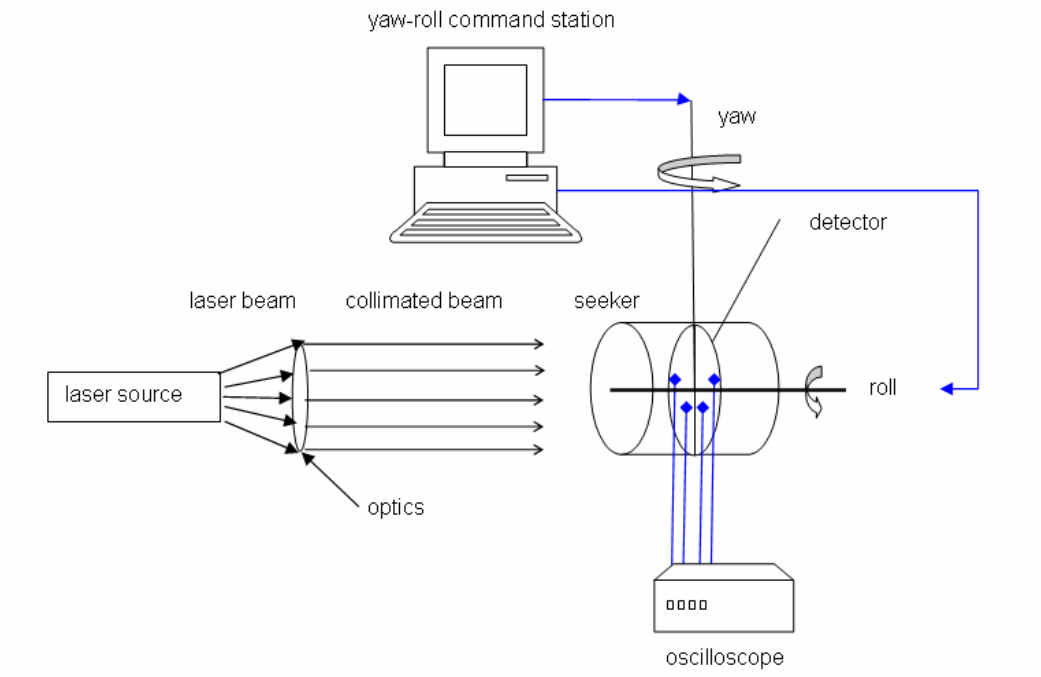

Figure 3-1 Laser test setup sketch

After handling the difficulties above, the data obtained can be used for a lead angle-voltage analysis. All data from the detector had to be taken as near as possible from the detector signal exit to eliminate any electronic processing and other system logics that may intervene the true signal values. The laser level had to be increased in order to discriminate the peak signal from the apparent noise.

In order to obtain the voltage–angle relationship, voltage outputs of the half circles are measured. Half circle channels output the summation of upper (right side) and lower (left side) quadrants. Since voltages that enter the related circuits can not be read in some cases due to low signal voltage levels and high noise experienced at test setup, it is decided to read the voltages after the amplification circuitry. Data for 10 degrees yaw angles between –30º and +30º, and 30 degrees roll increments between 0º and 360º roll angles are recorded. Since these readings give only an idea about general behavior of system; no usable conclusion is obtained by this approach.

Another approach is followed in order to accurately determine the voltage-lead angle relationships which will be used in the modeling phase. Voltages at the quadrants are of prime importance, not the up and down decision commands. So, voltages taken from the detector are recorded in a new test phase with two degrees increments for yaw angle (between –12º and +22º) and 10 degrees for roll angle (between 0º and -360º). Also a sweep test is performed. at zero roll angle with one degree yaw increments between -24º and +24º.

After the data is obtained, relative locations of quadrants are determined, a proper convention is established, and yaw-roll pairs of data are converted to equivalent yaw-pitch lead pairs. Lead angle errors are calculated and tabulated.

3.3.2 DATA ANALYSIS

By using the data obtained from seeker tests, several unknowns are determined, data is processed and all required information about the laser detector has been extracted.

First of all, the unknowns involving the test setup and seeker system are determined, such as relative locations and numbering of the quadrants, and positioning of the detector at the test setup.

After a convention is established, the laser misalignment (boresight) angle is estimated by utilizing various yaw-roll to yaw-pitch conversions, taking a possible non-zero boresight angle into account.

All data obtained are processed to obtain a voltage versus angle of arrival relationship. The general behavior of the data is shown in Figure 3-2. Figure 3-3 shows stacked view of all quadrants in 3D graph. It can be seen that all quadrants behave similarly as the laser beam sweeps on them. A data in this form only provides an information about the behavior difference of quadrants and can not be used directly in the seeker modeling. To obtain a more comprehensive knowledge, this data is further processed to produce the behavior of seeker at the corresponding yaw-pitch lead angles.

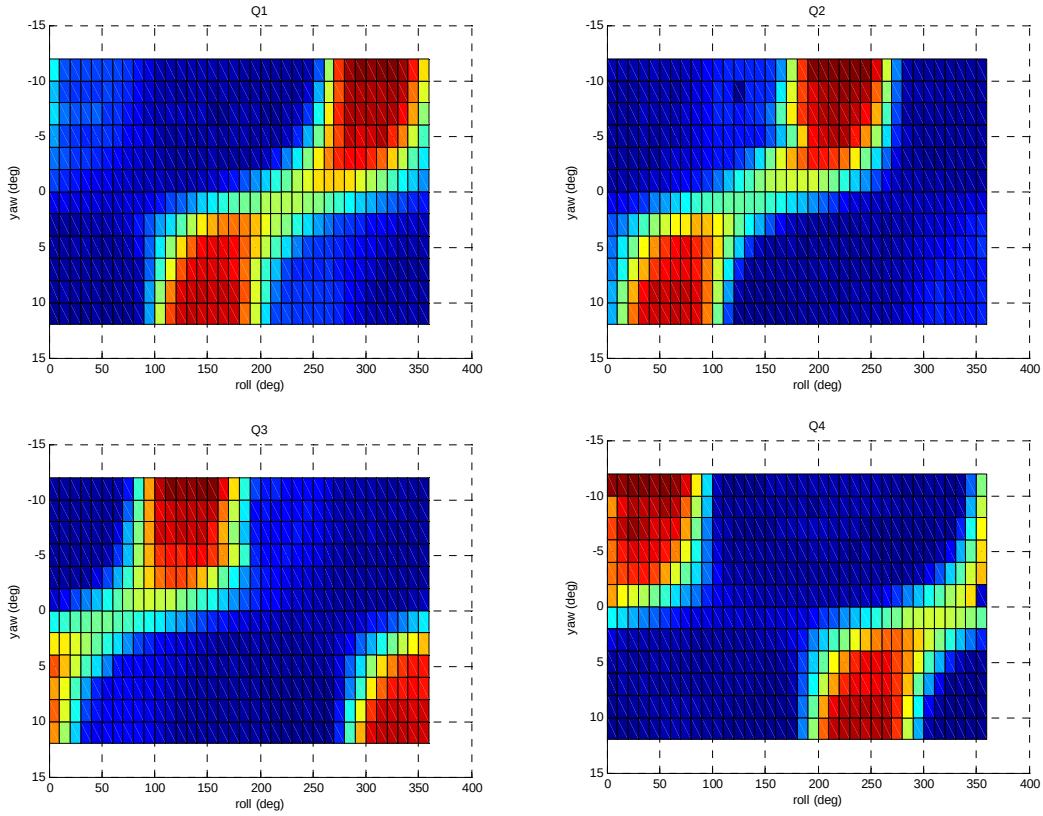

Figure 3-2 Voltage intensity of all quadrants for yaw-roll span.

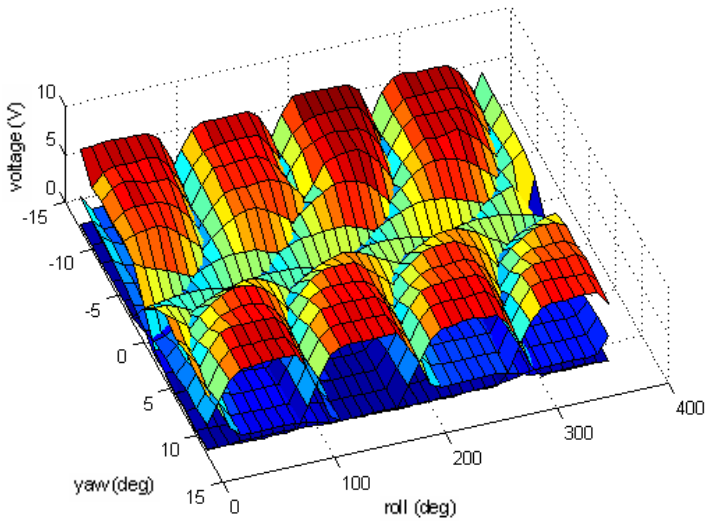

Figure 3-3 3D view of voltage levels in all quadrants.

3.3.2.1 Relative Location of the Quadrants

Since there is no physical evidence about the locations of the data ports, namely the quadrants with respect to the weapon frame, it is necessary to determine the relative locations of the quadrants.

According to the data obtained and knowledge indicating that the angle of arrival is about a specified degrees from up to down, one can understand that the laser spot falls mostly to the lower two quadrants. The lower two quadrants can be named by looking at the data at zero degrees yaw and roll.

During the experiments, it is seen that voltage readings from Q3 and Q4 are higher than the other two quadrants. So Q3 and Q4 can be assumed to be the lower half quadrants. The seeker is rotated CW (clockwise) when looked from the back as seen in Figure 3-4. This means that the voltage of one of the lower half quadrants will increase up to an extent. This quadrant will be the one on the right when looked from the back. Analyzing the data set again, it can be stated that the voltage reading of Q3 increases as the seeker is rotated CW. The voltage reading of the upper right quadrant must be increasing as the seeker is rotated CW (clockwise) in 90 degree range. The upper right quadrant is found as Q2. The reading of the upper left quadrant must be increasing when the seeker is rotated more than 90 degrees (~ 90º-180º range). This sets the upper left quadrant as Q1. The final form of the quadrants are shown in Figure 3-4.

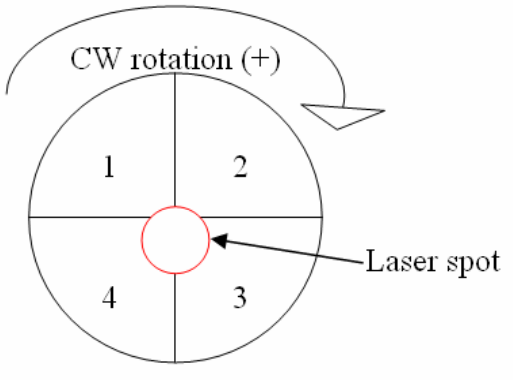

Figure 3-4 General layout of quadrants (Back view)

3.3.2.2 Yaw-Roll to Yaw-Pitch Conversion

The test setup is not suitable to obtain yaw-pitch pairs, directly. It can only turn in yaw direction and roll over this yaw direction. Tests are performed from –12º to +22º yaw and from 0º to 360º roll with 10 degrees increments. It is necessary to process the data in order to obtain yaw-pitch pairs. This can be achieved by the following procedure.

The location of the spot center is considered first. The detector is swept in yaw direction between –12º and +22º with 2 degrees increments. This action causes the spot to move on the x-axis of the detector from left to right (looking from back) at each yaw angle. The detector is rotated in CW direction for roll angles. This movement causes an effective spot motion on the detector as if the detector is stationary but the spot is moving on a circle starting from corresponding yaw place on x-axis of the detector and continuing on a circle in CCW direction (viewing from the back).

A transformation from yaw-roll pairs to yaw-pitch pairs is done as shown in Figure 3-5. A given (+) yaw angle causes the spot center to have a position on the right side of the detector. This displacement is called r. After this displacement, the rotation of the test set in CW direction causes the spot to move in a circle having a radius of r and angle Θ. The angle Θ is the test set roll angle measured from detector x-axis in CCW direction.

For any yaw-roll pair, the actual yaw and pitch displacements can be found by resolving the components of r into x and y axes.

So, r.cosΘ is defined as the equivalent yaw displacement and r.sinΘ as the equivalent pitch displacement.

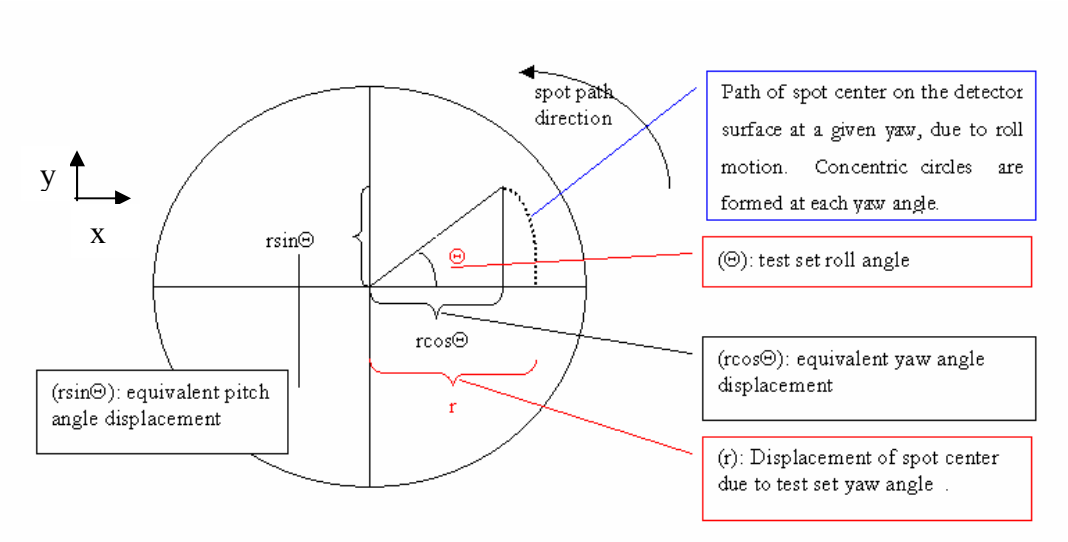

Figure 3-5 Spot motion on detector

It is necessary to convert the test set yaw angle to a displacement, r and then after finding the equivalent yaw r.cosΘ and pitch r.sinΘ displacements, it is necessary to re-convert these displacements to real angle of arrivals.

In order to have a mapping, the knowledge about the distance between the lens and the detector is used.

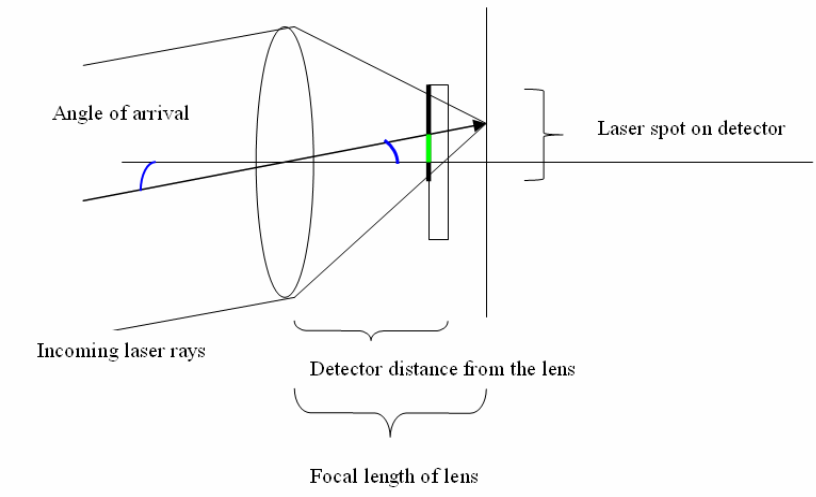

Figure 3-6 Basic seeker geometry

The displacement of laser spot center due to an arrival angle (lead angle, α in this case) can be found by

$$r = K.\tan(\alpha) \tag{3.3}$$

where, K is the distance between the detector's active surface and the lens.

Since the reflection distance from the target is long and the seeker's cross section is much smaller than laser reflection hemisphere, incoming rays are assumed to be collimated, thus parallel to each other. In the test setup, the laser source is converted to a collimated light source by the use of a proper optics in order to simulate real life situation.

By the formula given in Equation (3.3), it is possible to convert test device yaw angles to spot center displacement and then reconvert the equivalent yaw-pitch displacements to real lead angles.

Since the laser energy, therefore voltage values read from quadrants increase very much as the target is approached, it is necessary to work with normalized values of these voltages.

Real yaw and pitch lead angles are calculated and tabulated for each possible boresight angle along with the corresponding quadrant voltage values in Matlab. These quadrant voltages are used to calculate yaw and pitch lead angle error signals by using Equation (3.1) and (3.2).

3.3.2.3 Test Results

The seeker is given arrival angles in yaw plane between –12º and +22º, and at each yaw angle, roll rotations with 10 degree increments are done. The detector outputs are taken by oscilloscope probes at each location and recorded. Results can be seen in Figures 3-7 through 3-9. Figure 3-7 shows the three dimensional yaw lead angle - voltage relationship graph as function of yaw and pitch angles. Figure 3-8 and Figure 3-9 are two dimensional cross section views of yaw and pitch lead errors respectively.

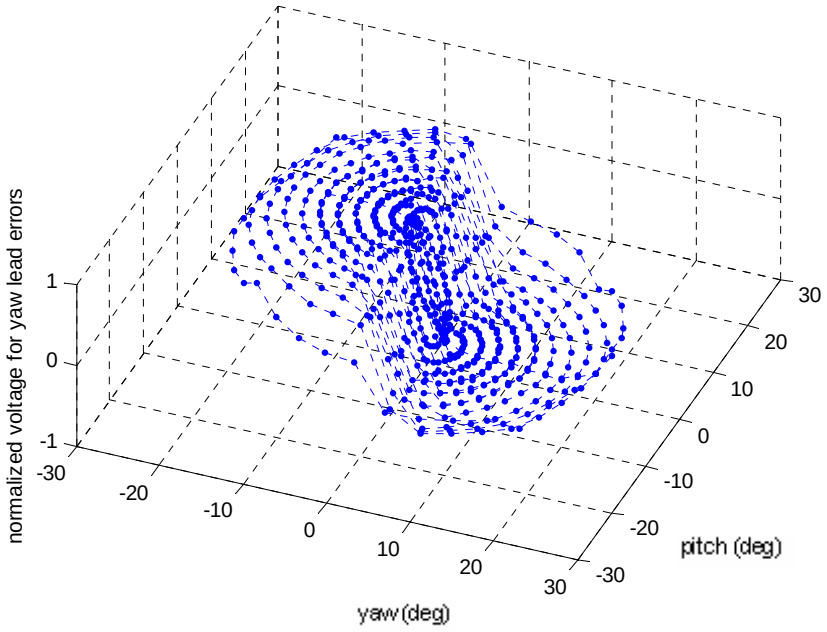

Figure 3-7 Yaw lead angle error in 3D view

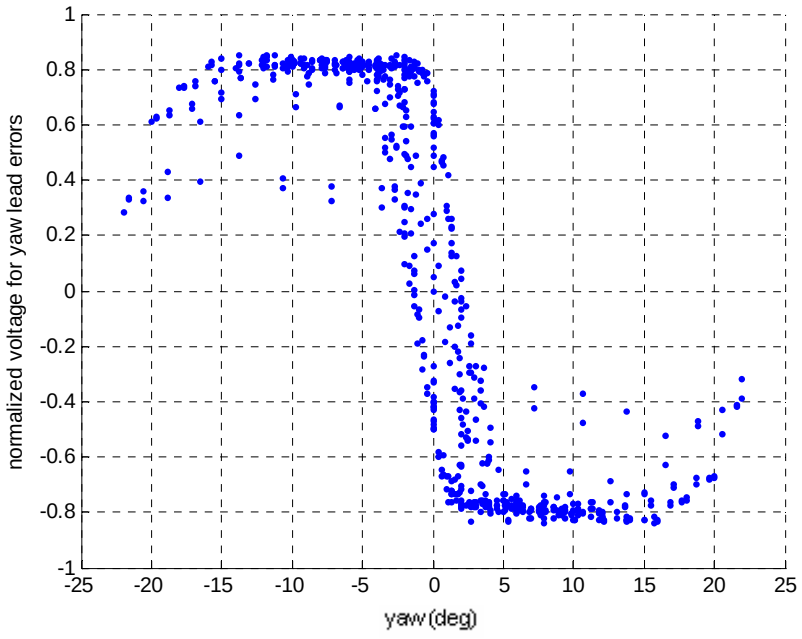

Figure 3-8 Normalized yaw lead angle error.

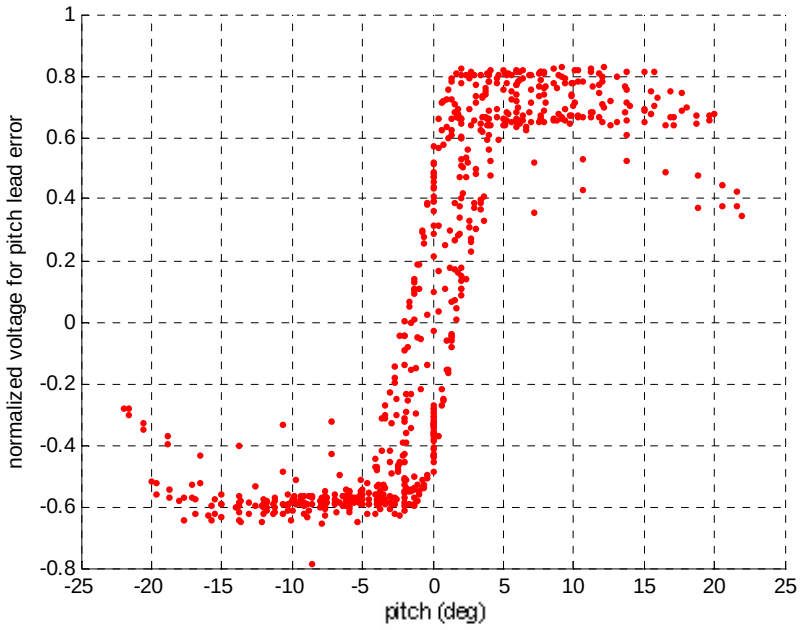

Figure 3-9 Normalized pitch lead angle error

The results show that, the detector has a linear region between ±3 degrees yaw lead angle and is saturated above ±3 degrees. It can be seen that there is a high uncertainty and a wide region of possible error (±2 degrees) in angle of arrival. Similar properties are observed for both yaw and pitch lead angle behaviors. Linear regions are nearly same for yaw and pitch error signals.

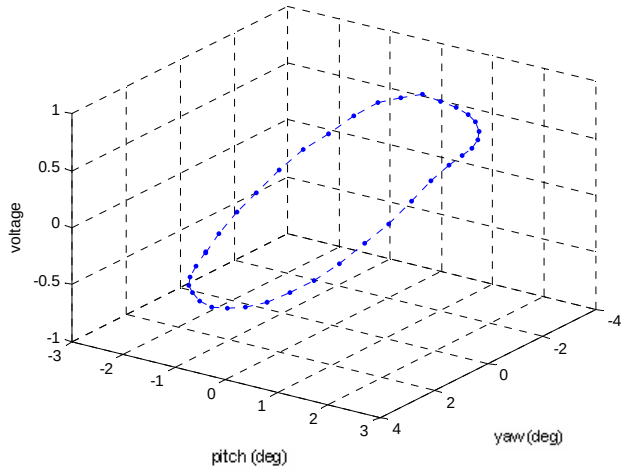

Figure 3-10 Pitch lead angle error at one turn of seeker

Pitch and yaw error signals must coincide under ideal conditions. However, a voltage difference is experienced while rolling at the same yaw angle as seen in Figure 3-10. This voltage difference leads to an uncertainty region. The ±2 degrees uncertainty region is created by different readings of quadrants passing from the same angle of arrival. This is a cue of asymmetry in the impact point of the laser spot. Another important aspect is that, when the detector is positioned at directly 90 degrees vertical to the laser beam, the amount of laser falling on quadrants must be same and only a small error signal must be produced. This signal must not be heavily affected by the roll motion since the spot will remain at the center of the detector. However, results show that the error signal shows a change with the roll angle even at zero degree yaw. The reason for this behavior may be the laser's misalignment problem. The laser may not be properly boresighted with the detector's normal direction. This finite spot displacement causes an induced yaw and/or pitch lead angle. So another approach in lead angle-voltage relationship determination is followed.

In this approach, a non-zero boresight error is also taken into account. It is suspected that at the test setup, the laser source is illuminating the detector with an incidence angle of specified degrees. This means that the spot is at the lower half of the detector.

The effect of boresight error is implemented in data conversions. The original location of the spot causes a down displacement. Any yaw angle turn performed by the test set adds an additional yaw displacement to the spot, effectively forming a new r. which can be defined as,

$$r_{effective} = \sqrt{(r_{boresight}{}^2 + r_{yaw}{}^2)} \tag{3.4}$$

The boresight error not only contributes to r but also creates an induced roll angle, whose magnitude is calculated as,

$$|\theta| = a\tan\frac{r_{boresight}}{r_{yaw}} \tag{3.5}$$

This angle starts the rolling motion at another location other than x-axis. The CCW rotation of the detector starts from (-Θ) angular position as seen in Figure 3-11. this shifts all data points on the detector surface in CW direction as depicted in Figure 3-12.

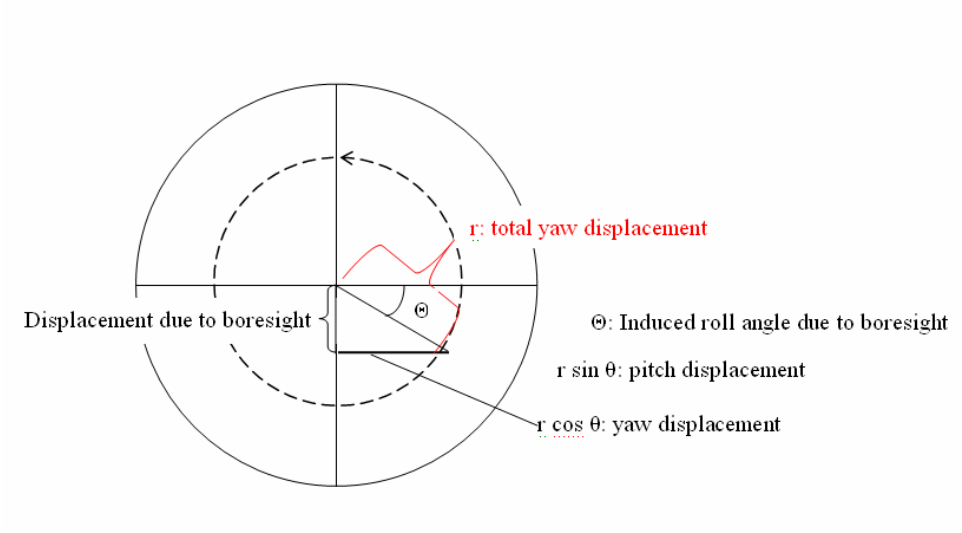

Figure 3-11 Laser misalignment effect on spot motion

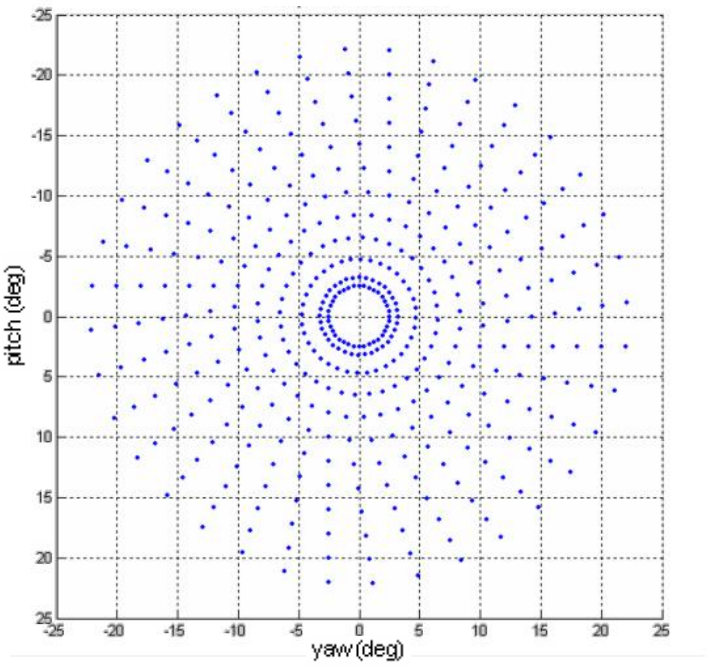

Figure 3-12 Data points on detector surface

This correction makes the size of the uncertainty region smaller at the linear range without disturbing its behavior as seen in Figure 3-13 and Figure 3-14.

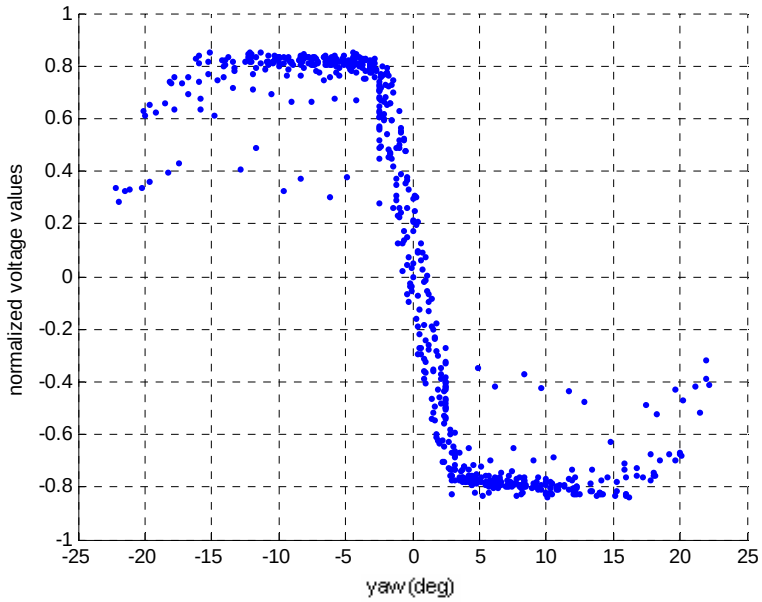

Figure 3-13 Normalized yaw lead angle error after initial boresight correction (2.5 degrees)

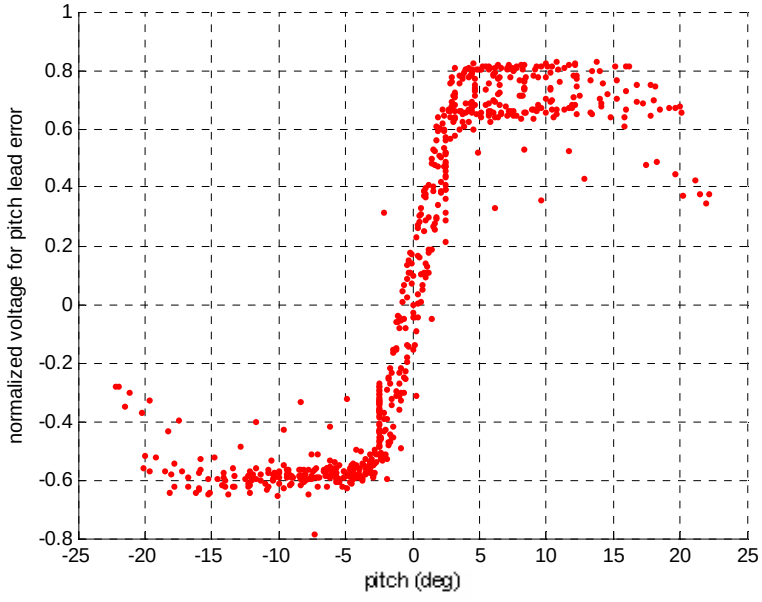

Figure 3-14 Normalized pitch lead angle error after initial boresight correction (2.5 degrees)

The linear range can still be considered as ±3 degrees. With the initial boresight angle correction, there is still an uncertainty region with a decreased magnitude around ±1 degree.

Various boresight corrections are employed to analyze their effects on the uncertainty region. At the first analysis, only pitch boresight corrections are changed between 1 degree and 4 degrees with 0.1 degree increments. It is seen that increasing boresight correction value above 2.5 degrees expands the uncertainty region to almost ±3 degrees which is the limit of linear region, and collapses data integrity. A sample comparison between 2.5 and 4 degrees is seen in Figure 3-15.

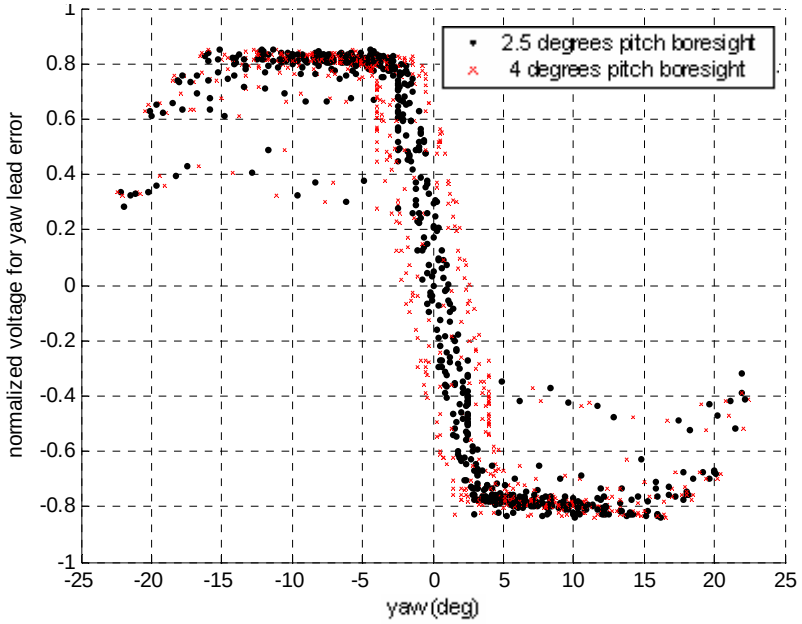

Figure 3-15 Effect of increasing pitch boresight angle

The uncertainty region decreases as the boresight correction is reduced from 2.5 degrees to 1.75-1.8 degrees range as seen in Figure 3-16. The uncertainty bound becomes ±0.5 degrees, and the behavior of seeker resembles the ideal case. A further decrease in boresight angle from 1.7 degrees causes the uncertainty region to expand again. The uncertainty region again reaches near 3 degrees when the correction takes a value of 1 degree (Figure 3-17).

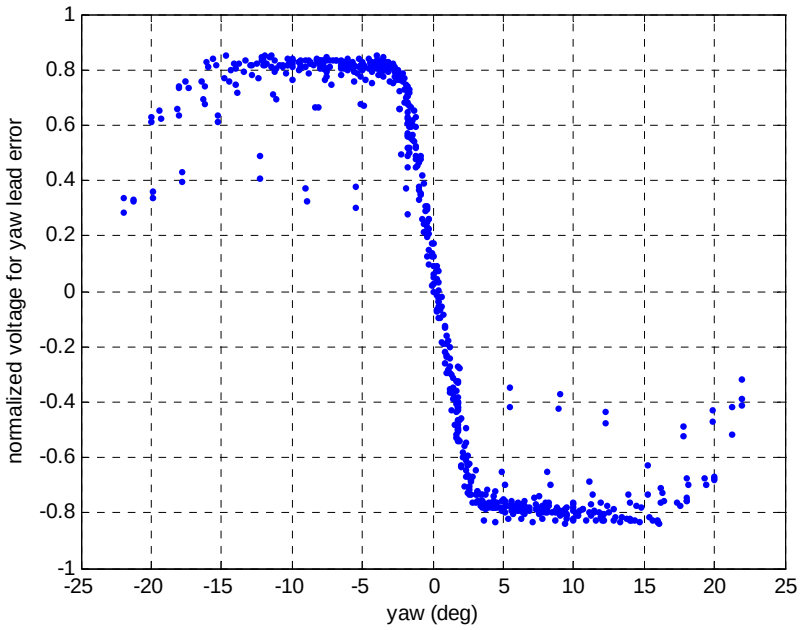

Figure 3-16 Effect of 1.8 degrees pitch boresight correction

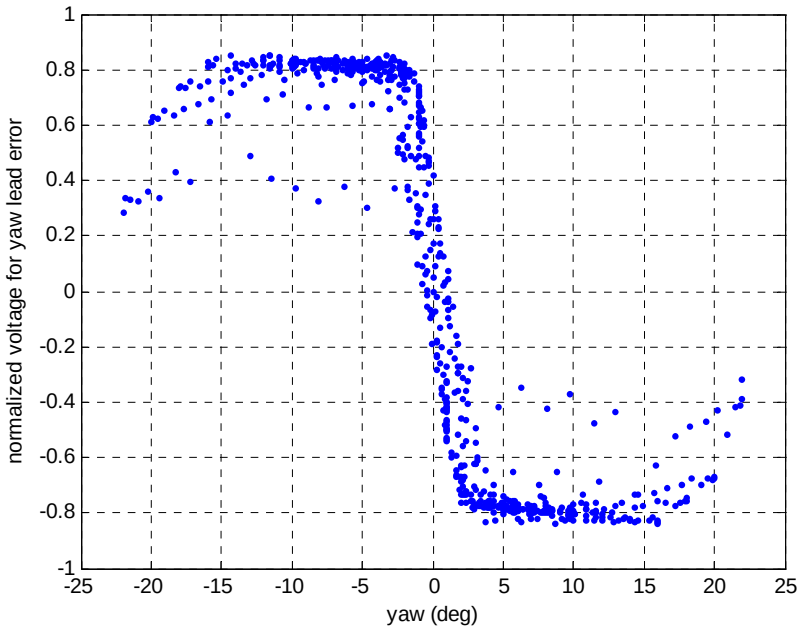

Figure 3-17 1.0 degrees pitch boresight correction increases uncertainty

Negative values of pitch boresight cause a huge uncertainty region and there is no possibility of negative boresight angle even with the existence of yaw error (Figure 3-18).

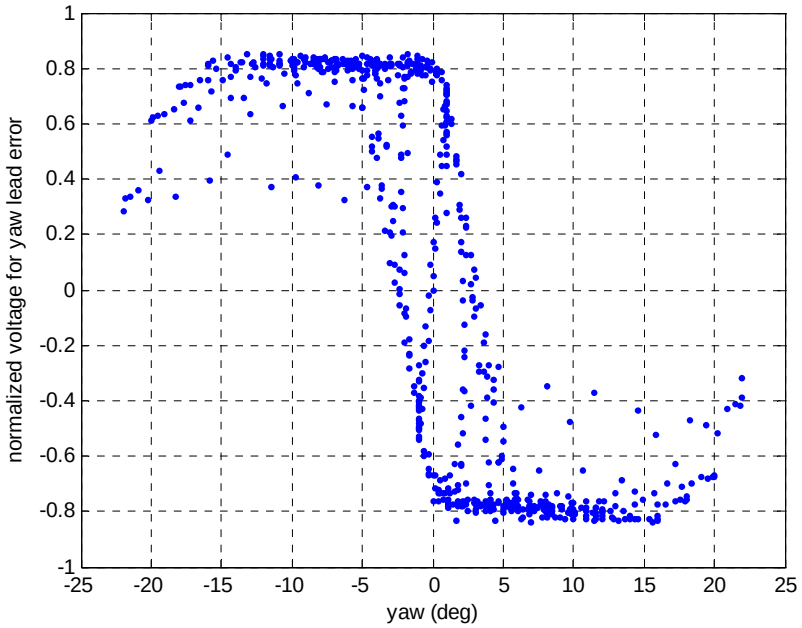

Figure 3-18 Sample for negative boresight correction case (-1 degrees correction)

An analysis of yaw boresight angle effect is also performed. Increasing positive yaw boresight angle increases uncertainty region for both 1.8 and 2.5 degrees pitch boresight values. Increasing negative yaw boresight angle also expands uncertainty region. Introducing yaw boresight has no apparent useful effect in obtaining better data. A sample dataset is shown in Figure 3-19.

As a result the graphical interpretations show that introducing a pitch boresight angle between 1.7 and 1.8 degrees provides a smaller uncertainty region, better organized data as shown in Figure 3-20.

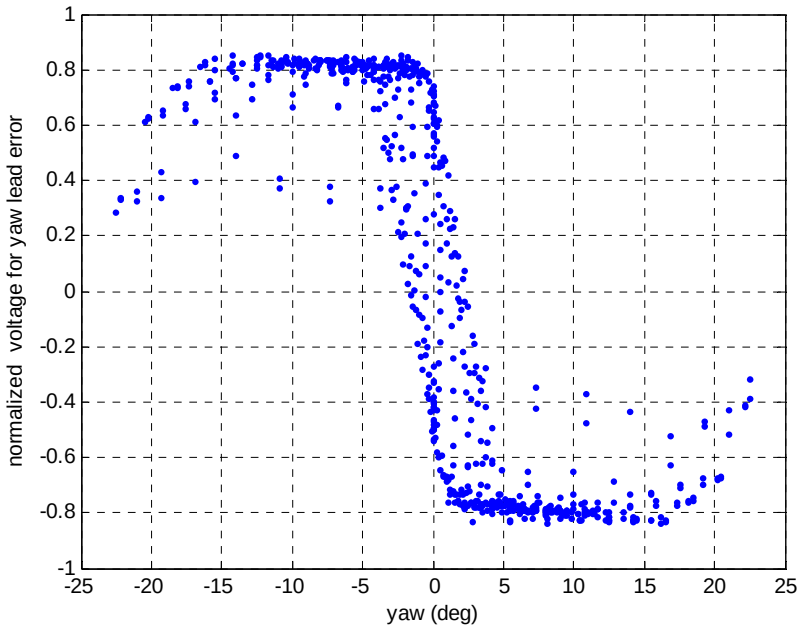

Figure 3-19 Effect of 0.5 degrees yaw boresight correction

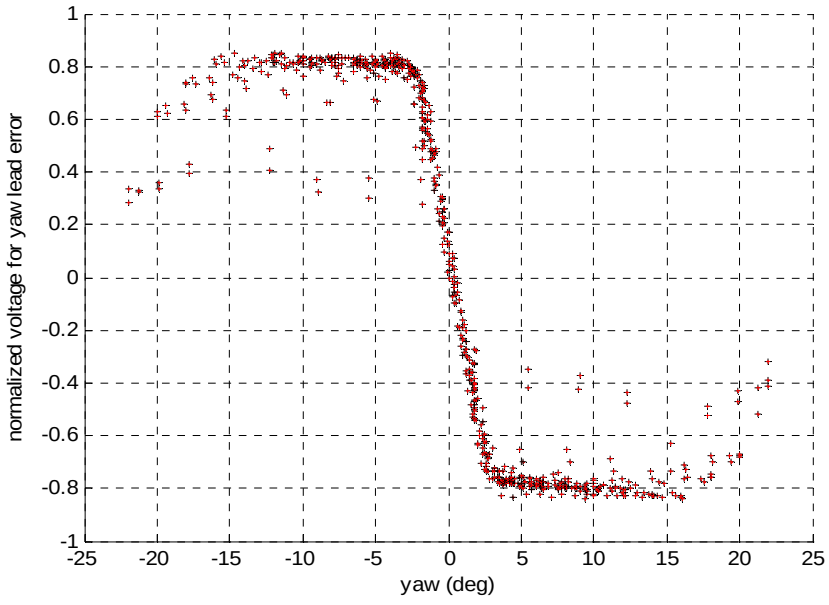

Figure 3-20 1.7 and 1.8 degrees pitch boresight corrections, limit of graphical interpretation

3.3.2.4 Boresight Determination with Curve Fitting Tool

By graphical interpretation, it is determined that the exact angle of arrival is between 1.6 and 1.8 degrees in the pitch plane with a negligible yaw boresight. In order to obtain more accurate data, curve fitting capabilities of Matlab [27] are utilized to obtain the exact boresight angle. Each linear region dataset is fitted with a line, and goodness of fit measures are used to find the exact boresight angle.

The goodness of the dataset, therefore the exact boresight angle of the test setup can be determined by a data analysis in the linear region since the saturated region is useless in the angle determination process.

By using Matlab's curve fitting toolbox and the curve fit tool, data sets for each boresight angle are analyzed. Each dataset are fitted with a straight line and measures of goodness parameters are monitored.

The goodness of fit can be measured in both graphical and numerical quantities. For example, residuals and their behavior around the zero can be used as a graphical measure of goodness. Also numerical measures of goodness can also be employed. Since it becomes harder to discriminate the graphical aspects, numerical goodness of fit measures are employed to determine the exact boresight angle combination at the suspected region.

The analysis is made at the region where the exact boresight angle lies. From graphical interpretations it was known that the exact boresight angle could be between 1.7 and 1.82 degrees pitch boresight.

For all suspected values, the dataset is re-calculated according to 1.7 to 1.82 degrees boresight angles with 0.1 degrees increments. The best dataset is the one that has the minimum uncertainty region in "voltage" since the lead angle is the input at the 6-DOF simulation and the test setup.

Both residuals and goodness of fit statistics are monitored to obtain the best compact dataset. Same samples from fit results are given in Figures 3-21 to 3-24. Figure 3-21 displays the goodness of fit measures for datasets between 1.7 and

1.81 degrees boresight cases. Figure 3-22 depicts graphical interpretation between 1.7 and 1.8 degrees boresight angles. Figure 3-24 shows how the data integrity is collapsed and uncertainty region expands beyond 1.7 degrees.

Table of Fits

Name	Data set	Type	SSE	R-square	Adj R-sq	RMS
.7 degrees line fit	boresight=1.7 degrees	Polynomial	1.60445	0.97162	0.9715	0.08482
.72 degrees line fit	boresight=1.72 degrees	Polynomial	1.53861	0.97279	0.97267	0.08306
.73 degrees line fit	boresight=1.73 degrees	Polynomial	1.50953	0.9733	0.97318	0.08228
.74 degrees line fit	boresight=1.74 degrees	Polynomial	1.47629	0.97325	0.97313	0.08173
.75 degrees line fit	boresight=1.75 degrees	Polynomial	1.4519	0.9737	0.97358	0.08105
.76 degrees line fit	boresight=1.76 degrees	Polynomial	1.43001	0.97409	0.97398	0.08044
.77 degrees line fit	boresight=1.77 degrees	Polynomial	1.41058	0.97444	0.97433	0.07989
.78 degrees line fit	boresight=1.78 degrees	Polynomial	1.3936	0.97475	0.97464	0.07941
.79 degrees line fit	boresight=1.79 degrees	Polynomial	1.37904	0.97502	0.9749	0.07899
.8 degrees line fit	boresight=1.8 degrees	Polynomial	1.36688	0.97524	0.97512	0.07864
.81 degrees line fit	boresight=1.81 degrees	Polynomial	1.42261	0.97468	0.97457	0.07987

Figure 3-21 Sample view from Matlab Curve Fit tool

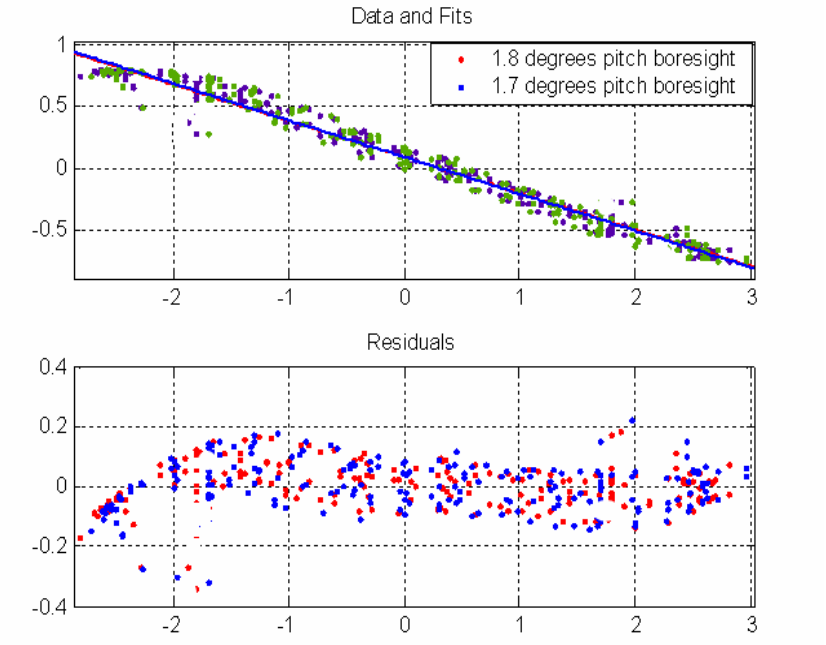

Figure 3-22 Linear fit for 1.7 and 1.8 degrees boresight angle datasets (Data-fits and residuals displayed)

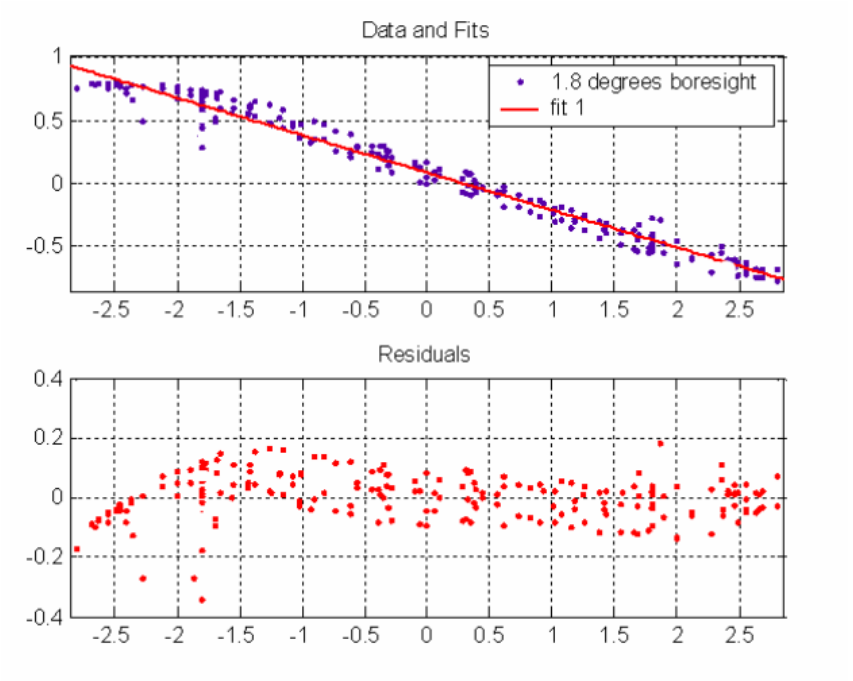

Figure 3-23 Linear fit for 1.8 degrees boresight angle dataset. (Data-fits and residuals displayed)

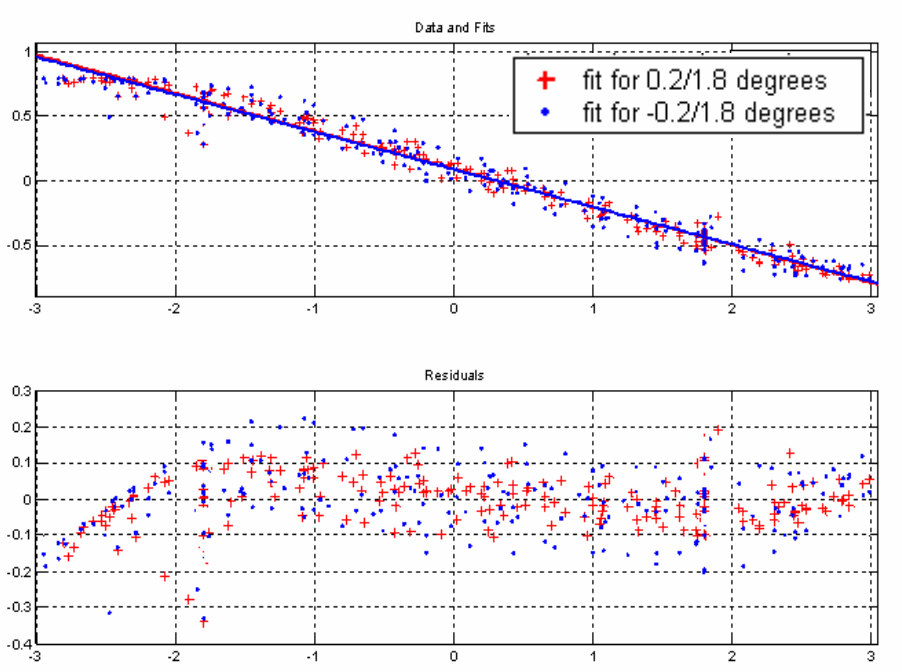

Figure 3-24 Difference between 1.6 and 1.7 degrees boresight angles.

Analysis results show that the best compact dataset occurs at 1.8 degrees pitch boresight angle having the largest R-square value as seen in Figure 3-21 and 3-23.

R-square value measures how successful the fit is, in explaining the variation of the data. In another way, R-square is the square of the correlation between the response values and the predicted response values. It is also called the square of the multiple correlation coefficient and the coefficient of multiple determination. R-square is defined as the ratio of the sum of squares of the regression (SSR) and the total sum of squares (SST). SST is also called the sum of squares about the mean. R-square is expressed as [27]

$$Rsquare = \frac{SSR}{SST} = 1 - \frac{SSE}{SST} = \frac{\sum_{i=1}^{n} w_i (\hat{y}_i - \overline{y})^2}{\sum_{i=1}^{n} w_i (y_i - \overline{y})^2} \tag{3.6}$$

where w_i is the weight of each data point, $\hat{y}_i$ is the predicted value of y. R-square can take on any value between 0 and 1, with a value closer to 1 indicating a better fit. It was estimated that the test setup also has a small misalignment at yaw plane but the graphical inspection is not enough to determine the exact yaw boresight angle.

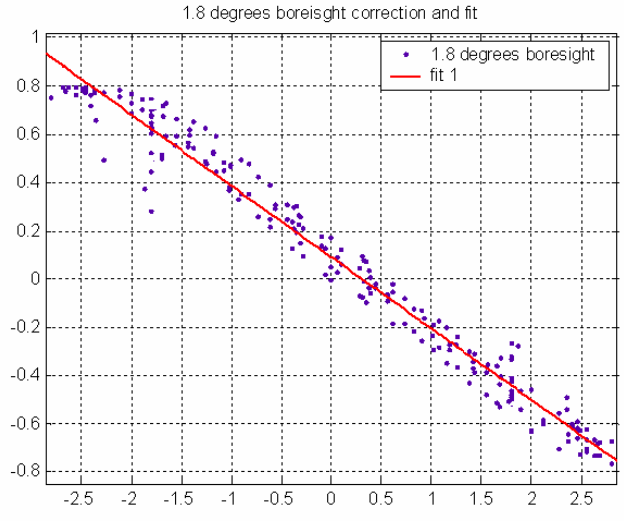

Figure 3-25. 1.8 degrees boresight angle misalignment

A similar analysis is performed to determine the yaw boresight angle when the pitch boresight angle is at 1.8 degrees. It is understood that yaw boresight angles are not positively effective in decreasing the uncertainty region as seen in Figure 3-26 and Figure 3-27. So, yaw boresight angle is neglected.

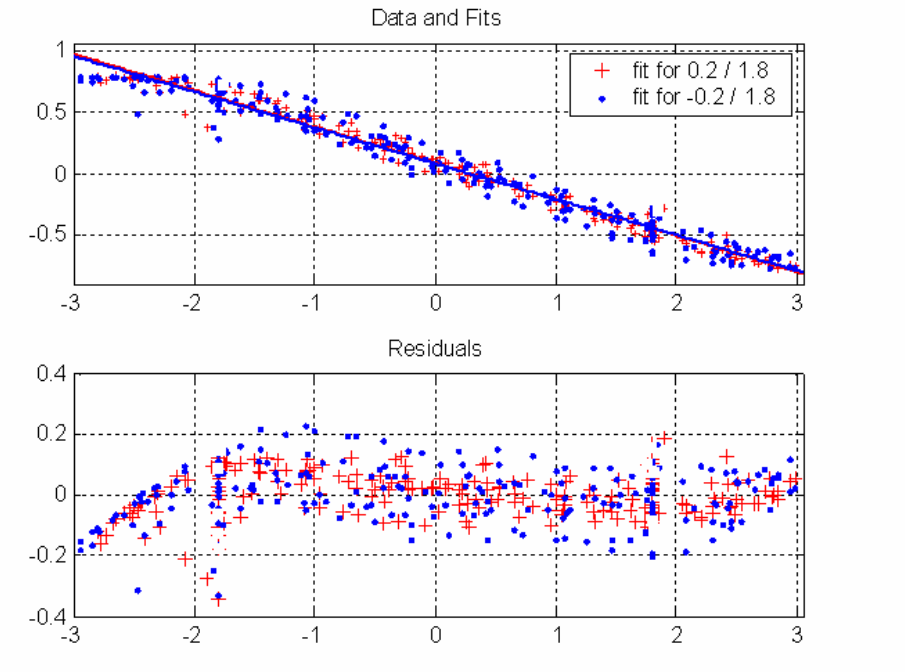

Figure 3-26 Comparison for +0.2 and -0.2 degrees yaw boresight angles at 1.8 degrees pitch boresight

Table of Fits

Name	Data set	Type	SSE	R-square	Adj R-sq	RMSE
1.8 degrees boresight	1.8 degrees boresight	Polynomial	1.36688	0.97524	0.97512	0.07864
1.8-0.1 fit	1.8 ve 0.1	Polynomial	1.23368	0.97765	0.97755	0.07471
1.8-0.2 fit	1.8-0.2	Polynomial	1.22749	0.97827	0.97818	0.07419
1.8-0.3 fit	1.8-0.3	Polynomial	1.33371	0.97639	0.97629	0.07734

Figure 3-27 Yaw boresight analysis at 1.8 degrees boresight.

3.3.2.5 Error Sources

After the analysis of these new datasets, it is seen that the uncertainty region is reduced to ±0.5 degree but could not be eliminated completely. There may be several reasons effective in data uncertainty.

- The exact value of laser misalignment (boresight) angle is not known.
- Voltage output from the detector has to be recorded manually due to test setup limitations.
- Heating of the test setup may change the sensitivity of the detector and increase detector noise.
- Several noise effects such as external light sources and/or electromagnetic interference might exist.

Due to limitations of the test setup, the test data are to be taken in long time periods, each dataset taking almost 6 hours, and tests are performed at different days These working conditions result in some noisy readings due to thermal effects on the detector and the test setup. However, this situation also simulated a worst case for the seeker system. Actual noise level on the seeker is expected to be much smaller in a limited flight time of the weapon.

3.4 CONCLUSIONS

The results obtained through the detector tests can be summarized as follows:

It is understood that the laser seeker design has a finite linear region where a linear lead angle-voltage relationship may be established. This result is very useful since the possibility of using multiposition or continuous canard deflection schemes with the existing seeker is verified. If the seeker had no linear region, it would have been impossible to extract linear angle relationship from the seeker, and no other canard deflection logic could have been implemented without the modification or change in the seeker section. This result leads to the way that additional

improvement methodologies may be based on the existing seeker section, without any modifications.

Another important aspect of the tests is that, the tests provide the behavior of the seeker at several angle of arrivals. The results show that, the seeker has ±3 degrees linear region where proportional canard deflection commands can be generated. The linear region will be the base of all newly proposed control methods, and will be the most important information source for the means which act in order to preserve energy.

The linear region uncertainty bounds that are ±2 degrees in the first conversions, can be decreased to ±0.5 degrees by the use of boresight angle corrections.

The final form of seeker consists of a low uncertainty region with ±3 degrees linear mapping and a saturated region beyond ±3 degrees. It will be necessary to shrink the weapon flight path in the linear region by full canard deflections and then small lead angle errors must be corrected by the use of proportional commands. This approach will reduce the drag and oscillations that the system is subjected to, and will be helpful in increasing the range and impact speed.

Thanks to the seeker tests, a lead angle–voltage relationship is obtained, noise levels are determined, and a seeker model has been constructed. After the implementation of other simulation components such as flight dynamics, the whole simulation model will be obtained.

CHAPTER IV

FLIGHT MECHANICS

In this chapter, equations of motion for the simulation of a laser guided weapon system are derived and presented with their important aspects. Aerodynamic coefficients are found by Missile Datcom software.

4.1 REFERENCE FRAMES

All calculations and simulations involving navigation and guidance require some well defined appropriate coordinate frames. There are a number of Cartesian co-ordinate reference frames which are used widely in aerospace applications. Each of them is an orthogonal right handed co-ordinate frame or axis set. Several widely used frames are as follows: [28]

The inertial frame: (i-frame) has its origin at the center of the Earth and axes which are non-rotating with respect to some fixed stars, defined by the axes x_i, y_i, z_i with z_i coincident with the Earth's polar axis (which is assumed to be invariant in direction)(Figure 4-1).

The Earth frame: (e-frame) has its origin at the center of the Earth and axes which are fixed with respect to the Earth, defined by the x_e, y_e, z_e with z_e along the Earth's polar axis. The axis x_e lies along the intersection of the plane of the Greenwich meridian with the Earth's equatorial plane. The Earth frame rotates, with respect to the inertial frame at a rate Ω about the axis z_i (Figure 4-1).

The Navigation frame: (n-frame) is a local geographical frame which has its origin at the location of the navigation system, and axes aligned with the directions of north (N), east (E) and the local vertical (D) (Figure 4-1). The x-axis (therefore y-axis) can also be defined with a known deviation from the north direction (wander-azimuth frame).

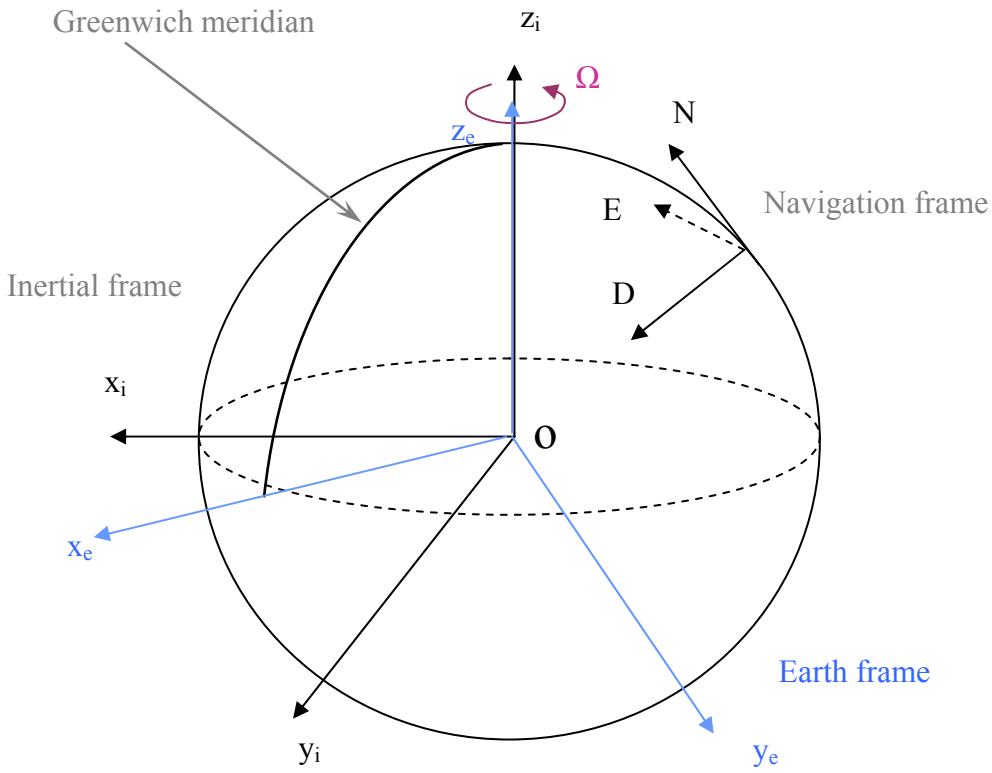

Figure 4-1 Reference frames

The body frame: (b-frame) is an orthogonal axis set which is aligned with the roll, pitch and yaw axes of a moving rigid body. The center of the axis system is, by definition, located at the center of mass (CM) of the body. The frame is fixed to the moving body and rotates with it. The axes definitions are as follows

- x-axis positive from stern to nose when looked from top of the moving object.

- y-axis from left to right when looked from the top and positive in the direction of right wing.
- z-axis downward positive when seen from starboard or port.

For short range tactical missiles, it is possible to make flat Earth assumption and use NED (north-east-down) frame (or any wander-azimuth frame) as stationary (excluding coriolis, Earth rate effects, etc.)

The wind frame (w-frame) is an axis set attached to body center of mass, whose x axis points through the total velocity vector of the body.

In this thesis, an Earth fixed reference frame is used and treated as an inertial reference where Newton's laws of motion are valid. The rotational velocity of the Earth is neglected.

4.2 EQUATIONS OF MOTION IN A MOVING / ROTATING AXIS SYSTEM

In general, vector quantities may be measured with respect to a frame and can be expressed in another frame. Most quantities such as velocity of missile have to be expressed in various frames other than an inertial one. It is one of the fundamental concepts to know what "with respect to" and "expressed in" mean especially in dealing with rotating frames. For example, "velocity with respect to the inertial frame expressed in the body frame" means that the magnitude of the vector has been measured with respect to an inertial frame and resolved into the components of a body frame. At any instant, a missile has a velocity vector with respect to the inertial space. This vector is resolved into the instantaneous missile axes to obtain the velocity components as u, v, and w. This resolution also applies to the angular velocity. The instantaneous angular velocity vector, with respect to inertial space, can be resolved into the instantaneous body axes to obtain p, q, and r which are the components of total angular velocity of the missile with respect to the inertial space, where Newton's laws apply.

4.2.1 EULER ANGLES

A transformation from one coordinate frame to another sharing a common origin can be carried out as three successive rotations about different axes. For example, a transformation from a reference frame to a new coordinate frame (say body axes) may be expressed as follows.

- Rotation about the reference z-axis by an amount φ
- Rotation about the new y-axis by an amount θ
- Rotation about the new x-axis by an amount ϕ

where φ, θ, and ϕ are called Euler angles.

In transforming the location information of a point between the new body fixed coordinate system and the fixed reference frame, each of these three rotations can be expressed as 3 separate direction (transformation) matrices as

$$C_1 = \begin{bmatrix} \cos\varphi & \sin\varphi & 0 \\ -\sin\varphi & \cos\varphi & 0 \\ 0 & 0 & 1 \end{bmatrix} \tag{4.1}$$

$$C_2 = \begin{bmatrix} \cos\theta & 0 & -\sin\theta \\ 0 & 1 & 0 \\ \sin\theta & 0 & \cos\theta \end{bmatrix} \tag{4.2}$$

$$C_3 = \begin{bmatrix} 1 & 0 & 0 \\ 0 & \cos\phi & \cos\phi \\ 0 & -\sin\phi & \cos\phi \end{bmatrix} \tag{4.3}$$

The expression representing the total rotation from one frame to another can be obtained by various φ, θ, and ϕ sequences. One of them is the 3-2-1 rotation sequence. The transformation from the reference frame to the body frame for 3-2-1 sequence can be expressed as the product of three separate transformations like

$$C_n^b = C_3 C_2 C_1 \tag{4.4}$$

$$C_b^n = C_1^T C_2^T C_3^T \tag{4.5}$$

or when expressions for C_1, C_2, and C_3 are used

$$C_b^n = \begin{bmatrix} \cos\theta\cos\psi & \sin\phi\sin\theta\cos\psi - \cos\phi\sin\psi & \cos\phi\sin\theta\cos\psi + \sin\phi\sin\psi \\ \cos\theta\sin\psi & \sin\phi\sin\theta\sin\psi + \cos\phi\cos\psi & \cos\phi\sin\theta\sin\psi - \sin\phi\cos\psi \\ -\sin\theta & \sin\phi\cos\theta & \cos\phi\cos\theta \end{bmatrix} \tag{4.6}$$

Since the matrix C_n^b is formed by multiplication of orthogonal matrices, it is itself orthogonal too and therefore its inverse is equal to its transpose. The normality characteristics of this matrix assure that the absolute magnitude of any vector remains unchanged by the operation of this transformation matrix. The C_b^n matrix transforms any vector expressed in body frame to components in reference frame.

4.2.2 EQUATIONS OF MOTION

The equations of motion for any vehicle can be derived from the Newton's second law which states that the summation of all external forces acting on a body must be equal to time rate of change of its momentum. Also, the summation of all external moments acting on a rigid body in motion must be equal to time rate of change of its angular momentum. That is,

$$\sum \vec{F} = \frac{d\vec{p}}{dt} \tag{4.7}$$

$$\sum \vec{M} = \frac{d\vec{H}}{dt} \tag{4.8}$$

where time rates of change should all be taken with respect to an inertial space, $\vec{p}$ and $\vec{H}$ denote respective linear and angular momenta of the rigid body in motion, $\sum \vec{F}$ and $\sum \vec{M}$ are respective summations of external forces and moments acting on the rigid body, as a result of effects like lift, drag, thrust, and gravity. The motion of the aircraft with respect to the navigation frame can be found by using

these force and moment equations. For short range missiles, the Earth rate can be neglected, and therefore this frame can be treated as an inertial frame.

4.2.2.1 Translational Dynamics

Since the linear momentum of a rigid body with fixed mass m is given as

$$\vec{p} = m\vec{v} \tag{4.9}$$

where $\vec{v}$ is the total (absolute) velocity of the body CM, Equation (4.7) can be expressed as

$$\sum \vec{F} = m\frac{d\vec{v}}{dt} \tag{4.10}$$

In order to write this equation in the body frame, one needs to express the total velocity vector $\vec{v}$ of the body CM with respect to the inertial frame expressed in moving / rotating body frame as

$$\vec{v} = u\vec{i} + v\vec{j} + w\vec{k} \tag{4.11}$$

and the angular velocity vector $\vec{\omega}$ of the body with respect to the inertial frame expressed in moving / rotating body frame as

$$\vec{\omega} = p\vec{i} + q\vec{j} + r\vec{k} \tag{4.12}$$

where $\vec{i}$, $\vec{j}$, and $\vec{k}$ are the unit vectors along the body's x-, y-, and z-axes, respectively.

Using these components of $\vec{v}$ and $\vec{\omega}$, the dynamic equations of linear motion of the body CM can be obtained as [29]

$$\sum \vec{F}_x = m\left(\frac{du}{dt} + qw - vr\right) \tag{4.13}$$

$$\sum \vec{F}_y = m\left(\frac{dv}{dt} - ur + pw\right) \tag{4.14}$$

$$\sum \vec{F}_z = m\left(\frac{dw}{dt} + pv - uq\right) \tag{4.15}$$

where subscripts x, y, and z denote the components of the total external forces $\sum \vec{F}$ acting on the body CM, which consist of aerodynamic $\sum \vec{F}_A$, propulsive $\sum \vec{F}_P$, and gravitational $\sum \vec{F}_G$ forces as

$$\sum \vec{F} = \sum \vec{F}_A + \sum \vec{F}_P + \sum \vec{F}_G \tag{4.16}$$

In this thesis, a free fall weapon is considered; therefore there exists no propulsive force, that is

$$\sum \vec{F}_P \equiv 0 \tag{4.17}$$

In order to express the gravitational force, it is necessary to find the components of the gravity vector expressed in the body frame. The gravity vector can be written in the navigation frame as $[0\ 0\ g]^T$. In order to express the gravitational force components in the force equations, it is necessary to know the expressions of gravitational components g_x, g_y, and g_z in the body frame. According to the 3-2-1 rotation sequence; the first rotation, as the rotation about reference frame z-axis (axis of gravity acceleration), does not effect (rotate) the gravity vector. But the next two rotations C_2 and C_3 are effective in distributing the magnitude of the gravity vector along associated axes. So it is possible to write

$$\begin{bmatrix} g_x \\ g_y \\ g_z \end{bmatrix}_b = \begin{bmatrix} 0 \\ 0 \\ 0 \end{bmatrix} + C_3 \begin{bmatrix} 0 \\ 0 \\ 0 \end{bmatrix} + C_3 C_2 \begin{bmatrix} 0 \\ 0 \\ g \end{bmatrix} = \begin{bmatrix} 1 & 0 & 0 \\ 0 & \cos\phi & \cos\phi \\ 0 & -\sin\phi & \cos\phi \end{bmatrix} \begin{bmatrix} \cos\theta & 0 & -\sin\theta \\ 0 & 1 & 0 \\ \sin\theta & 0 & \cos\theta \end{bmatrix} \begin{bmatrix} 0 \\ 0 \\ g \end{bmatrix} \tag{4.18}$$

$$\begin{bmatrix} g_x \\ g_y \\ g_z \end{bmatrix}_b = \begin{bmatrix} -g\sin\theta \\ g\sin\phi\cos\theta \\ g\cos\phi\cos\theta \end{bmatrix} \tag{4.19}$$

Inserting the gravitational force components in Equations (4.13), (4.14), and (4.15) rearranging give the final form of translational dynamic equations as

$$\frac{du}{dt} = \frac{1}{m} F_{Ax} - g \sin\theta + rv - qw \tag{4.20}$$

$$\frac{dv}{dt} = \frac{1}{m} F_{Ay} + g \sin\phi \cos\theta + ru - pw \tag{4.21}$$

$$\frac{dw}{dt} = \frac{1}{m} F_{Az} + g \cos\phi \cos\theta + qu - pv \tag{4.22}$$

where F_{Ax}, F_{Ay}, F_{Az} are the components of the aerodynamic forces expressed in the body frame.

4.2.2.2 Rotational Dynamics

Since the angular momentum of a rigid body with fixed mass is given as

$$\vec{H} = I\vec{\omega} \tag{4.23}$$

where I is the constant mass moment of inertia matrix, Equation (4.7) for the rotational dynamics of a rigid body can be expressed as

$$\sum \vec{M} = I \frac{d\vec{\omega}}{dt} \tag{4.24}$$

which can also be expressed in the body frame as

$$\sum \vec{M} = I \frac{d\vec{\omega}}{dt} + \vec{\omega} \times (I\vec{\omega}) \tag{4.25}$$

Defining the components of total external moments in the body frame as

$$\sum \vec{M} = L\vec{i} + M\vec{j} + N\vec{k} \tag{4.26}$$

and using the fact that the I is a diagonal matrix (that is all product of inertia terms are zero) since the weapon is symmetrical about its xy and xz planes setting the body axes as principle axes, one obtains the following equations

$$L = I_x \frac{dp}{dt} + (I_z - I_z)qr = I_x \frac{dp}{dt} \tag{4.27}$$

$$M = I_y \frac{dq}{dt} + (I_x - I_y)rp \tag{4.28}$$

$$N = I_z \frac{dr}{dt} + (I_y - I_x)pq \tag{4.29}$$

and their final forms as

$$\frac{dp}{dt} = \frac{1}{I_x} L \tag{4.30}$$

$$\frac{dq}{dt} = \frac{1}{I_y} M + \frac{I_y - I_x}{I_y} pr \tag{4.31}$$

$$\frac{dr}{dt} = \frac{1}{I_z} N + \frac{I_x - I_y}{I_y} pq \tag{4.32}$$

4.2.2.3 Translational Kinematics

In order to find the position of the weapon with respect to Earth fixed navigation frame, the velocities need to be expressed with respect to this frame.

The weapon's velocity vector expressed in body frame can be transformed to velocity components in the Earth fixed navigation frame by using the transformation matrix C_b^n defined in (4.6) as

$$\begin{bmatrix} \dot{x} \\ \dot{y} \\ \dot{z} \end{bmatrix} = C_b^n \begin{bmatrix} u \\ v \\ w \end{bmatrix} \tag{4.33}$$

$$\begin{aligned} \dot{x} &= u\cos\theta\cos\psi + v(\sin\phi\sin\theta\cos\psi - \cos\phi\sin\theta) + w(\cos\phi\sin\theta\cos\psi + \sin\phi\sin\psi) \\ \dot{y} &= u(\cos\theta\sin\psi + v(\sin\phi\sin\theta\sin\psi + \cos\phi\cos\psi) + w(\cos\phi\sin\theta\sin\psi - \sin\phi\cos\psi) \\ \dot{z} &= -u\sin\theta + v(\sin\phi\cos\theta) + w(\cos\phi\cos\theta) \end{aligned} \tag{4.34}$$

4.2.2.4 Rotational Kinematics

Derivation of Euler rate equations as function of body rates and Euler angles can be carried out as follows.

Let p, q, and r be the body rotation rate components with respect to the inertial frame expressed in the body frame, and $\dot{\phi}$, $\dot{\theta}$, and $\dot{\psi}$ be the body rotation rate components with respect to the inertial frame expressed in the inertial frame. Then, using the following transformation equation

$$\begin{bmatrix} p \\ q \\ r \end{bmatrix} = \begin{bmatrix} \dot{\phi} \\ 0 \\ 0 \end{bmatrix} + C_3 \begin{bmatrix} 0 \\ \dot{\theta} \\ 0 \end{bmatrix} + C_3 C_2 \begin{bmatrix} 0 \\ 0 \\ \dot{\varphi} \end{bmatrix} = \begin{bmatrix} \dot{\phi} \\ 0 \\ 0 \end{bmatrix} + \begin{bmatrix} 0 \\ \cos\phi\dot{\theta} \\ -\sin\phi\dot{\theta} \end{bmatrix} + \begin{bmatrix} -\sin\theta\dot{\varphi} \\ \sin\phi\cos\theta\dot{\varphi} \\ \cos\phi\cos\theta\dot{\varphi} \end{bmatrix} \tag{4.35}$$

one gets

$$p = \frac{d\phi}{dt} - \frac{d\varphi}{dt}\sin\theta \tag{4.36}$$

$$q = \frac{d\theta}{dt}\cos\phi + \frac{d\varphi}{dt}\cos\theta\sin\phi \tag{4.37}$$

$$r = \frac{d\varphi}{dt}\cos\theta\cos\phi - \frac{d\theta}{dt}\sin\phi \tag{4.38}$$

or solving for $\dot{\phi}$, $\dot{\theta}$, and $\dot{\psi}$ as

$$\frac{d\varphi}{dt} = (r\cos\phi + q\sin\phi)\sec\theta \tag{4.39}$$

$$\frac{d\theta}{dt} = q\cos\phi - r\sin\phi \tag{4.40}$$

$$\frac{d\phi}{dt} = p + (q\sin\phi + r\cos\phi)\tan\theta \tag{4.41}$$

The dynamic and kinematic translational/rotational equations (4.20), (4.21), (4.22), (4.30), (4.31), (4.32), (4.34), (4.39), (4.40), and (4.41) constitute the necessary base for a flight mechanics model.

4.3 AERODYNAMICS

It is customary to express aerodynamic forces and moments appearing in dynamic equations in terms of a set of nondimensional coefficients as

$$\begin{bmatrix} F_{Ax} \\ F_{Ay} \\ F_{Az} \end{bmatrix} = Q_d A \begin{bmatrix} C_x \\ C_y \\ C_z \end{bmatrix} \tag{4.42}$$

$$\begin{bmatrix} L \\ M \\ N \end{bmatrix} = Q_d Ad \begin{bmatrix} C_L \\ C_M \\ C_N \end{bmatrix} \tag{4.43}$$

where A is the maximum cross section of the missile, d is the diameter, Q_d is the dynamic pressure which is a function of air density (ρ) and weapon's total speed (V_T) as shown in Equation (4.44).

$$Q_d = \frac{1}{2}\rho V_T^2 \tag{4.44}$$

Aerodynamic coefficients C_i are functions of several variables as [30]

$$C_i = C_i\left(M, \alpha, \beta, \delta_e, \delta_r, \delta_a, p, q, r, \dot{\alpha}, \dot{\beta}\right) \tag{4.45}$$

where M stands for the Mach number (not the second component of moment vector), α and β are angle of attack and sideslip respectively. δ_e is the elevator deflection δ_r is the rudder deflection, and δ_a stands for the aileron deflection.

One straightforward way to accurately determine these coefficients is to hold one variable while changing others and calculate the coefficient in all possible cases. However, this approach leads to a complicated n-dimensional lookup table even if all required experimental conditions are provided. In order to avoid this complication, the following Taylor series approximations are commonly used. [30]

$$C_x = C_{x0} \tag{4.46}$$

$$C_y = C_{y\beta}.\beta + C_{y\delta r}.\delta_r + C_{yr}.r.\frac{d}{2V_T} \tag{4.47}$$

$$C_z = C_{z\alpha}\alpha + C_{z\delta e}\delta_e + C_{zq}q\frac{d}{2V_T} \tag{4.48}$$

$$C_L = C_{L\delta a}\delta_a + C_{Lp}p\frac{d}{2V_T} + C_{L\beta}\beta \tag{4.49}$$

$$C_M = C_{M\alpha}\alpha + C_{M\delta_e}\delta_e + C_{Mq}q\frac{d}{2V_T} \tag{4.50}$$

$$C_N = C_{N\beta}\beta + C_{N\delta r}\delta_r + C_{Nr}r\frac{d}{2V_T} \tag{4.51}$$

where V_T is the total speed of weapon, and C_x, C_y, and C_z stand for axial, side force and normal force coefficients respectively. C_L is the rolling moment coefficient, C_M is the pitching moment coefficient and C_N stands for yawing moment coefficient.

The nondimensional aerodynamic coefficients dC_i/dx, which are also called stability derivatives, show the rate of change of the force and moment coefficients (i) with angle of attack, sideslip, roll,/pitch,/yaw rates, and control surface deflections (x). Thanks to the Maple Synge rotational symmetry which is valid for symmetrical missiles about y and z axes, the number of coefficients to be determined is reduced to the following set. [30]

$$\begin{aligned} C_{z\alpha} &= C_{y\beta} \\ C_{z\delta e} &= C_{y\delta r} \\ C_{zq} &= -C_{yr} \\ C_{M\alpha} &= -C_{N\beta} \\ C_{Mq} &= C_{Nr} \\ C_{M\delta e} &= -C_{N\delta r} \end{aligned} \tag{4.52}$$

4.3.1 DETERMINATION OF AERODYNAMIC COEFFICIENTS

Currently, there are four basic methods that are used in combination for the prediction of aerodynamic data for flying objects, namely [31]

i) Computational methods,

ii) theoretical and empirical aerodynamics,

iii) experimental aerodynamics (wind tunnel testing), and

iv) experimental flight mechanics (aeroballistic range testing).

The aerodynamic coefficients of the generic shape used in this thesis are generated by using the Missile Datcom software package [32]. The Missile Datcom version used at the analysis is Version 6 (release 6/93). It is understood that the results obtained by different versions of Datcom show some differences in magnitudes of some coefficients. The outputs are slightly different when the same input file is run with 6/93 and 5/97 versions.

The shape generated is a generic weapon shape, which has a blunted spherical nose, accompanying conical nose structure, and general boattail type tail section with tail stability surfaces. The system is assumed to be canard controlled by 4 trapezoidal fins and stability is achieved by 4 inline tail structures.

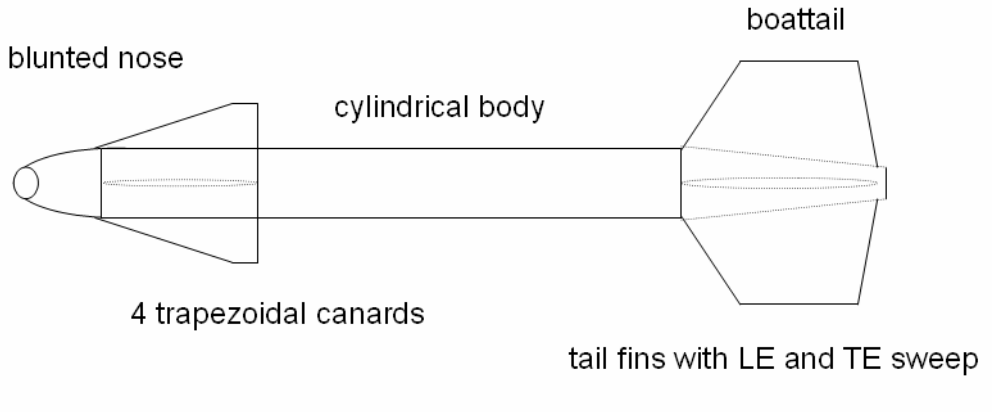

Figure 4-2 Sketch of the generic weapon shape

The input file is constructed to obtain the aerodynamic coefficients as functions of Mach number and angle of attack. Since the weapon experiences various angle of attack values due to bang-bang control, it is necessary to take the angle of attack effect on coefficients.

Runs for a Mach number range between 0.1 and 1.3 with 0.1 degree increments and angle of attack range between -10º and +10º with 1 degree increments are performed. Results are then implemented to form 2D (two dimensional) lookup tables which take the angle of attack and Mach number as inputs. Coefficients that depend on sideslip angle take sideslip and Mach number as inputs. Mach number and altitude are given as inputs to the program to calculate aerodynamic coefficients. The sideslip angle and roll angle are taken as zero.

The results at the transonic region between Mach 0.8 and 1.1 are important due to the nature of weapon. However, it is known that Datcom's capabilities are limited at transonic region calculations. The results from computer programs must be verified with experiments if possible or used cautiously.

4.3.1.1 Missile Datcom Outputs

The following outputs, which are written as same as their appearance in the output file, are obtained from Missile Datcom software.

CN: (Normal Force Coefficient) CN=-CZ and it is used to find the $Cz_{\delta e}$ by the following formula using a central difference of two runs at +1 and -1 degrees equivalent elevator deflections.

$$C_{z\delta e_{ij}} = \frac{C_{z\delta e=1}(mach_i, \alpha_j) - C_{z\delta e=-1}(mach_i, \alpha_j)}{2} \tag{4.53}$$

CM: (Pitching moment coefficient.) This coefficient is used to calculate $C_{M\delta e}$ in the same manner by central difference as functions of Mach number and angle of attack.

CA: (Axial force Coefficient.) CA=CX and equal to Cd since drag coefficient at

the body axis is used at the simulation.

CY: Side force coefficient

CLN: Yawing moment coefficient

CLL: Rolling moment coefficient

CNA: Normal force coefficient derivative with angle of attack. $C_{n\alpha} = -C_{z\alpha} = C_{y\beta}$

CMA: Pitching moment coefficient derivative with angle of attack. $C_{M\alpha}$ is directly obtained from the output file.

CYB: Side force coefficient derivative with sideslip angle. Since the simulations are run for Mach and angle of attack, and due to rotational symmetry $C_{z\alpha}$ values are used for $C_{y\beta}$, with the only difference that sideslip angle enters the lookup tables of $C_{y\beta}$ and $C_{N\beta}$.

CLNB: Yawing moment coefficient derivative with sideslip. $C_{N\beta}$ values are not used since the runs are made for angle of attack and Mach number. Rotational symmetry is used.

CLLB: Rolling moment coefficient derivative with sideslip. $C_{l\beta}$.

CNQ: Normal force coefficient due to pitch rate. $C_{Nq} = -C_{zq} = C_{yr}$

CNAD: Normal force coefficient due to angle of attack rate.

CMQ+CMAD: Pitching moment coefficient due to pitch rate. This output is assumed as C_{Mq}.

Since Cl_p value is not directly given as output, it is found in the following manner. Aileron deflections for 1 degree right and left are given, and C_l (CLL) values for each Mach number and angle of attack configuration are found by using the following formula. [30]

$$C_{lp} = -2.15.C_{l\delta a}.\left(\frac{y_c}{d}\right) \tag{4.54}$$

where y_c is the distance from the rolling body axis to the area center of one fin panel and d is the diameter of the missile.

Sample results of Missile Datcom are given in Figure 4-3, Figure 4-4, and Figure 4-5.

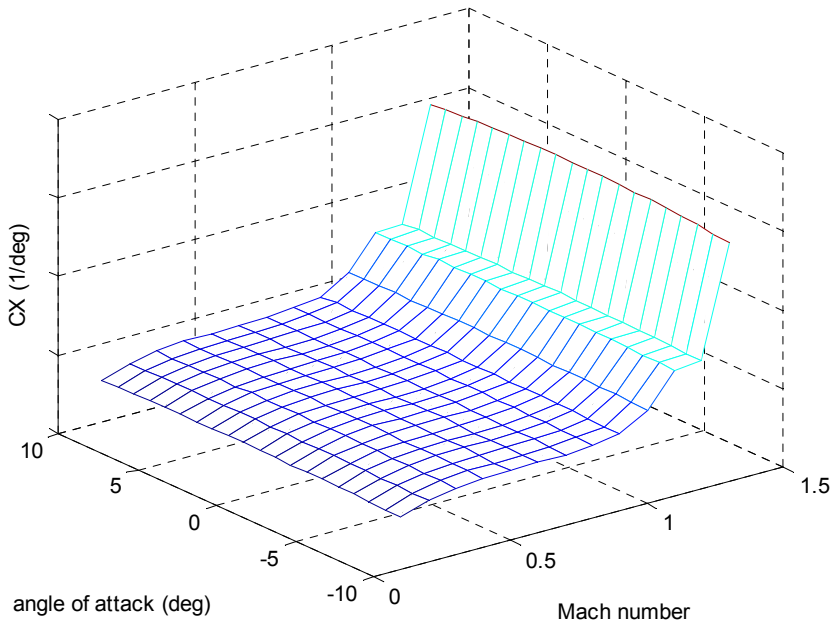

Figure 4-3 Drag coefficient as function of Mach number and angle of attack

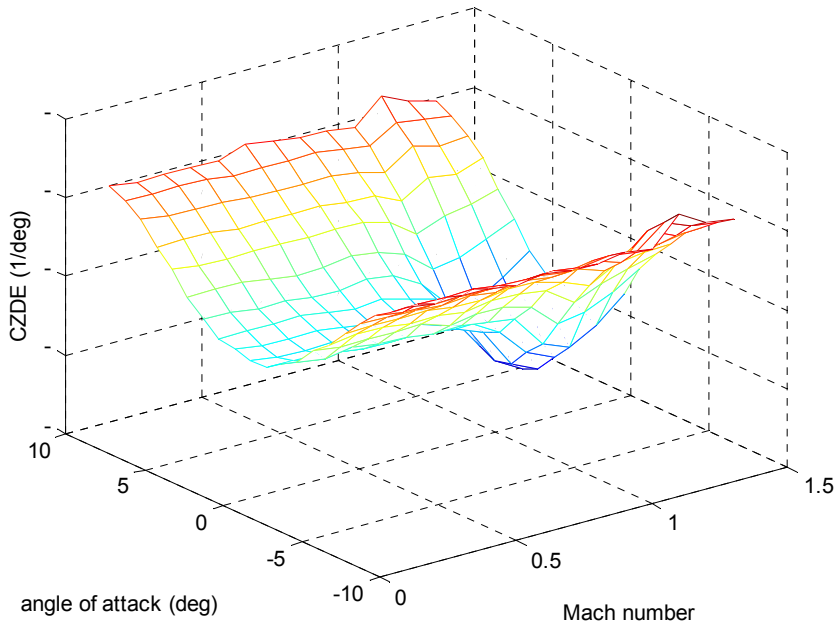

Figure 4-4 Normal force coefficient derivative with elevator deflection as function of Mach number and angle of attack

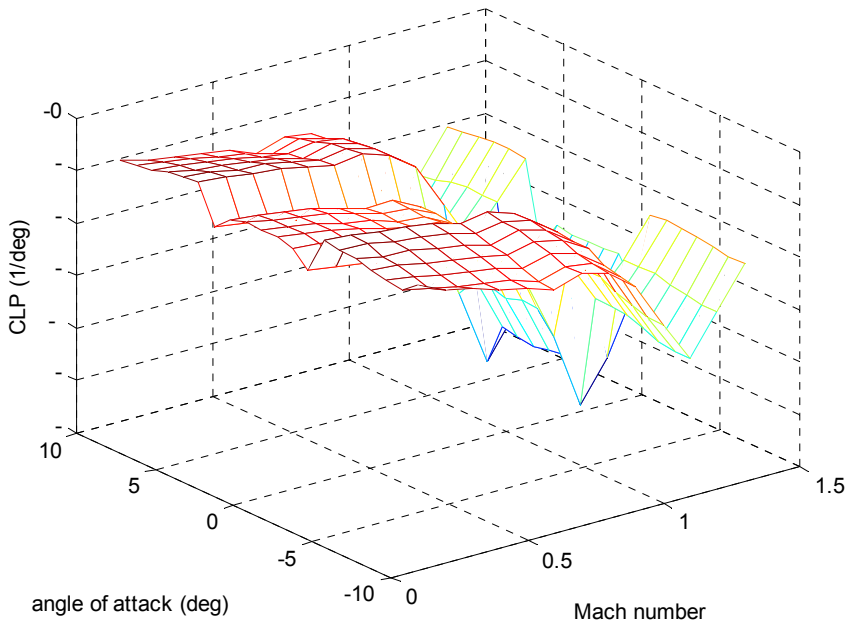

Figure 4-5 Roll stiffness as function of Mach number and angle of attack

CHAPTER V

GUIDANCE AND CONTROL SYSTEM

5.1 INTRODUCTION

This chapter is primarily about the general layout of guidance and control modeling.

Widely used angles in missile guidance are defined. Velocity pursuit guidance method is described. A block diagram of the guidance and control modeling is given. The calculation procedure for the lead angles is narrated since these angles have to be calculated mathematically in the simulation studies whereas they are directly sensed in a real application.

Some special control schemes subject to study, such as the bang-bang, bang-trail-bang, multiposition and continuous canard deflection methods are described and the modeling of control schemes is narrated.

5.2 IMPORTANT ANGLES IN MISSILE GUIDANCE

Before proceeding with the guidance and control schemes, it will be helpful to define some widely used terminology and angles in guidance studies which are depicted in Figure 5-1.

LOS (line of sight): The line between the center location of seeker and the target (the aiming mark or spot on the target).

Impact angle: The angle between the surface (which is to be hit) of the target and the longitudinal axis of missile. This angle is especially important when attacking

hard targets such as bunkers, aircraft shelters with penetrator warheads or kinetic energy rods in anti-armor missions.

Lead angle: The initial angle of missile velocity vector with respect to the LOS is known as the missile lead angle.

LOS angle: The angle between the reference line (Earth horizontal) and the LOS.

Flight path angle: The angle between the velocity vector and the inertial reference.

Look angle: The angle between the missile longitudinal axis and the LOS.

A gimbaled inertially stabilized seeker senses the LOS rate, and corrects small misalignments within seeker linear region very accurately.

An airstream stabilized seeker senses the lead angle since seeker centerline direction will always coincide with the missile velocity vector as shown in Figure 5-2.

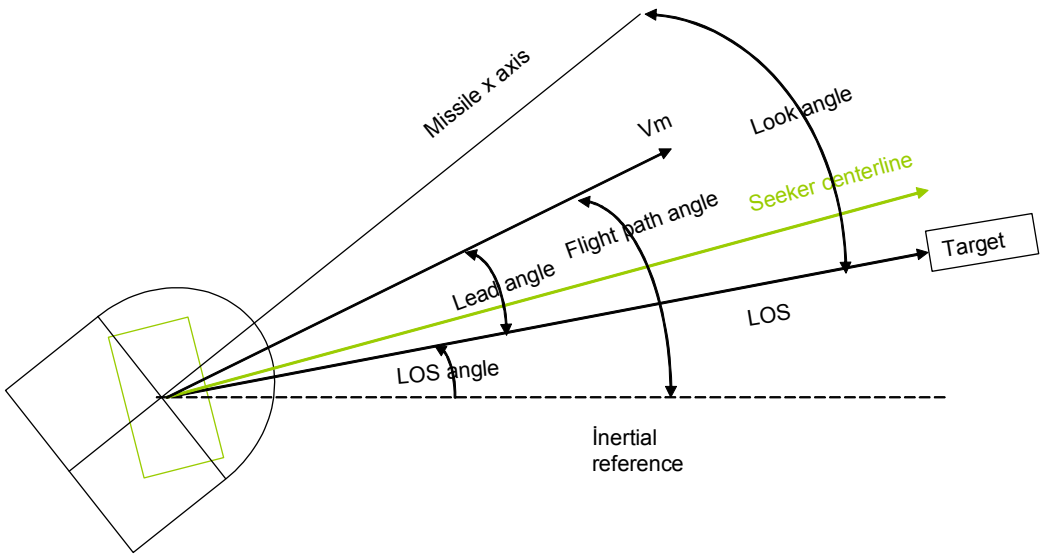

Figure 5-1 Important angles in guidance (general case)

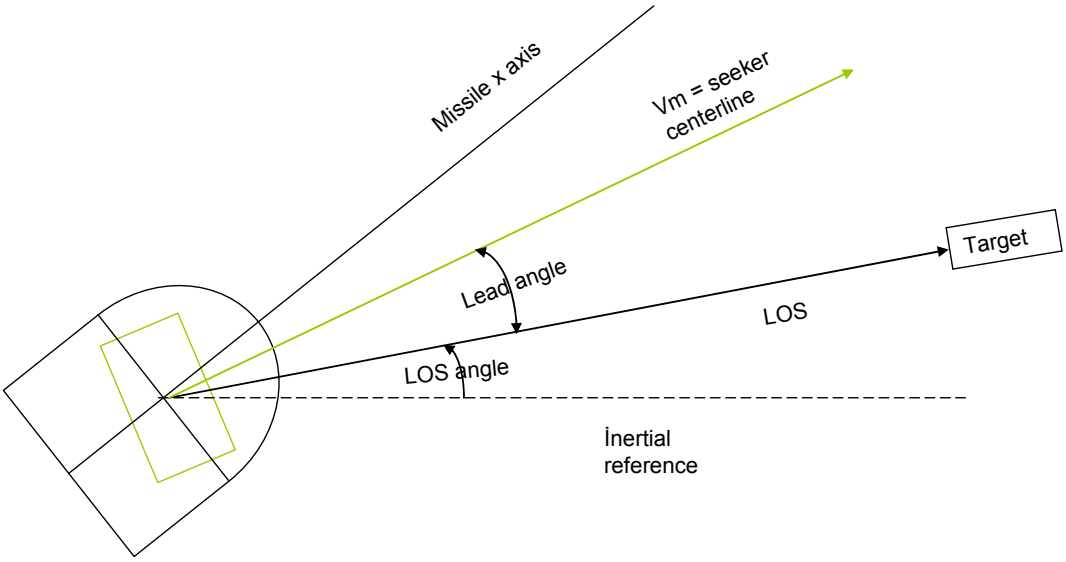

Figure 5-2 Velocity aligning probe mounted seeker

5.3 GENERAL LAYOUT OF GUIDANCE SYSTEM

The generic weapon used in this study employs the velocity pursuit guidance law since it has no additional sensors to utilize other guidance methods. This guidance law mainly stands on the fact that, the target can be hit if the velocity vector of the missile can be forced to coincide with the LOS between the missile and the target.

To implement this law, the laser sensor is sometimes located on a special structure called as “birdie” which aligns itself (and the seeker) with the airstream (missile velocity vector). This birdie is mounted on the missile nose by a swivel joint. The missile body assumes the angle of attack with the birdie to fly the required path.

The general layout of weapon model used in this thesis is shown in Figure 5-3. The laser seeker, whose normal line direction is the same as the weapon’s velocity vector, senses the collimated laser beam when the laser spot falls on the detector surface. Voltages generated by the seeker as a response to the incident laser beam are sent to the guidance system. The guidance system converts these voltages into commanded elevator and rudder deflections.

Four control schemes are modeled. Bang-bang (BB), bang-bang with deadzone (BTB), multiposition, and fully continuous. These commanded deflections are sent

to the control actuation system which tries to realize the commanded deflections as close as its dynamic response allows. The weapon flies with these control surface deflections and gains a new position and attitude. The only feedback sensor in this structure is the seeker itself.

The control actuation system (CAS) is modeled by using a fourth order transfer function whose response time is fast enough to perform commanded deflections in a short time without disturbing the guidance command sequence.

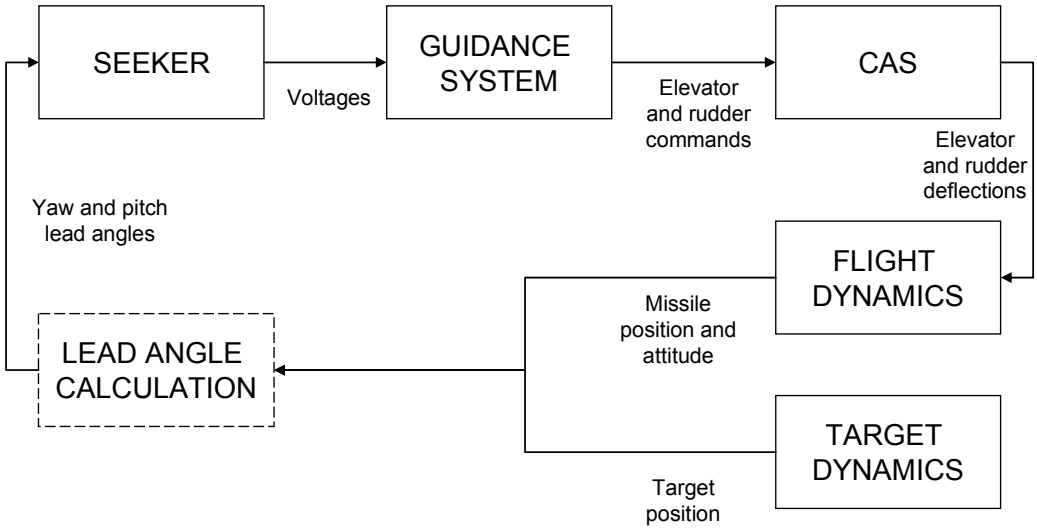

Figure 5-3 Guidance and control model block diagram

Elevator and rudder deflections enter to the flight dynamics model which is used to simulate the flight of the weapon system.

The target model constitutes both stationary and moving targets. Moving targets are modeled as main battle tanks with some sinusoidal and random directional maneuvers.

In real life, the seeker senses lead angles directly. But in mathematical modeling, lead angle values are obtained by the help of some calculations using the weapon-target range vector and weapon attitude as explained in the following section.

5.4 LEAD ANGLE DETERMINATION

The determination of the lead angle is important for the guidance and control system modeling since lead angles are used in voltage-yaw/pitch error functions with respect to the seeker axis system. In order to determine the lead angle (angle between the velocity vector of the weapon and LOS) the following procedure is employed.

Since the seeker is mounted on a probe-like structure which aligns its direction with the apparent velocity vector, the seekers vision will be directly centered at the velocity direction. Thus, the seeker will be measuring the lead angle directly. It is possible to orient any vector to any direction by two successive rotations in azimuth and elevation with respect to say, seeker frame.

In order to calculate the lead angle, it is necessary to know the line that connects the seeker's position and the target's position with respect to the fixed navigation frame. (LOS) Then this position vector can be resolved into its components and a two dimensional LOS angle can be obtained.

The equations of motion are written according to the CM (center of mass) of the weapon and its position is actually the CM position with respect to inertial frame. In order to find the real LOS between the seeker and the target, the distance between the seeker and CM of the weapon must be taken into account.

The position vector $\vec{R}_g\big|_b$ of weapon seeker with respect to body frame in the body frame can be written as,

$$\vec{R}_g\big|_b = \begin{bmatrix} D & 0 & 0 \end{bmatrix} \tag{5.1}$$

where D is the distance from center of mass to detector centerline in body x-axis.

The position $\vec{R}_g\big|_n$ of the detector with respect to the navigation frame can be written as,

$$\vec{R}_g\Big|_n = \vec{R}_m\Big|_n + C_b^n.\vec{R}_g\Big|_b \tag{5.2}$$

where $\vec{R}_m\Big|_n$ is the position of the missile CM in the navigation frame and C_b^n is the transformation matrix which transforms a vector from the body frame to the navigation frame.

Denoting the target position in the inertial frame as $\vec{R}_T\Big|_n$, the gimbal to target slant range can be found as,

$$\vec{R}_{gT}\Big|_n = \vec{R}_T\Big|_n - \vec{R}_g\Big|_n \tag{5.3}$$

In order to find the lead angle, it is necessary to resolve the components of this slant range into wind axes (i.e., seeker axis) and then obtain the horizontal and vertical components of the lead angle with respect to seeker axes. The slant range vector can be expressed in wind frame as

$$\vec{R}_{gT}\Big|_w = C_n^w\,\vec{R}_{gT}\Big|_n \tag{5.4}$$

where C_n^w is the transformation matrix which transforms a vector from the navigation frame to the wind frame and can be written as

$$C_n^w = C_b^w C_n^b = C_b^w (C_b^n)^T \tag{5.5}$$

where C_b^n is given in Equation (4.6) and C_b^w can be found by using the angle of attack and sideslip angle in the following manner.

The transformation matrix C_b^w from the body frame to the wind frame can be found by two successive rotations of the body axis system, first about the second body axis (y-axis) by an amount α (angle of attack) and then a rotation about the new z-axis by an amount β (sideslip angle). The positive direction of angle of attack shown in Figure 5-4

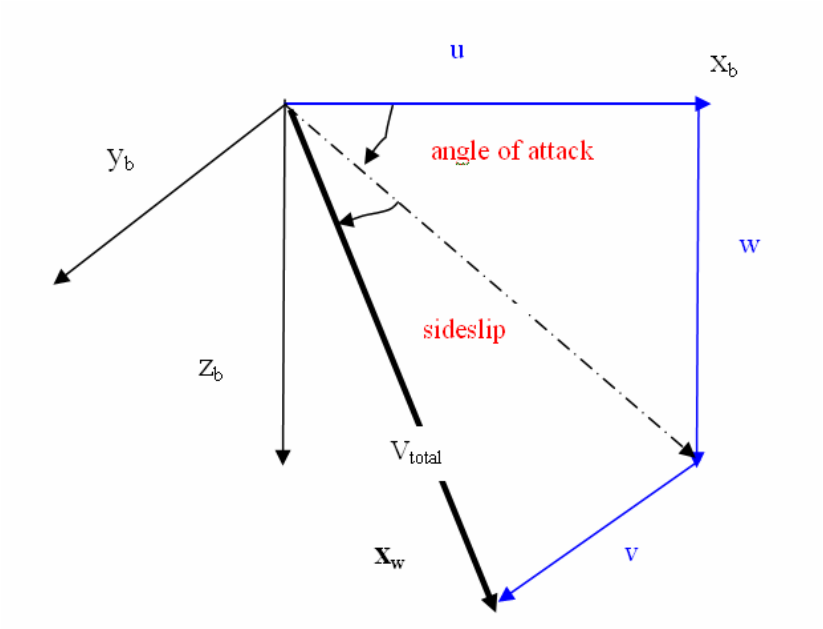

Figure 5-4 Transformation from body to wind axes

$$C_b^w = C3(\beta).C2(-\alpha) = \begin{bmatrix} \cos\beta & \sin\beta & 0 \\ -\sin\beta & \cos\beta & 0 \\ 0 & 0 & 1 \end{bmatrix} . \begin{bmatrix} \cos\alpha & 0 & \sin\alpha \\ 0 & 1 & 0 \\ -\sin\alpha & 0 & \cos\alpha \end{bmatrix}$$

$$= \begin{bmatrix} \cos\alpha\cos\beta & \sin\beta & \cos\beta\sin\alpha \\ -\cos\alpha\sin\beta & \cos\beta & -\sin\beta\sin\alpha \\ -\sin\alpha & 0 & \cos\alpha \end{bmatrix} \tag{5.6}$$

So the slant range vector can be expressed in wind frame as

$$\vec{R}_{gT}\Big|_{wind} = C_b^w \vec{R}_{gT}\Big|_b \tag{5.7}$$

So it is now possible to directly find the lead angle in relative horizontal and vertical planes with respect to the missile seeker as

$$leadyaw = a\tan 2(y_{gT}\Big|_w, x_{gT}\Big|_w) \tag{5.8}$$

$$pitchlead = a\tan 2\left(z_{gT}\Big|_w, \sqrt{\left(x_{gT}\Big|_w\right)^2 + \left(y_{gT}\Big|_w\right)^2}\right) \tag{5.9}$$

where $x_{gT}\big|_w$, $y_{gT}\big|_w$, and $z_{gT}\big|_w$ are the components of $\vec{R}_{gT}\big|_w$.

5.5 CONTROL MODELS

In this thesis, four primary control methodologies are investigated as seen in Figure 5-5. They differ by their processing styles of information coming from the seeker.

Due to the nature of laser guidance, pulsed laser return signals are sensed by the seeker at 10 Hz rate. This means that the feedback information can be obtained at most 0.1 seconds after a control surface deflection. The models are constructed by taking this feature into account. The guidance system will sense the same lead angle value until a new correction is received.

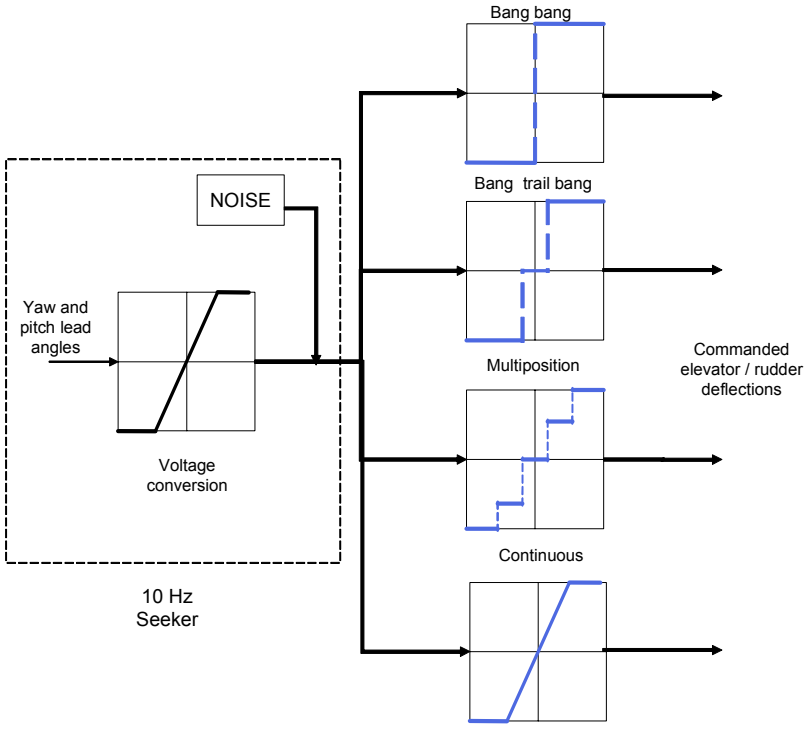

Figure 5-5 General guidance / control system

The seeker model provides a linear region of lead angle-voltage relationship up to a limit and a saturated region where only directional information can be obtained. The seeker tests, whose details are given at Chapter III, reveal that the seeker has a linear region up to ±3 degrees lead angle, and further lead angle values can only be sensed in a directional manner due to the saturation of seeker. So, even in employing a fully proportional control strategy, the seeker limits the range of proportional signals.

Noise levels in the seeker are taken into consideration. The maximum margins of noise levels are determined and fed to the ideal linear region data in a Gaussian distribution manner.

5.5.1 BANG-BANG CONTROL

One of the control methodologies examined is the bang-bang control. The bang-bang control is an on-off type control strategy which appears to be the simplest control method. The control actuation system needs not to be complicated, either.

In this control strategy, control surfaces are deflected at their maximum deflection limits regardless of the magnitude of error. The result is a very oscillatory behavior around the desired position. In this model, the magnitude of the lead angle error is not taken into consideration. The commands will be cyclic like left/down, right/up and so on.

5.5.2 BANG-TRAIL-BANG CONTROL

A modified version of bang-bang control is the bang-trail-bang (BTB) method. Due to oscillations faced in bang-bang control, a deadzone is created. The aim of the deadzone concept is to open a small region about the desired position, where the controller does not produce any corrective action. For the weapon in study, the deadzone is defined as the limit of lead angle error (or the voltage value from the seeker) where no canard deflection command is produced.

In this case unnecessary maneuvers can be prevented up to an extent. The width of the deadzone must be determined regarding the primary launch conditions of the weapon. In this thesis, a preliminary analysis for the deadzone width is also performed.

5.5.3 MULTIPOSITION CONTROL

One further step in the control system model is the multiposition control, which is a control strategy somewhere between the fully proportional control and the bang-bang control. The effect of using multiposition control on the weapon performance is also analyzed in this study.

The aim for the employment of this control strategy is to examine if a multiposition controller can be utilized instead of continuous (fully proportional) control and to determine the amount of performance increase gained by this method.

The multiposition scheme selected is 5-position controller which is capable of creating -10, -X, 0, +X, +10 degrees canard deflections. Increasing the amount X of mid-step deflection positions shifts this method closer to the continuous control. No deflection case (X=0 degrees) is obtained by the use of deadzone concept in the same manner as the BTB method.

This control method requires analysis of three important parameters. One of them is the width of the deadzone. The other is the value of the deflection which will eliminate the necessity of full deflections in most phases of flight. The last parameter is the decision criteria of “when to use this deflection”, namely, the magnitude of the lead angle error, which is the limit for the full or the mid-deflection position.

All these parameters are investigated and results of multiposition control are obtained.

5.5.4 CONTINUOUS CONTROL

The ultimate limit of the control strategies is the fully proportional control methodology, which provides an output proportional to the input.

Canard deflections are produced according to the magnitude of voltages from the seeker. However, since the seeker has a limit in linear region, fully proportional elevator and rudder deflections can only be generated at the limited linear region. Full scale deflections have to be employed beyond the linear region.

This method is employed in order to provide an overall picture of the control methods and their effects on weapon performance starting from the bang-bang, ending with the continuous control.

It is expected that the continuous control methodology would give the best results. The main purpose is to see how much improvement with respect to multiposition control can be gained and to decide if the multiposition control will be adequate in increasing weapon performance without the necessity of utilizing continuous control.

5.6 CONCLUSIONS

The properties and models of control methods used in this study are narrated in this chapter. The general weapon model is described, seeker information rate is specified. The working logic of guidance system is briefly explained.

Bang-bang control method is described. Bang-bang control with deadzone (BTB) is also modeled. A multiposition controller with five stations is created. The three important decision parameters which are deadzone width, canard deflection values and lead angle limit in using canard deflection values are introduced. The last control method which is the continuous control is described.

Now it is possible to convert the mathematical model of the weapon system to 6-DOF simulation in computer environment, and analyze the effects of different control methodologies with this simulation.

CHAPTER VI

6-DOF SIMULATION

6.1 INTRODUCTION

This chapter summarizes the primary aspects of 6-DOF simulation of the flight dynamics of the weapon and gives information about how the mathematical models are implemented into the simulation.

After the environment and the simulation parameters such as integration method, etc. are introduced, information about the implementations of laser guidance, seeker, control types (BB, BTB, multiposition and continuous) and target dynamics are given in the following sections.

6.2 GENERAL STRUCTURE OF THE SIMULATION

The 6-DOF simulation of the flight dynamics of the weapon is constructed in the Matlab 6.5 Simulink 5.0 environment. The simulation consists of following subsystems.

- Weapon and target initialization parameters
- Pulsed laser signal
- Seeker model
- Control system models
    - Bang-bang / bang-trail-bang control
    - Multiposition control

    - Continuous control
    - Continuous control with a theoretical down sensor
- Field of view and laser detection range controls
- Laser reflection model
- Lead angle calculator
- Flight dynamics model
- Aerodynamic coefficients pool
- Target dynamics model

The simulation parameters are configured to use Runge-Kutta integration scheme with fixed step size. The step size is selected to be 0.001 seconds. Normally the step size is selected as 1/5 or 1/10 of the fastest dynamics of the system. Various step sizes are tried and several important variables such as rotation rates, etc. are monitored to catch a difference. It is assured that a step size of 0.001 is adequate to accurately simulate the situation.

Overall simulation works in a continuous manner. However, some models use low sampling rate information (e.g., seeker at 10 Hz rate) in order to adequately simulate the system. Variables are transferred between blocks by using goto/from flags and long lines and connections are avoided where possible.

6.2.1 FIELD OF VIEW AND DETECTION RANGE CONTROLS

The primary control mechanisms for the weapon system's flight type are the field of view limitation and the laser detection range check (Figure 6-1). According to these checks the weapon initiates either the ballistic mode or activates guidance modules.

The seeker system has a predetermined field of view (FOV). If any of the yaw or pitch lead angles becomes bigger than this limit, the acquisition is said to be lost

and the weapon flies ballistically. No return algorithms are employed since there are no other aids onboard to determine what the weapon's attitude was, at the time of acquisition loss.

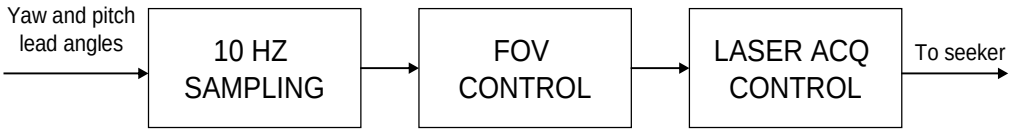

Figure 6-1 Guidance start check schematic

The other control mechanism is the laser detection range. For a given visibility condition, the detection range of the weapon is calculated and the guidance system is not activated till the target-weapon slant range is smaller than this value.

If one of these checks fail, (the target gets out of field of view or the weather conditions do not let acquisition at a given range), the guidance system becomes offline and weapon flies ballistic. A part of simulation about these checks is shown in Figure 6-2.

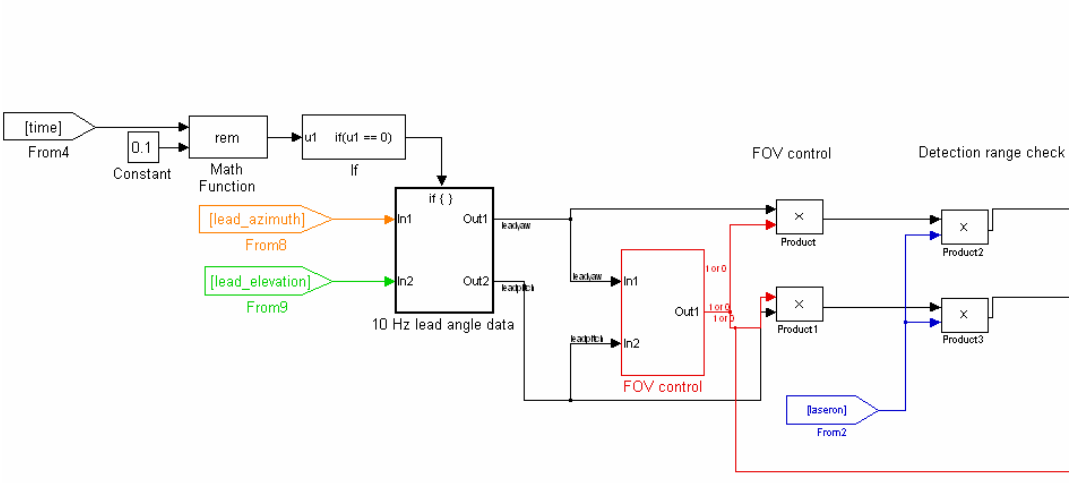

Figure 6-2 Detection range and FOV controls in Simulink

6.2.2 SEEKER MODEL IMPLEMENTATION

A laser seeker model constructed by using the data of seeker tests is implemented to the 6-DOF simulation in the following manner.

Lead angle values are calculated continuously by related lead angle calculator blocks. Due to the nature of laser guidance, their values are passed to the seeker model every 0.1 seconds. There is no delay, but the value corresponding to the 0.1 second sampling rate is taken and passed to the seeker model. During the 0.1 second period, this value is held and the system behaves as the same lead angle value is coming to the seeker.

As an output of seeker tests, it is determined that the seeker can be modeled as an ideal case with linear and saturated regions and noise characteristics with known variance.

In the light of this information, the seeker model is composed of two lookup tables for yaw and pitch, which convert incoming lead angle data to voltage scale, and a noise generator which generates continuous random noise signals with a Gaussian distribution. Since the lead angles are sensed at 10 Hz, the noise generator output is also taken at 0.1 second samples. So there is always one value of sensed lead angle at every 0.1 second interval containing noise effects in it.

The noise generator is selected to be the Simulink‘s random source block from DSP blockset. This block can generate random numbers in two methods, namely Ziggurat and sum of uniform values. The Ziggurat method is selected since the mean of the random variable is slightly closer to zero than the other method for a finite simulation time. (Details about Ziggurat method can be found at [33]). The inputs are the mean and variance. The repeatability is set to “nonrepeatable” in order to obtain different random sequences in each run.

The noise (variance) generated by the block is believed to be the highest level of noise that the seeker may face, due to the nature of the experiments performed at cold and hot setups in different conditions and times. The voltage outputs from the seeker enter to the control system blocks.

6.2.3 BANG-BANG AND BANG-TRAIL-BANG CONTROL MODEL

The bang-bang controller model and bang-trail-bang models use the same blocks with the only difference that the deadzone value is set to 0 in the bang-bang mode. For the BTB control, various deadzone widths can be specified.

The voltages coming from seeker lookup tables are converted to full scale deflections by the use of signum function which gives (+1) when voltage is greater than zero and (-1) when voltage difference is negative. The magnitude of the voltage is not taken into account in this control method.

In BTB mode, no canard deflection is generated if the absolute value of voltage is under a specified level which is called deadzone. Noise effects are not taken into consideration since the canard deflections are always at maximum. Figure 6-3 shows the blocks of bang-bang and bang-trail-bang models in Simulink.

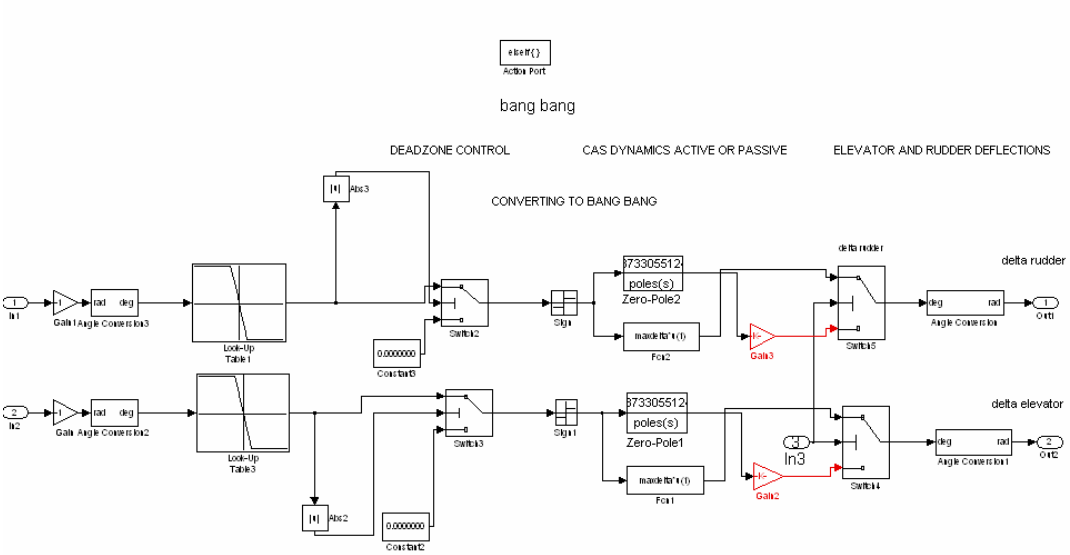

Figure 6-3 Bang-bang control blocks in Simulink

6.2.4 MULTIPOSITION CONTROL MODEL

The multiposition control model simulates a 5-position controller as shown in Figure 6-4. After the voltage values coming from the seeker lookup tables are added with noise signals, the resulting voltage value may be greater than 1. In order to avoid this, a saturation block is used to limit the normalized voltage value at absolute value of 1. Different from other schemes, this voltage value is compared with the deadzone width. If the voltage value is smaller than deadzone, canard deflection is set to zero. If the voltage value is smaller than the mid-deflection decision value, medium deflection is initiated. If it exceeds this decision criterion, it is understood that lead angle difference is high and maximum deflection is commanded. All decisions are constructed by if-action subsystems of Simulink.

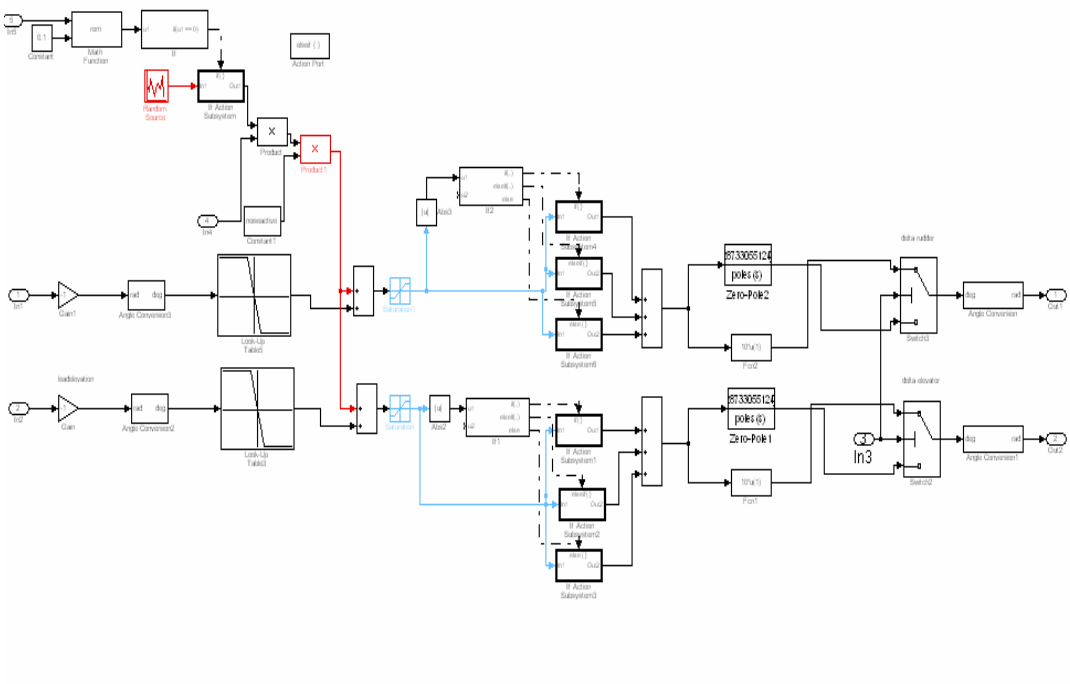

Figure 6-4 Multiposition control blocks in Simulink

6.2.5 CONTINUOUS CONTROL MODEL

The continuous control scheme uses the linear lead angle data to produce proportional elevator and rudder commands.

This scheme has no deadzone concept. Normalized voltage values as function of lead angle are mapped to the deflection range of canards linearly. Since the seeker is not a fully proportional sensor, only the ±3 degrees linear region had to be mapped to the full canard deflection scale. Lead angle errors greater than 3 degrees are corrected with maximum deflections as in the case of bang-bang control due to the nature of seeker.

The simulation can be configured to include or exclude CAS (control actuation system) dynamics. A fourth order transfer function which can achieve full control surface deflection within 0.1 seconds is used. Continuous control model blocks are seen in Figure 6-5.

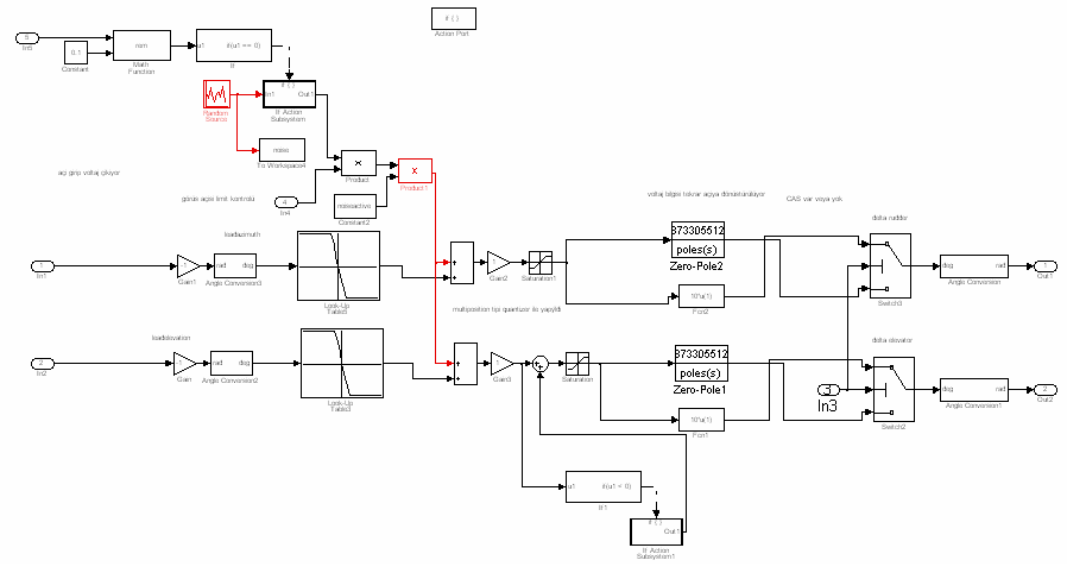

Figure 6-5 Continuous control blocks in Simulink

6.2.6 AERODYNAMIC COEFFICIENTS

The aerodynamic coefficients are implemented to the 6-DOF simulation in the form of two dimensional lookup tables as depicted in Figure 6-6. All aerodynamic coefficients are modeled as functions of Mach number and angle of attack. Coefficients like Cy_β and Cn_β which are functions of sideslip angle, take the sideslip angle and Mach number as inputs. An interpolation is used for Mach number and angle of attack values between data points. End values are used for out of range inputs.

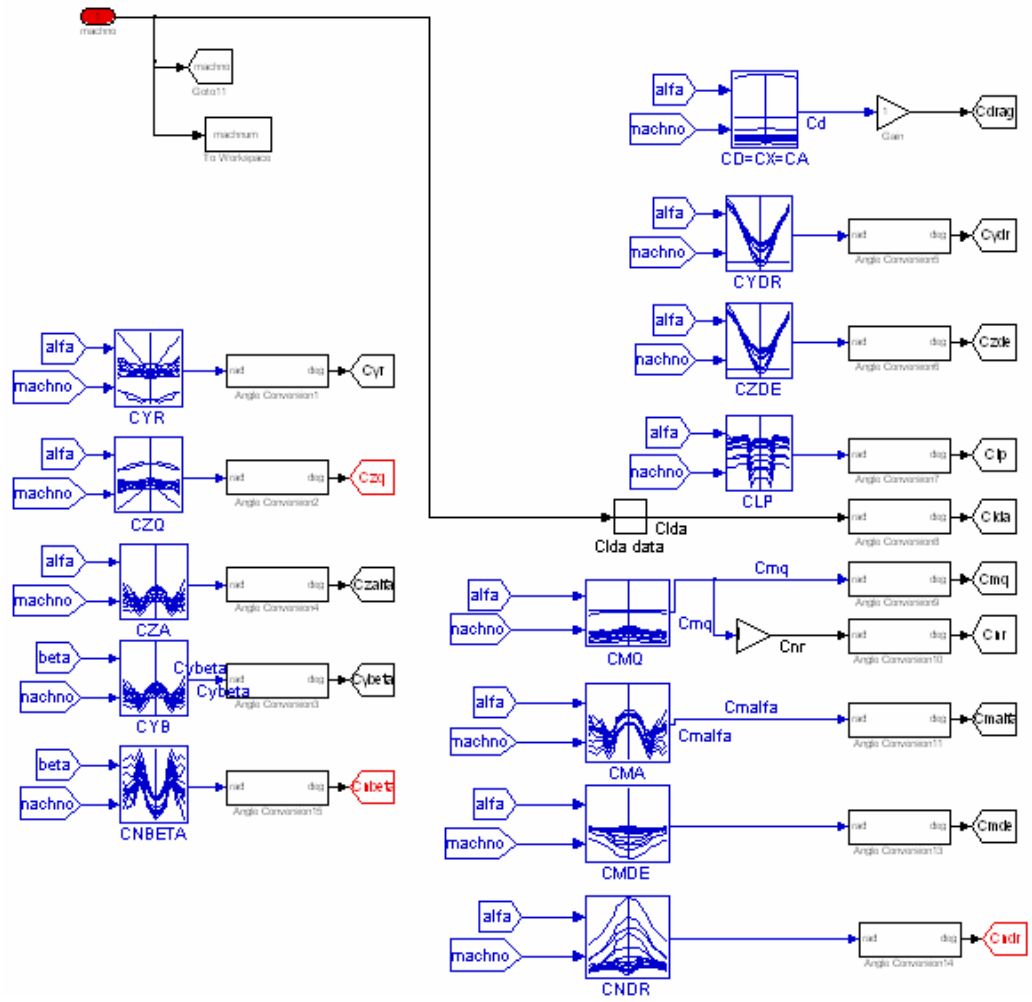

Figure 6-6 Aerodynamic coefficient lookup tables in Simulink

6.2.7 TARGET DYNAMICS

Two types of targets are modeled, namely stationary targets and moving point targets. Since the weapon is used against surface targets, moving targets are modeled with a planar motion capability. For moving target engagement simulations, main battle tanks are considered as the primary target type. Main battle tanks mostly have a maximum road speed between 48 and 72 km/h (13-20 m/s) and they can reach 0-32 km/h (9 m/s) speed in less then 6.5 to 8 seconds. [23] Cross country speeds of main battle tanks do not exceed 40 km/h (11 m/s) in most situations.

Considering an acceleration capability of 0 to 32 km/h in 6.5 seconds, an acceleration value of 1.37 m/s^2 is used in evasion maneuvers.

Deceleration capability of tracked vehicles is much higher than wheeled vehicles; for example, a second generation tank can stop from 45 km/h speed in less than 12 meters. Assuming a constant deceleration capability, the deceleration value of 6.5 m/s^2 can be used. Figure 6-7 shows the general layout of moving target model.

Armored vehicles are not equipped with capable radars to detect incoming threats and employ evasive maneuvers due to limitations of mobility and financial reasons. They can not utilize an optimum evasive maneuver pattern considering the movement of incoming weapon.

Some tanks also utilize active hard kill protection systems such as the Russian Drozd-1/2 and Arena APS (active protection system). Such systems rely on launching a small rocket or an explosive charge to the direction of incoming missile to hit the missile just before the impact, causing pre-explosion of warhead and loss of armor penetration effectiveness. Typical Arena APS radar can detect incoming rounds at 50 meters and can launch counter explosives in last few meters. These active protection systems are designed to counter the RPG's or anti-tank missiles and can not be used against heavy assault weapons. [34], [35]

As a result, the only defense against the incoming weapon is to make various sudden evasive maneuvers, accompanied by launching smoke grenades between

the designator and the tank for concealment and hoping that the laser guided weapon loses track. So the evasive maneuvers are modeled as random direction turns and sinusoidal path movements. Evasive maneuvers are started after laser spot on target is detected by the laser warning receiver, within 3 seconds.

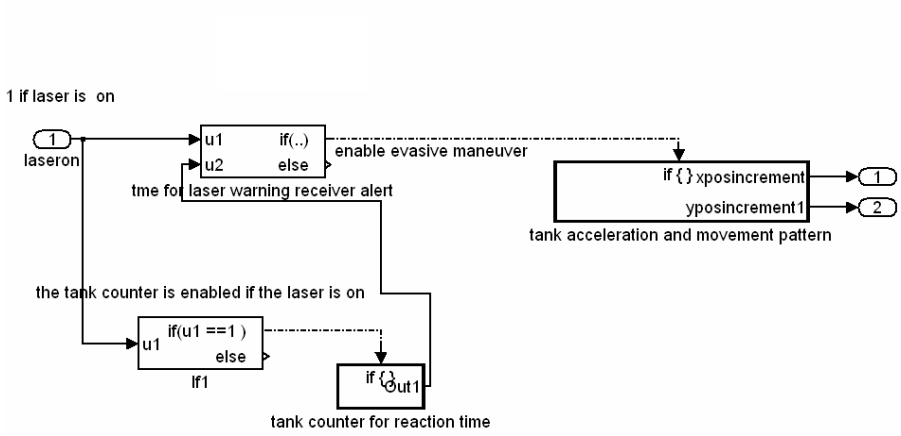

Figure 6-7 Moving target model in Simulink

6.3 CONCLUSIONS

With the completion of 6-DOF nonlinear system simulation, a base for the modeling of laser guided weapons is constituted. A computer model is formed to simulate the behavior of laser guided weapons under different conditions.

The flight dynamics of the weapon is modeled. Various control schemes are implemented to the 6-DOF simulation. Aerodynamic coefficients are integrated in the form of two dimensional lookup tables. Laser detection and guidance initiation checks are based on field of view and detection range parameters.

In the following section, primary launch scenarios for the weapon system are created and weapon's behavior under various conditions is investigated. The primary area of investigation is the determination of weapon performance in bang-bang, bang-trail-bang, multiposition and continuous control methods. The weapon's flight characteristics are also analyzed and effect of several parameters such as deadzone, down sensor, etc. on weapon performance are monitored.

CHAPTER VII

SIMULATIONS AND CASE STUDIES

7.1 INTRODUCTION

This chapter is dedicated to the analysis of various control implementations and their effects on the weapon performance. The results are obtained by using 6-DOF simulations and integrated models of subcomponents.

The main purpose of this chapter is to show the performance features of various control schemes and comment on their success under different release conditions. Comparisons of these schemes are also made to clarify their relative merits.

A general behavior of the bang-bang control scheme is given in the first section for a set of release conditions.

Results of the bang-trail-bang control are also given. Some primary scenarios are run in order to see if the claims about the weapon's performance are in accordance with the simulation results. The effect of deadzone width, as one of the important parameters in BTB control, on the weapon's performance is investigated.

Results of the multiposition control are shown with the selection of control surface position and other parameters such as deadzone.

Results of the continuous canard deflection are compared with the results of other methods and the amount of improvement for each strategy on the weapon's performance in terms of range, impact speed, miss distance, etc. is demonstrated.

The effect of adding a theoretical down sensor onboard is investigated. The weapon's maneuverability (g levels) is investigated in order to understand the kind of sensor that should be used with the weapon.

The Chapter ends with the summary of results obtained and the conclusions about the analysis of multiple methods.

7.2 PRIMARY SCENARIOS

In order to analyze the system performance, several scenarios are run with different release conditions and delivery types. Among these scenarios, three distinctive scenarios are characterized, namely, the high altitude level release, high altitude dive, and low altitude toss.

High altitude level delivery: High altitude level delivery is investigated for medium and high speed releases. The aim is to figure out the limits of the weapon's release envelope for different control schemes. The aircraft is level at the time of release and release speeds between 400-700 knots are employed.

High altitude dive delivery: High altitude dive delivery is characterized by a high speed dive onto the target where the high speed is used to avoid air defense systems. This delivery is included to the scenario analyses in order to investigate the effects of high initial energy on the weapon's performance. Both the release speed and release altitude of the weapon are kept as high as possible.

Low altitude toss delivery: This delivery is characterized by a high speed ingress at very low altitude, a sharp pitch up at release, and an egress. This delivery type is primarily used when there is a need to fly low to avoid being detected by enemy air-defense radar systems. It is used in interdiction and air support missions. The aircraft flies level at a low altitude, initiates a pitching up, releases the weapon with a positive pitch angle and provides the weapon with a trajectory to gain altitude. The guidance and control start when the seeker of the weapon sees the laser reflection.

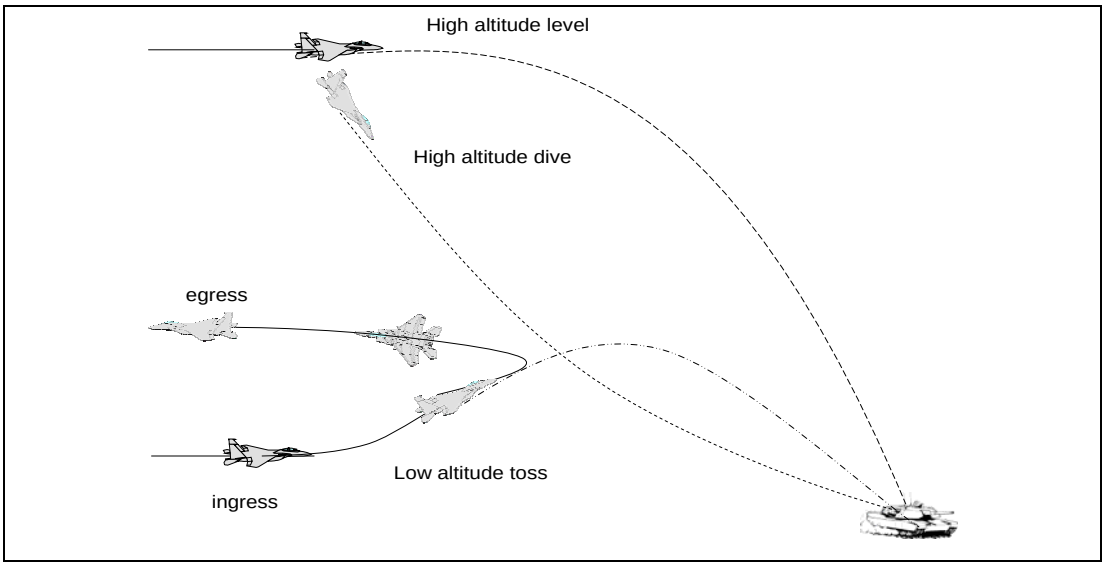

Figure 7-1 Launch scenarios

In this study, launches against

- stationary targets
- moving targets

with,

- bang-bang (with different maximum canard deflections)
- bang-trail-bang (with various deadzone widths)
- multiposition
- continuous (with and without theoretical down sensor)

control methods are investigated in ideal environments as well as in noisy environments.

In all simulations, the velocity pursuit guidance is used as the only guidance method.

7.3 RESULTS FOR BANG-BANG (BB) CONTROL SCHEME

The first control scheme investigated is the bang-bang control. Several launch scenarios are run in order to analyze the system behavior. Some of these launches and their results are given below which are used as examples about the weapon's flight characteristics.

BB Case 1: Parameters of this case are given in Table 7-1.

Table 7-1 High altitude level delivery parameters with bang-bang control

Launch Conditions		
Control scheme	Bang-bang	
Deadzone width	None	
Delivery type	High altitude level	
Release speed	600 knots (308 m/s)	
Release altitude	20,000 ft (6,096 m)	
Initial attitude in fixed frame		
Heading (deg)	Pitch angle (deg)	Roll angle (deg)
0	0	0
Initial rotation rates		
p (deg/s)	q (deg/s)	r (deg/s)
0	0	0
Target variables		
Target type	stationary	
	Downrange (m)	Crossrange (m)
Initial target location	10,000	0
Final target location	10,000	0
Performance variables		
Miss distance (m)	Time of flight (s)	Impact speed (m/s)
0.7	48	190

Figure 7-2 shows the flight path of the weapon when launched at a target at 10,000 meter downrange, from 20,000 ft (6,096 m) altitude with 600 knots (308 m/s) initial speed. As can be seen from Table 7-1, for high altitude level deliveries, the weapon's miss distance with the bang-bang control scheme is in the order of a meter, which seems to be a satisfactory performance for the given range envelope.

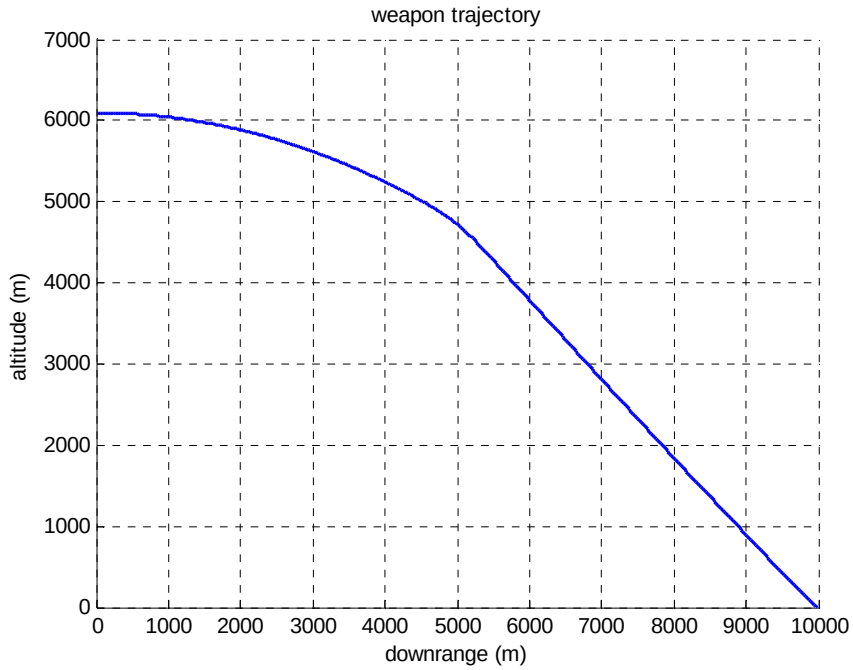

Figure 7-2 Weapon trajectory for a high altitude level delivery with BB control

One distinctive characteristic of the bang-bang control scheme is the continuous oscillations seen in some weapon variables. Important flight variables, especially the angle of attack, show an oscillatory behavior as seen for the lead angle in Figure 7-3. When the laser reflection enters the FOV of the seeker after the ballistic portion of flight, the weapon makes full down deflections until it falls beyond the LOS. After this phase, full up deflections are applied until the weapon again reaches above the LOS. When there is even a small-misalignment above the LOS, a full down command causes the weapon to dive again. The elevator deflections are seen in Figure 7-4. Longer up commands are required to compensate short down commands. Since the down direction can not be determined by the seeker as the only sensor of the weapon, the effect of gravity acts as a disturbance in all phases of flight. Note that the elevator deflections are cyclic during the guided phase of flight (Figure 7-4). Another important feature seen in Figure 7-5 is that as full canard deflections cause more drag and an increase in the angle of attack of the weapon system, this combined effect causes the weapon's velocity to decrease rapidly.

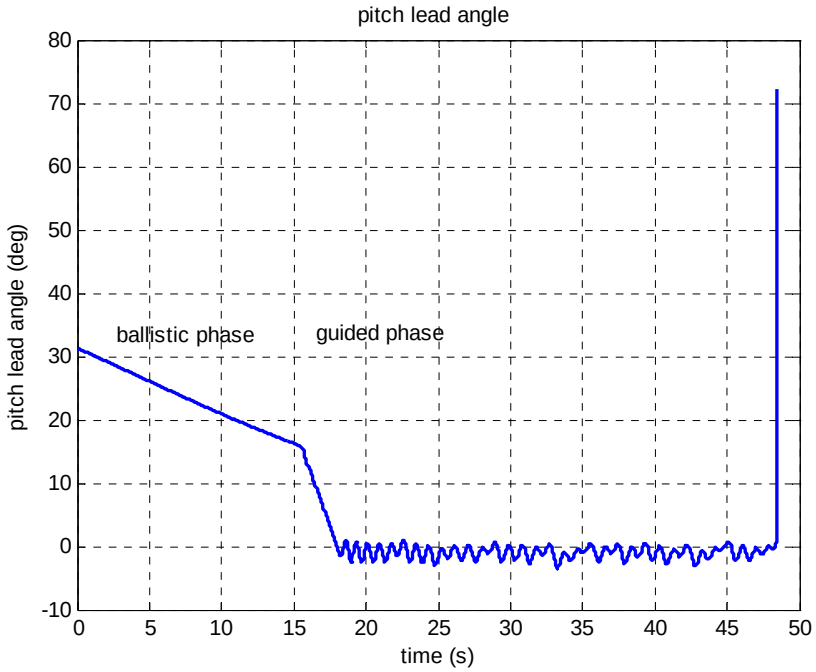

Figure 7-3 Pitch lead angle time history for a high altitude level delivery with BB control

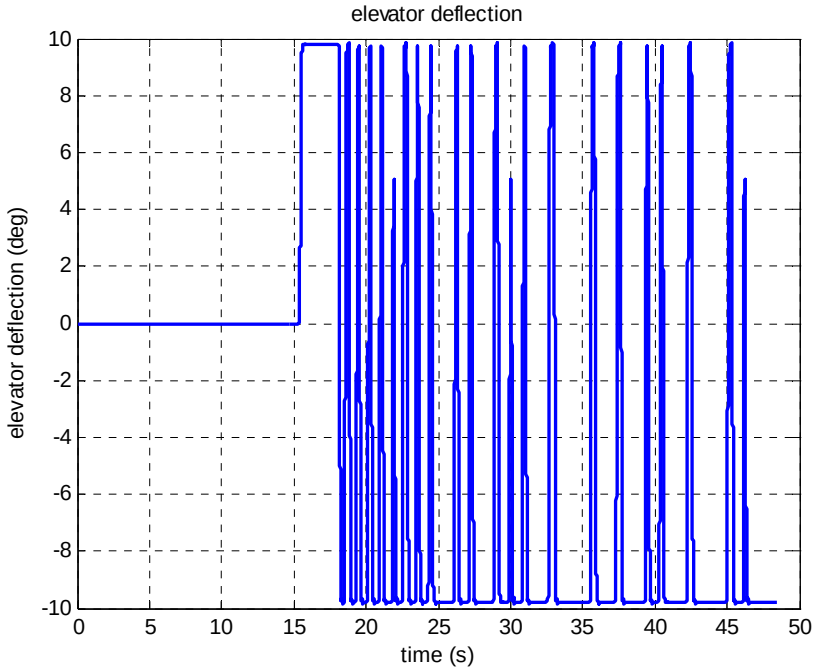

Figure 7-4 Elevator deflection time history for a high altitude level delivery with BB control

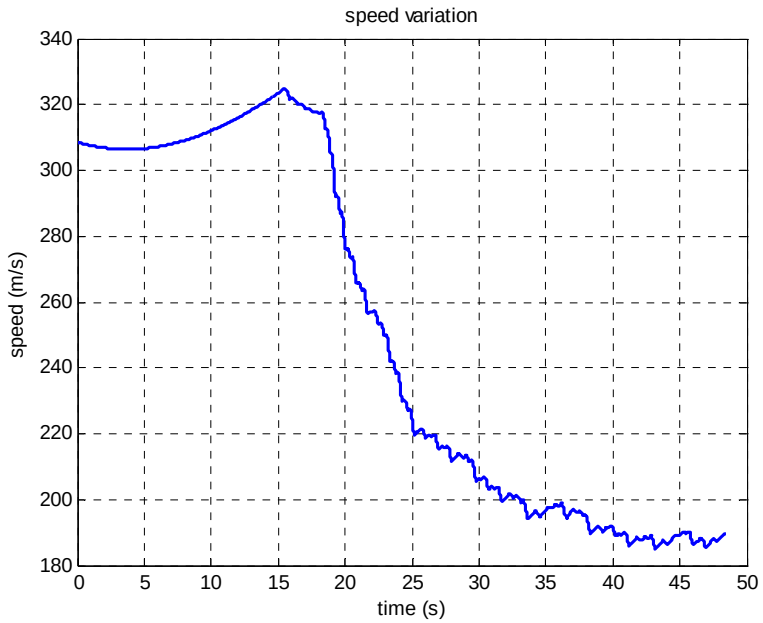

Figure 7-5 Total speed time history for a high altitude level delivery with BB control

BB Case-2: Parameters of this scenario are depicted in Table 7-2.

Table 7-2 High altitude dive delivery parameters with bang-bang control

Launch Conditions		
Control scheme	Bang-bang	
Deadzone width	None	
Delivery type	High altitude dive	
Release speed	600 knots (308 m/s)	
Release altitude	20,000 ft (6,096 m)	
Initial attitude in fixed frame		
Heading (deg)	Pitch angle (deg)	Roll angle (deg)
0	-30	0
Initial rotation rates		
p (deg/s)	q (deg/s)	r (deg/s)
0	0	0
Target variables		
Target type	stationary	
	Downrange (m)	Crossrange (m)
Initial target location	10,000	0
Final target location	10,000	0
Performance variables		
Miss distance (m)	Time of flight (s)	Impact speed (m/s)
11	55	181

Figure 7-6 shows the trajectory of the weapon in this high altitude dive scenario. The guided flight starts as soon as the weapon is released since the target is already in FOV. This can be seen in lead angle time history in Figure 7-7.

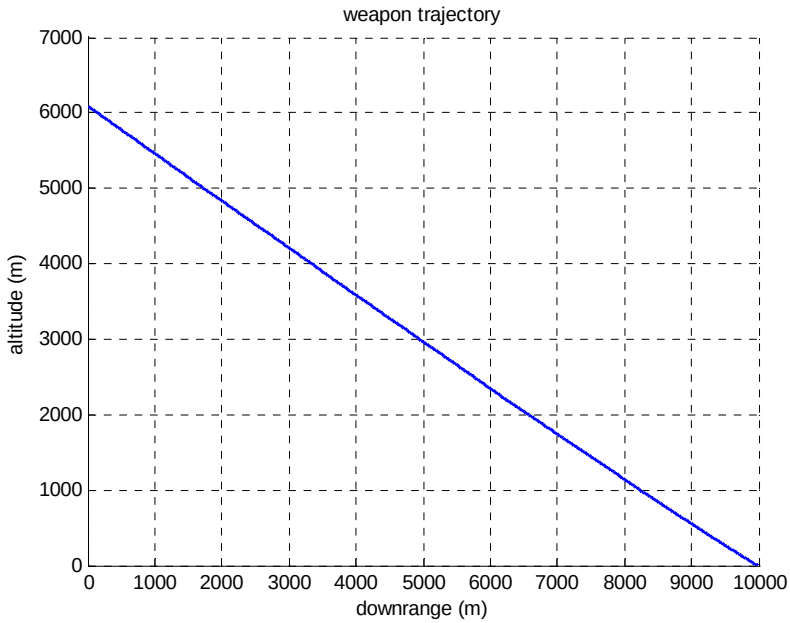

Figure 7-6 Weapon trajectory for a high altitude dive delivery with BB control

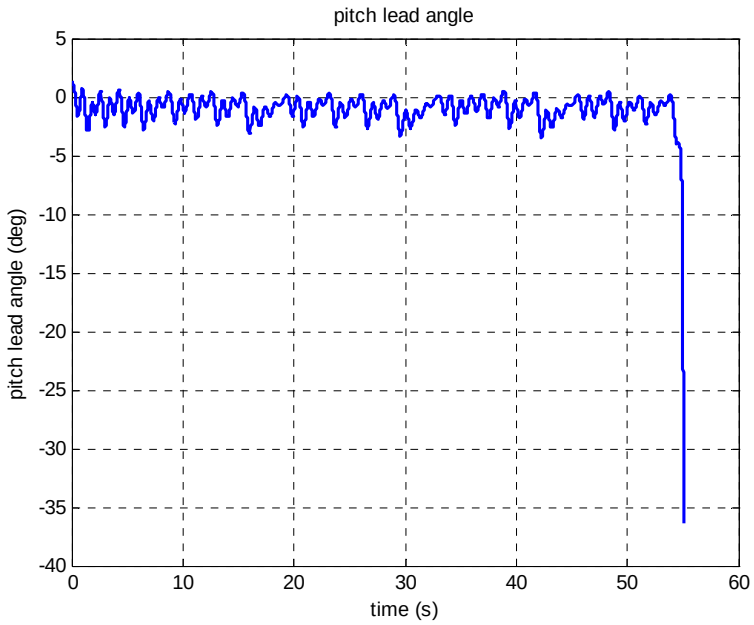

Figure 7-7 Pitch lead angle time history for a high altitude dive delivery with BB control

The elevator deflections start with the release of the weapon as seen in Figure 7-8. A longer guided flight time causes the weapon to lose more speed when compared with the high altitude level delivery as shown in BB case-I (Figure 7-9).

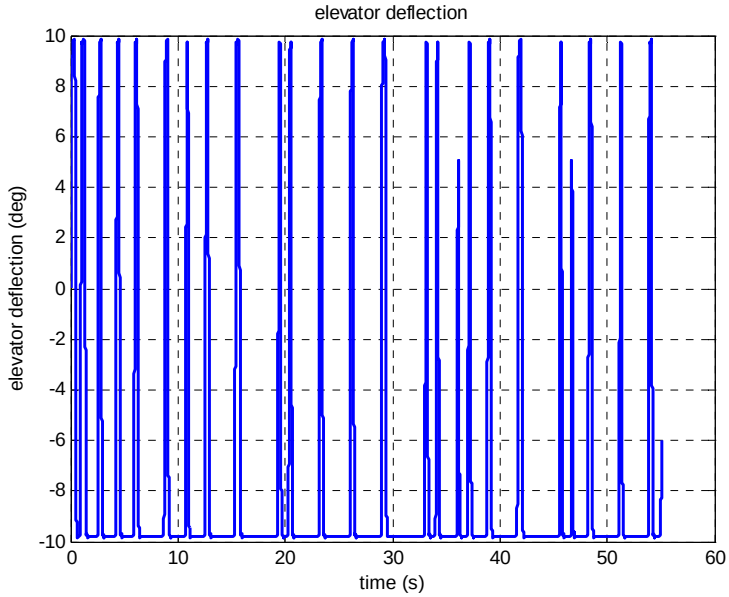

Figure 7-8 Elevator deflection time history for a high altitude dive delivery with BB control

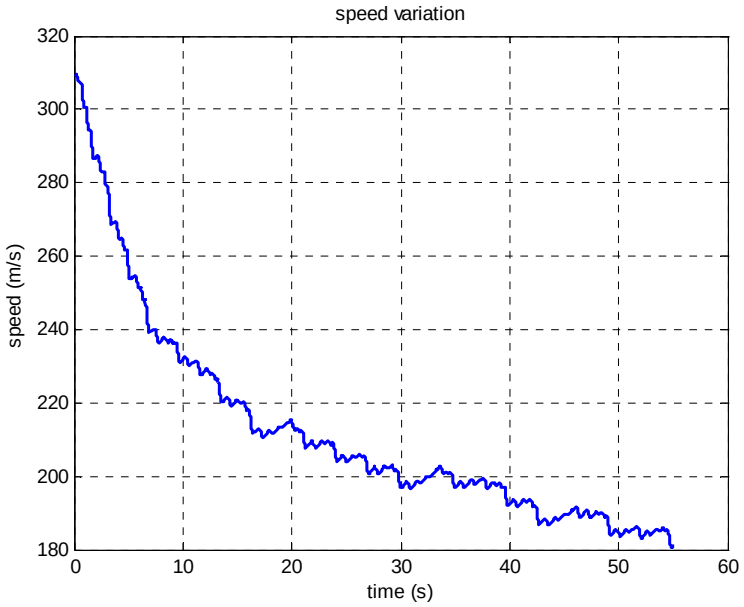

Figure 7-9 Total speed time history for a high altitude dive delivery with BB control

The weapon experiences high angle of attack values with BB control scheme due to full scale cyclic canard deflections as seen in Figure 7-10.

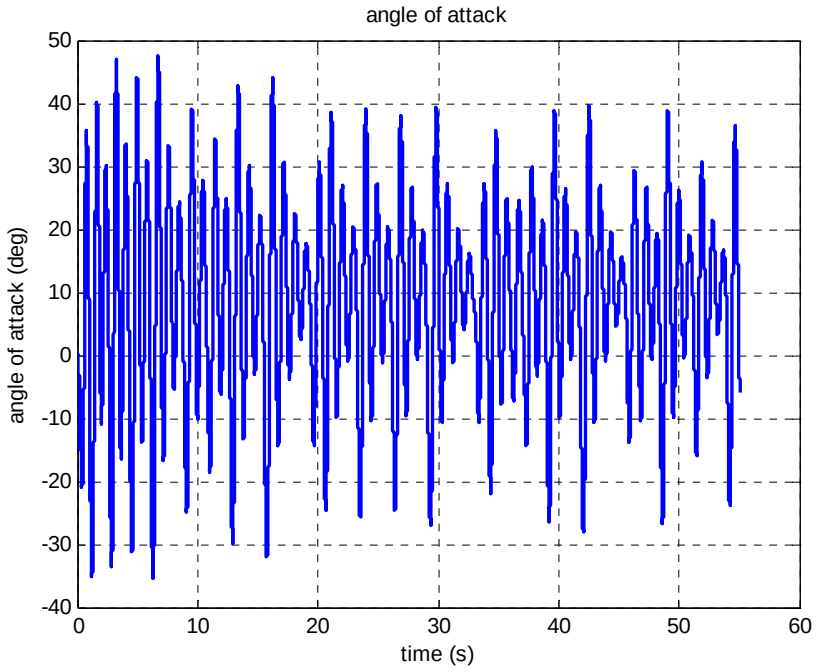

Figure 7-10 Angle of attack time history for a high altitude dive delivery with BB control

BB Case-3: Low altitude toss scenario parameters are seen in Table 7-3. The simulation results show that the weapon is turning down too early to boresight the laser energy especially in toss deliveries, reducing its range. All attempts to reach longer range targets are unsuccessful. For low level toss deliveries, if the weapon sees the laser energy too early, it tries to eliminate the lead angle by a full down command, which prevents the weapon from climbing further and achieving a higher altitude, thus a longer range. The miss distance value is much higher in this type of delivery since the weapon can not climb enough, and falls short of the target (Table 7-3). Figure 7-11 shows how the weapon prematurely turns down before reaching apogee of its ballistic flight path.

Table 7-3 Low altitude toss delivery parameters with bang-bang control

Launch Conditions		
Control scheme	Bang-bang	
Deadzone width	None	
Delivery type	Low altitude toss	
Release speed	600 knots (308 m/s)	
Release altitude	1,000 ft (305 m)	
Initial attitude in fixed frame		
Heading (deg)	Pitch angle (deg)	Roll angle (deg)
0	10	0
Initial rotation rates		
p (deg/s)	q (deg/s)	r (deg/s)
0	0	0
Target variables		
Target type	stationary	
	Downrange (m)	Crossrange (m)
Initial target location	3,000	0
Final target location	3,000	0
Performance variables		
Miss distance (m)	Time of flight (s)	Impact speed (m/s)
37	13	183

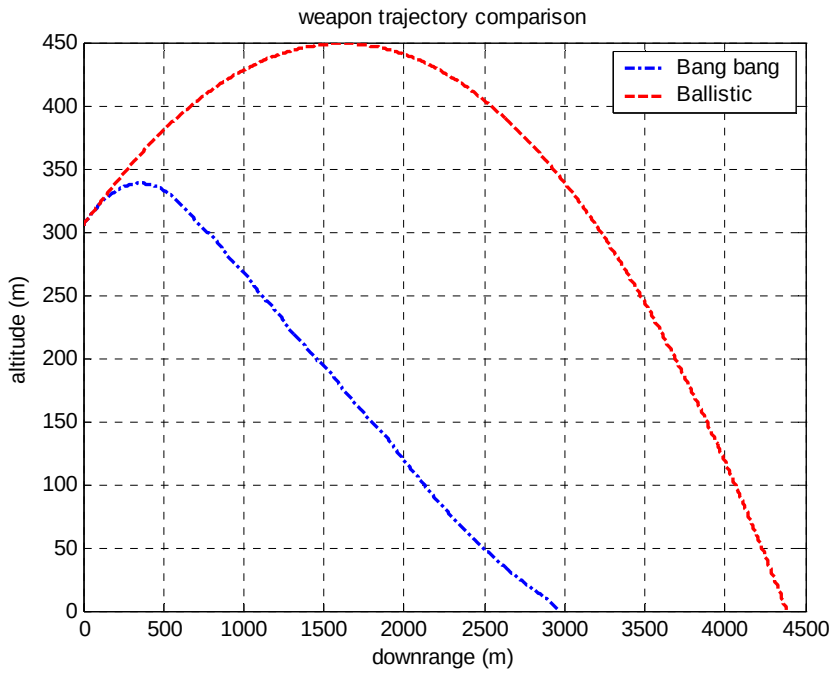

Figure 7-11 Comparison of BB and ballistic trajectories in toss delivery

The pitch lead angle value is reduced as soon as the laser reflection is in the FOV of the weapon by full deflections as seen in Figure 7-12, and Figure 7-13.

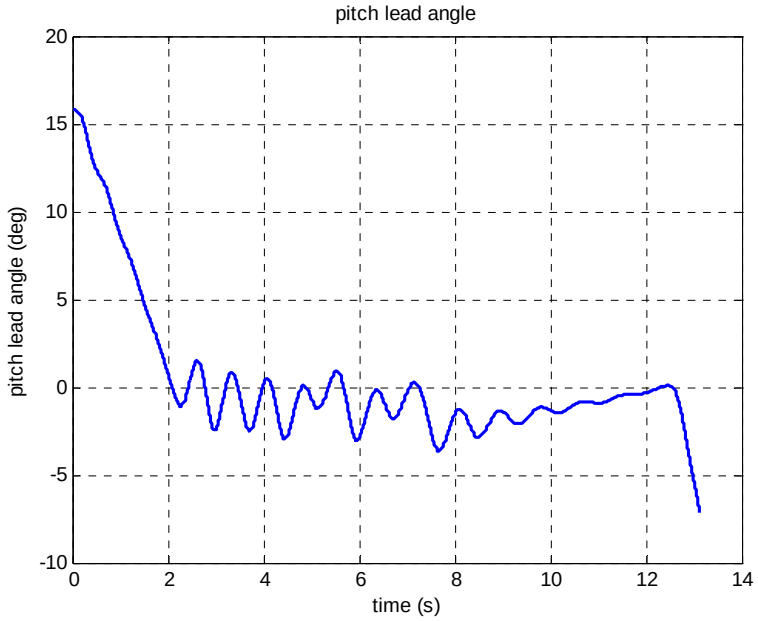

Figure 7-12 Pitch lead angle time history for a low altitude toss delivery with BB control

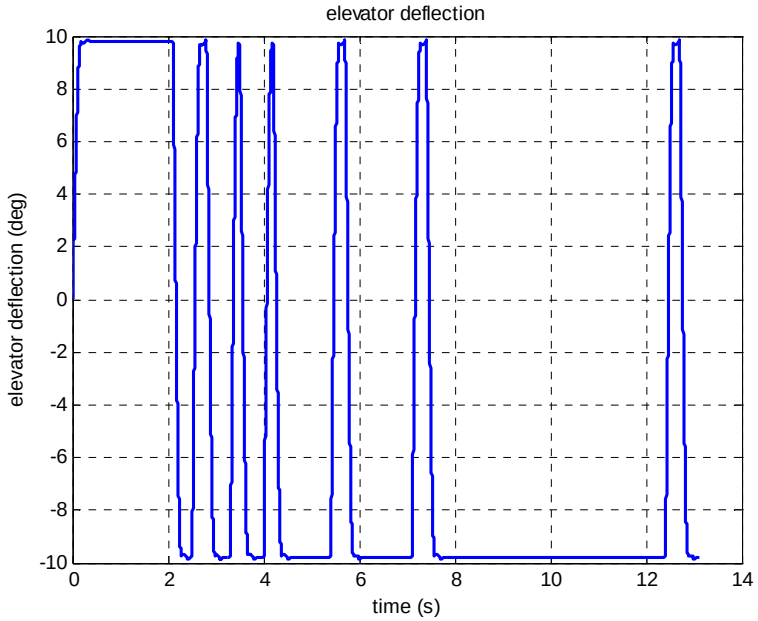

Figure 7-13 Elevator deflection time history for a low altitude toss delivery with BB control

The two second duration down deflection in the first phase of flight causes rapid turn down which is barely compensated with longer up commands at the terminal phase of flight (Figure 7-13).

The total speed shows the same decreasing behavior with previous cases. During constant canard deflection phase in 0-2'nd and 8-12'th second intervals, speed decrease becomes steady (Figure 7-14), and angle of attack converges around ±10 degrees (Figure 7-15).

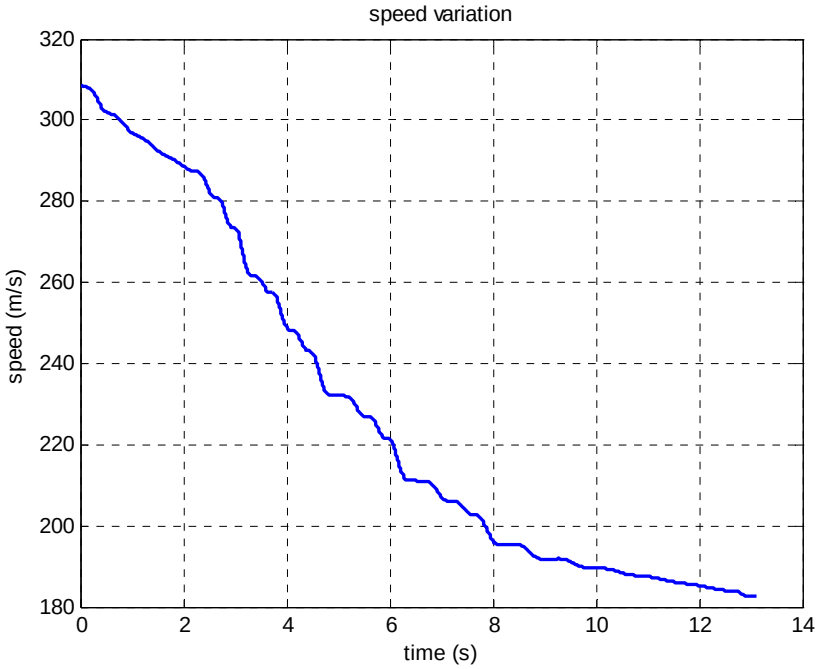

Figure 7-14 Total speed time history for a low altitude toss delivery with BB control

Another property of the weapon is noticed that, the release speed affects the weapon's miss distance. For a sample release condition from 10,000 ft (3,048 m) against a target located 10,000 meters downrange, the miss distance can be reduced by increasing the release speed as shown in Figure 7-16.

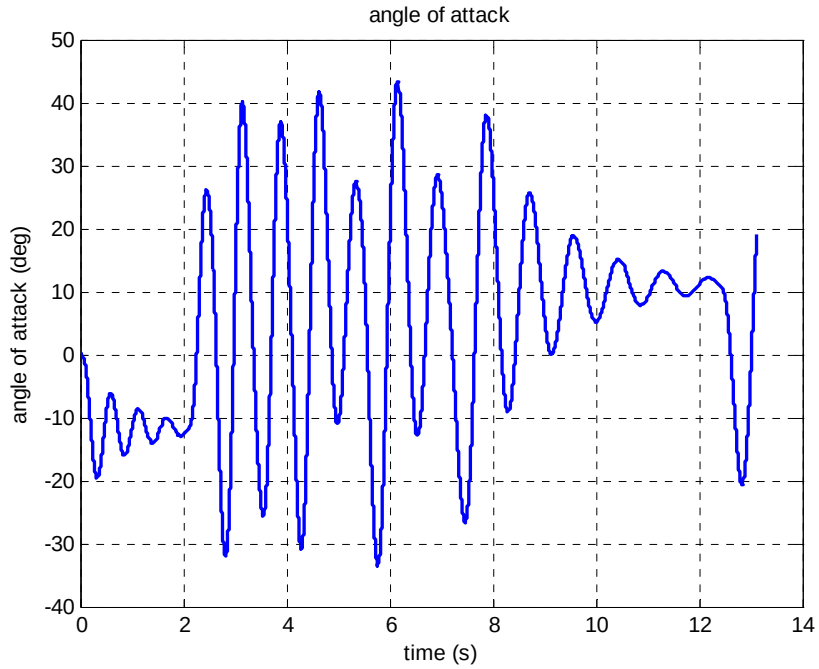

Figure 7-15 Angle of attack time history for a low altitude toss delivery with BB control

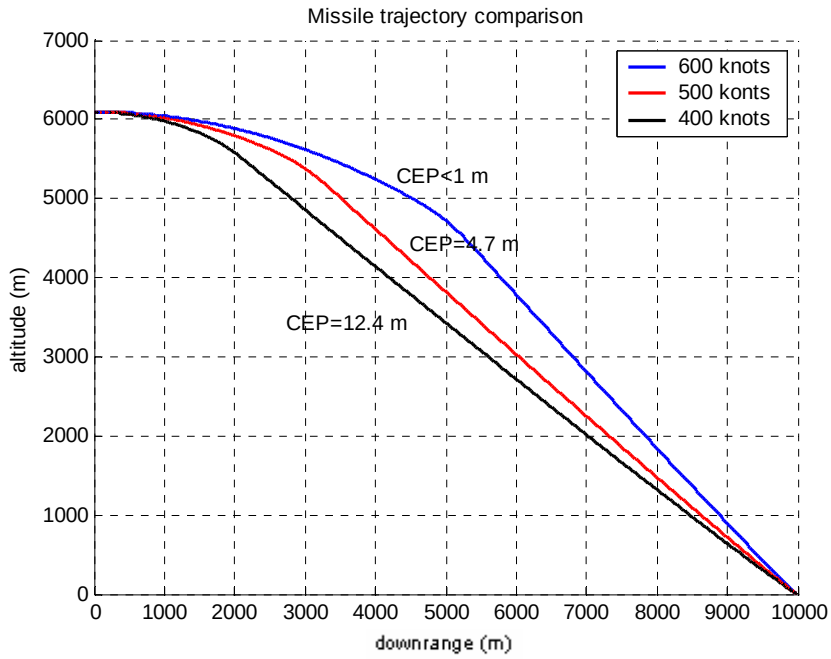

Figure 7-16 Effect of release speed on miss distance with BB control

BB Case-4: This scenario is given as an example to the moving target intercept capability of BB control. Scenario parameters are shown in Table 7-4. This scenario is selected at the limit where the target intercept becomes impossible as the range is further increased. The BB control scheme seems to be incapable when dealing with moving targets within medium and long ranges. The miss distance reaches unacceptable values as the target range increases. The weapon flight path is oscillatory both in yaw and pitch planes (Figure 7-17 and Figure 7-18).

Pitch lead angles tend to increase when the target is approached due to canard deflections and speed loss (Figure 7-19). Maintaining yaw lead angle becomes harder at the final seconds of flight (Figure 7-20). If the range is further increased, oscillations on the lead angle reach FOV limit. Full yaw and pitch canard deflections cause out of FOV maneuvers after which weapon flies ballistic This is mostly seen when the target is approached.

Table 7-4 Dive delivery parameters against moving target with BB control

Launch Conditions		
Control scheme	Bang-bang	
Deadzone width	None	
Delivery type	medium altitude dive	
Release speed	600 knots (308 m/s)	
Release altitude	10,000 ft (3048 m)	
Initial attitude in fixed frame		
Heading (deg)	Pitch angle (deg)	Roll angle (deg)
0	-20	0
Initial rotation rates		
p (deg/s)	q (deg/s)	r (deg/s)
0	0	0
Target variables		
Target type	sinusodial evading	
	Downrange (m)	Crossrange (m)
Initial target location	4,000	0
Final target location	3,992	207
Performance variables		
Miss distance (m)	Time of flight (s)	Impact speed (m/s)
109	26	121

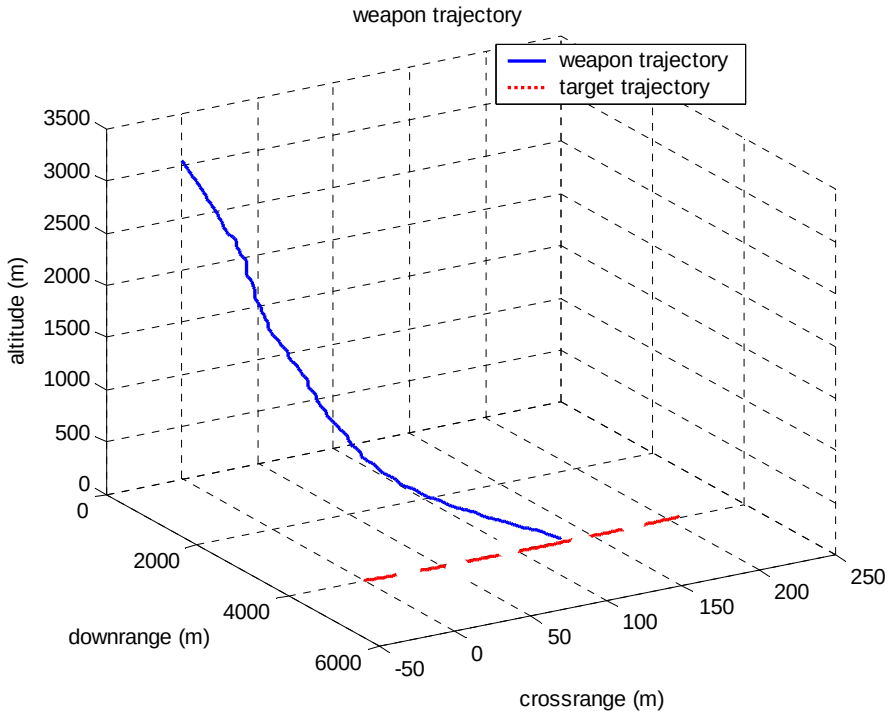

Figure 7-17 Weapon trajectory for a medium altitude high speed dive delivery against an evading target with BB control

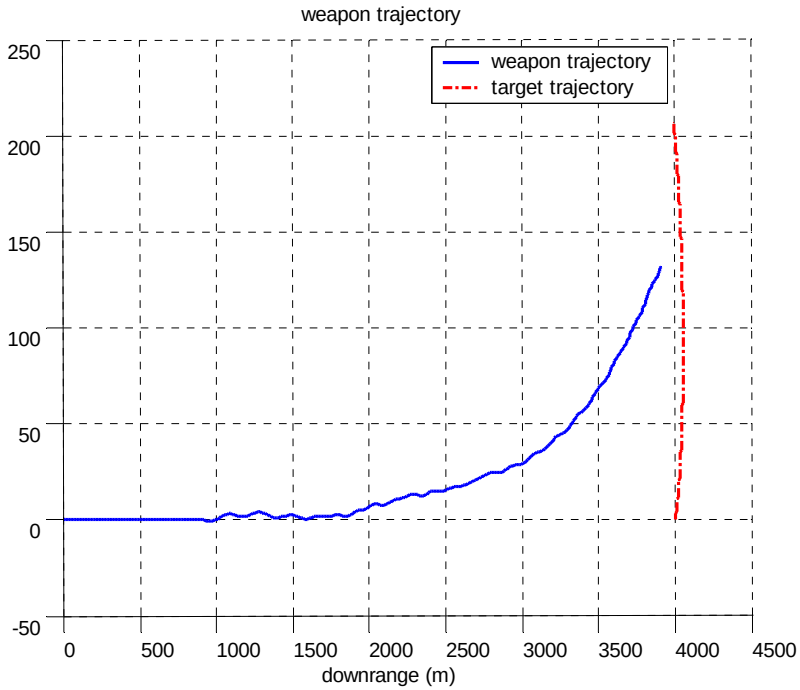

Figure 7-18 Weapon trajectory for a medium altitude high speed dive delivery against an evading target with BB control (top view)

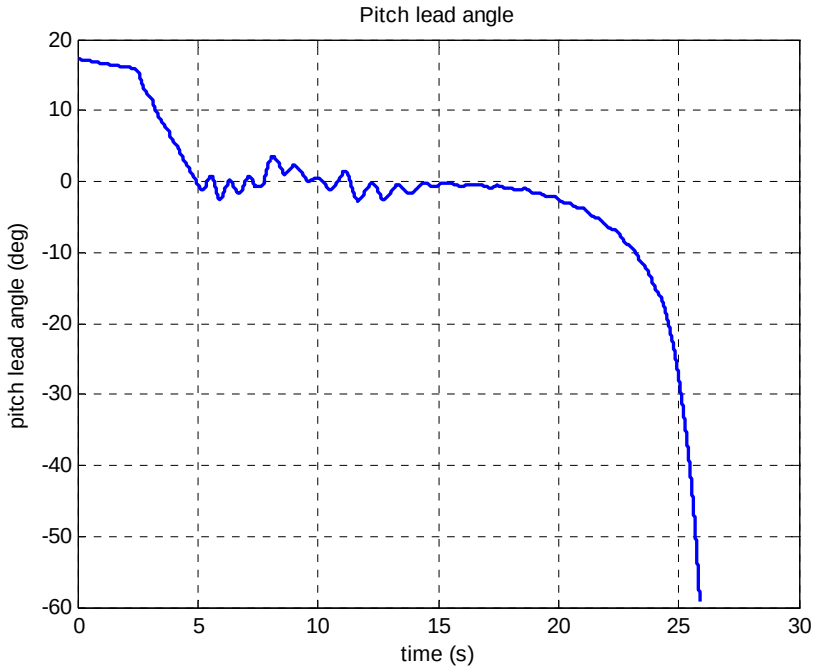

Figure 7-19 Pitch lead angle time history for a medium altitude high speed dive delivery against an evading target with BB control

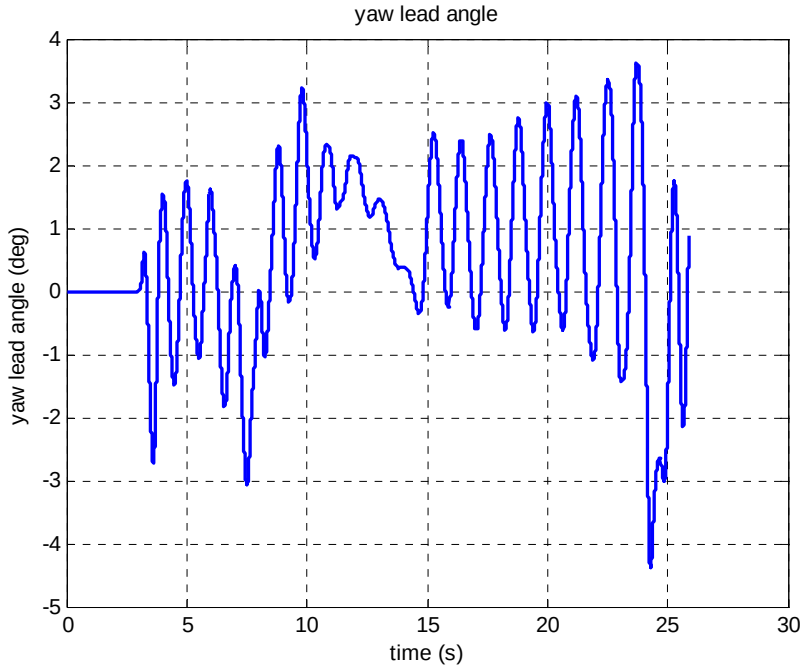

Figure 7-20 Yaw lead angle time history for a medium altitude high speed dive delivery against an evading target with BB control

The main characteristics of the bang-bang control scheme can be summarized in the light of simulation studies as follows.

- Within a specified range envelope, the weapon's performance is satisfactory when released from a high altitude and with a high speed in both dive and level launches.
- The speed decreases rapidly with time due to cyclic full canard deflections.
- Important weapon variables show oscillations due to cyclic canard deflections.
- The system's range is limited due to a high drag and energy dissipation.
- Moving target intercept efficiency decreases rapidly with range.

7.4 RESULTS FOR BANG-TRAIL-BANG (BTB) CONTROL SCHEME

7.4.1 DEADZONE ANALYSIS

In the bang-bang control, it is seen that, there are always up and down commands whatever the magnitude of error is. This causes high oscillations and degrades the weapon's performance. In order to improve the performance and decrease oscillations, a deadzone is introduced to the bang-bang control scheme. By this way, no canard deflections will be produced until the lead angle error exceeds a specified limit. This type of control is commonly named as "3-position" or "bang-trail-bang" (BTB) control.

In order to investigate the results of BTB control, it is necessary to decide on the deadzone width. For this purpose, several scenarios are run and range, miss distance, etc. are monitored.

Simulation results performed with very small deadzones such as 0.05 Volts resemble the results obtained with the bang-bang control. Figure 7-21, Figure 7-22, and Figure 7-23 shows the elevator deflections for a sample high altitude level launch scenario from 20,000 ft (6,096 m) with 600 knots (308 m/s) release speed. Down deflections are generated when the weapon has a slightly positive lead angle as seen in Figure 7-21. This degrades the accuracy of weapon by increasing the miss distance. Elevator deflections for 0.1 and 0.3V deadzone widths are given in Figure 7-22, and Figure 7-23.

A 0.1 Volt deadzone width gives better results than wider deadzones like 0.3 Volts. Wide deadzones reduce the performance of the weapon, since once the weapon enters below the LOS, all “up” commands are terminated before it reaches LOS again due to a large deadzone width, so there exists a greater offset in lead angle error as seen in Figure 7-24.

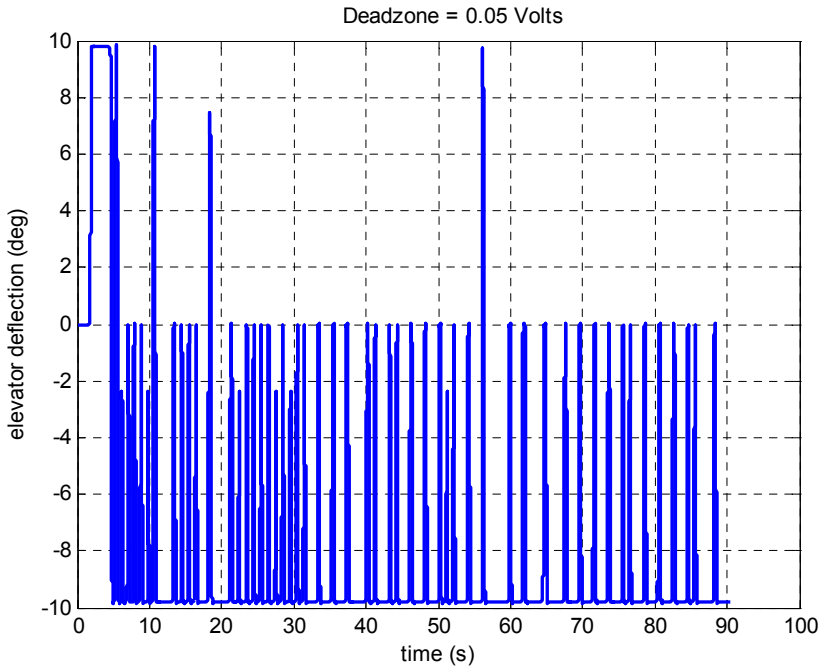

Figure 7-21 Elevator deflection time history with 0.05V deadzone width with BTB control

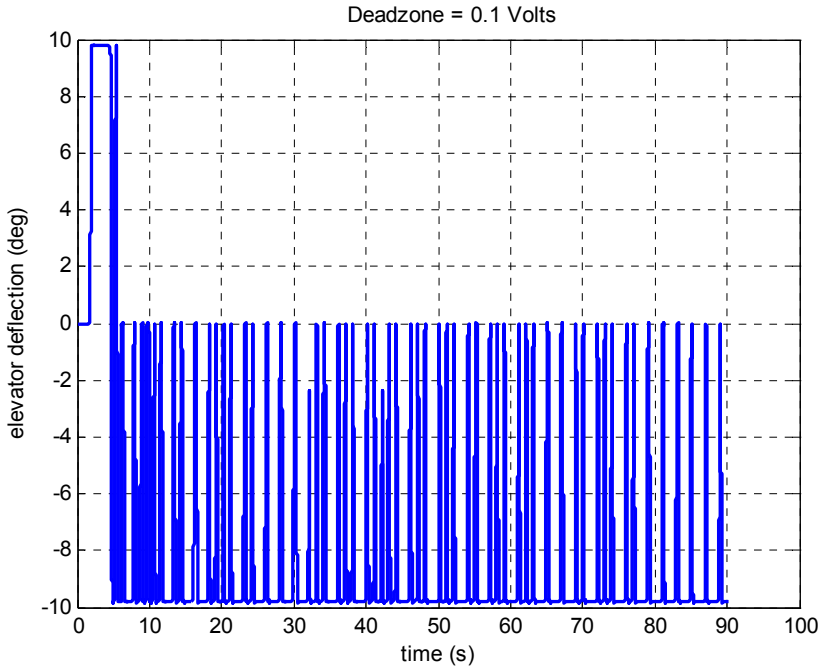

Figure 7-22 Elevator deflection time history with 0.1V deadzone width with BTB control

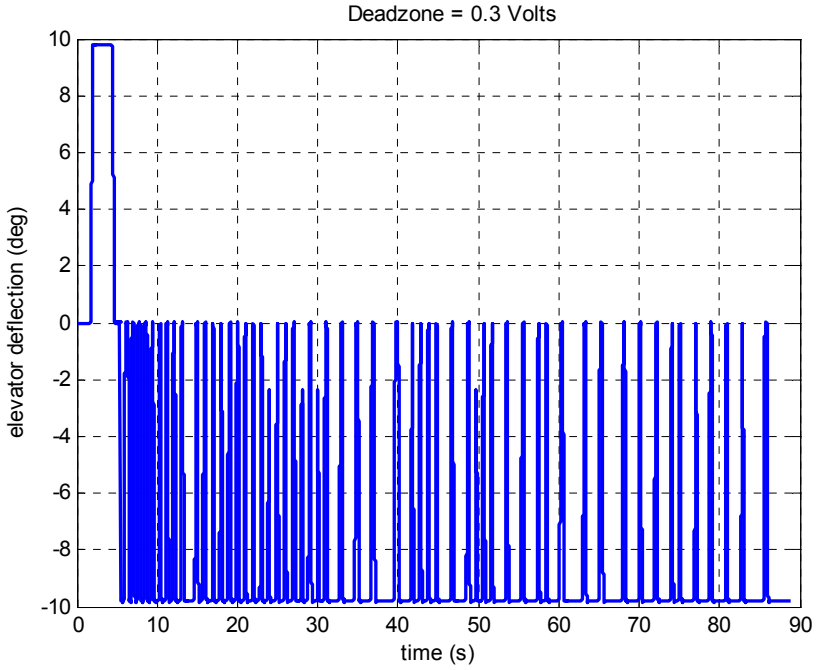

Figure 7-23 Elevator deflection time history with 0.3V deadzone width with BTB control

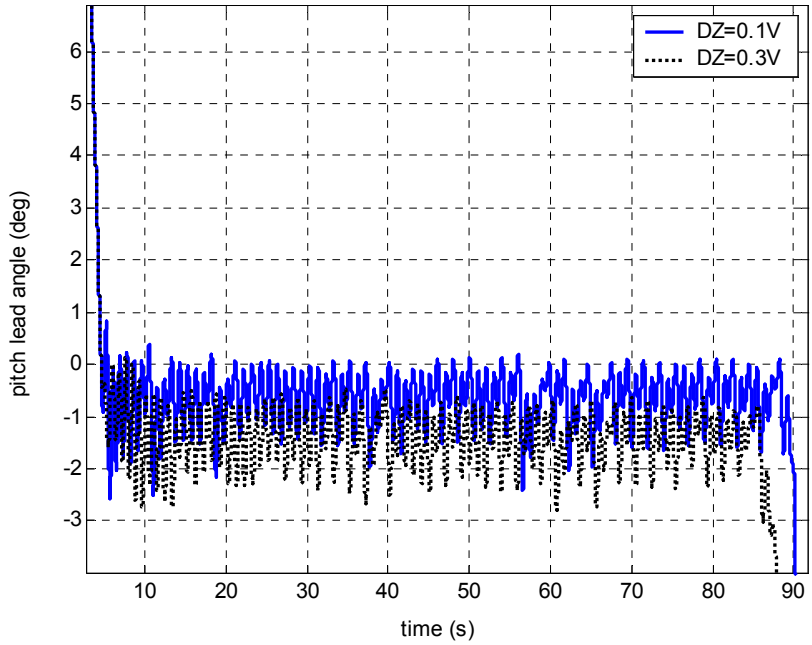

Figure 7-24 Effect of two different deadzones on pitch lead angle with BTB control

Deadzone width heavily effects the miss distance, and if the miss distance is taken as the primary criteria for weapon's success, wide deadzones are not much effective in increasing range. Another important fact is that, the deadzone is most useful in long range intercepts. There is no significant improvement in short range deliveries.

In the light of multiple scenario runs, it is decided to use a deadzone width of 0.1V for the rest of the studies.

7.4.2 RESULTS FOR SOME BTB SCENARIOS

BTB Case-1: Parameters of this case are given in Table 7-5. BTB control increases the range of the weapon when compared with BB control, especially in high altitude deliveries while maintaining the miss distance as seen from Table 7-5. An oscillatory lead angle behavior is seen in Figure 7-26.

Table 7-5 High altitude level delivery parameters with BTB control

Launch Conditions		
Control scheme	Bang-trail-bang (3 position control)	
Deadzone width	0.1 Volts	
Delivery type	High altitude level	
Release speed	600 knots (308 m/s)	
Release altitude	20,000 ft (6,096 m)	
Initial attitude in fixed frame		
Heading (deg)	Pitch angle (deg)	Roll angle (deg)
0	0	0
Initial rotation rates		
p (deg/s)	q (deg/s)	r (deg/s)
0	0	0
Target variables		
Target type	stationary	
	Downrange (m)	Crossrange (m)
Initial target location	18,000	0
Final target location	18,000	0
Performance variables		
Miss distance (m)	Time of flight (s)	Impact speed (m/s)
9	90	179

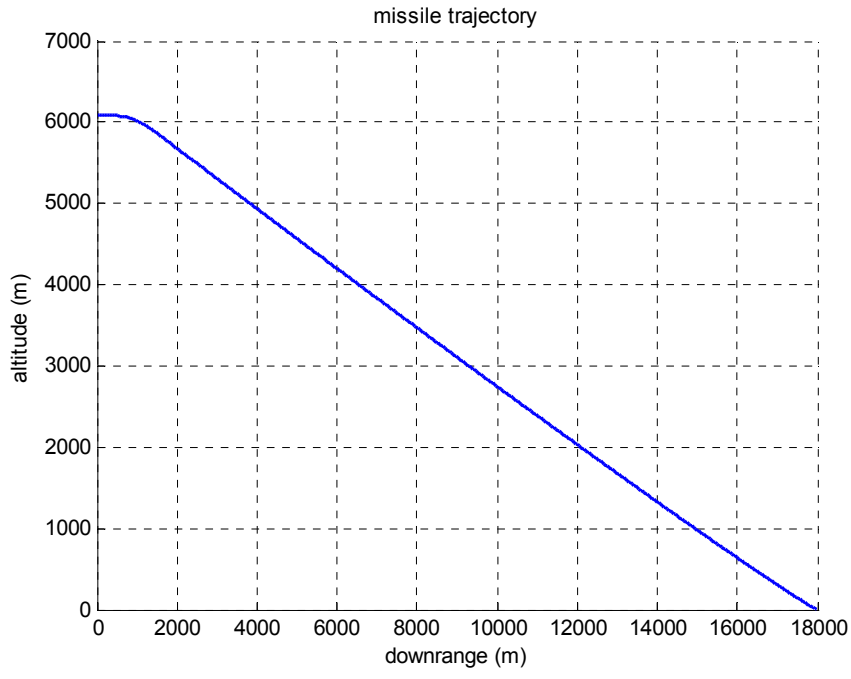

Figure 7-25 Weapon trajectory for a high altitude level delivery with BTB control

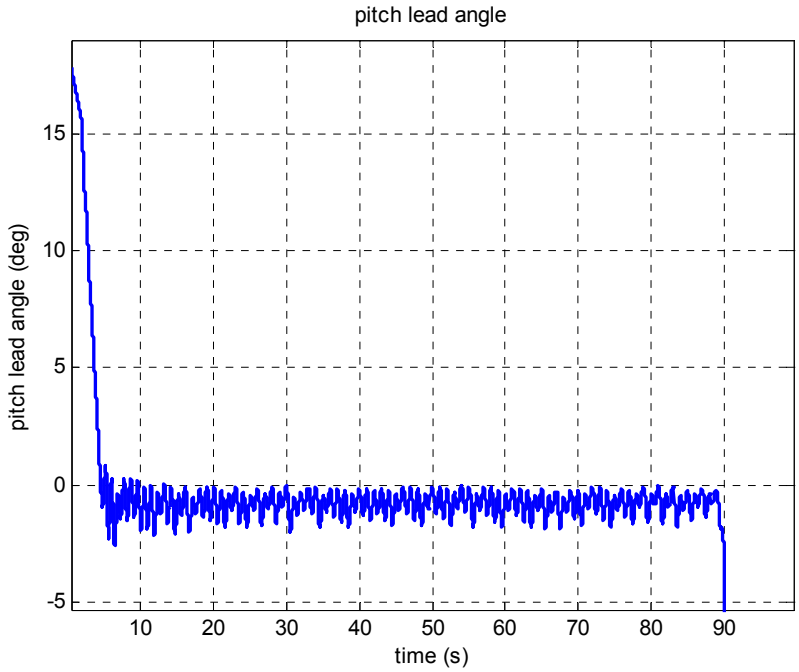

Figure 7-26 Pitch lead angle time history for a high altitude level delivery with BTB control

Unlike the BB control, cyclic elevator deflections are not seen except for the first seconds of flight. 0 degrees and 10 degrees up commands are seen in most of the flight time especially in long range deliveries where the weapon tries to maintain itself on the LOS (Figure 7-27).

The oscillatory behavior in flight variables still exists with the BTB control.(Figure 7-28, Figure 7-29). The deadzone does not eliminate the oscillations but decreases their magnitude slightly.

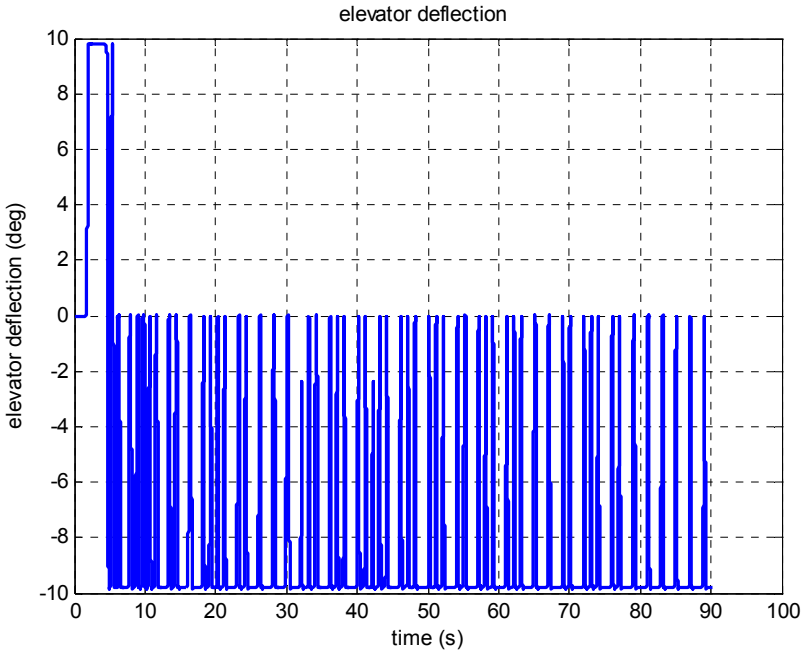

Figure 7-27 Elevator deflection time history for a high altitude level delivery with BTB control

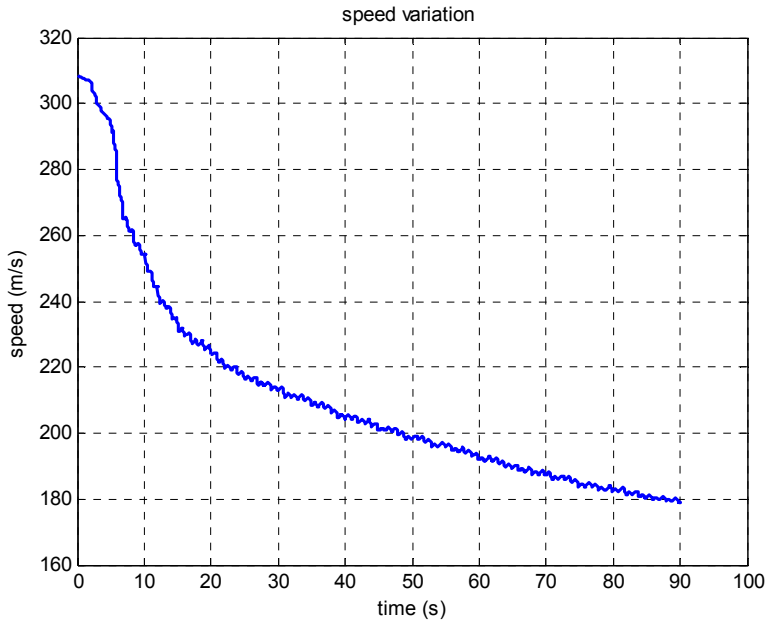

Figure 7-28 Total speed time history for a high altitude level delivery with BTB control

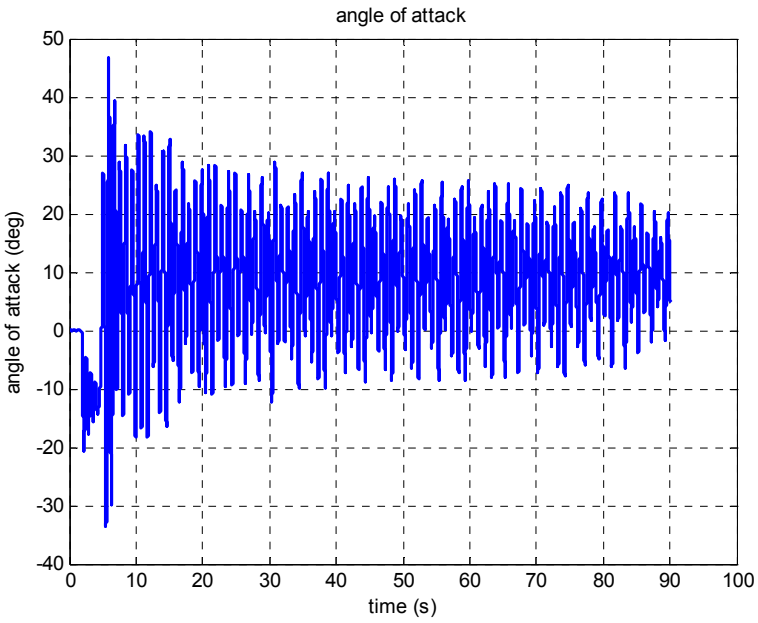

Figure 7-29 Angle of attack time history for a high altitude level delivery with BTB control

BTB Case-2: Simulation parameters for this scenario are seen in Table 7-6.

Table 7-6 High altitude dive delivery parameters with BTB control

Launch Conditions		
Control scheme	Bang-trail-bang (3 position control)	
Deadzone width	0.1 Volts	
Delivery type	High altitude dive	
Release speed	600 knots (308 m/s)	
Release altitude	20,000 ft (6,096 m)	
Initial attitude in fixed frame		
Heading (deg)	Pitch angle (deg)	Roll angle (deg)
0	-30	0
Initial rotation rates		
p (deg/s)	q (deg/s)	r (deg/s)
0	0	0
Target variables		
Target type	sationary	
	Downrange (m)	Crossrange (m)
Initial target location	16,000	0
Final target location	16,000	0
Performance variables		
Miss distance (m)	Time of flight (s)	Impact speed (m/s)
9	80	181

Figure 7-30 shows the weapon's trajectory in this dive delivery. The lead angle starts from negative values since a 30 degrees dive is performed (Figure 7-31).

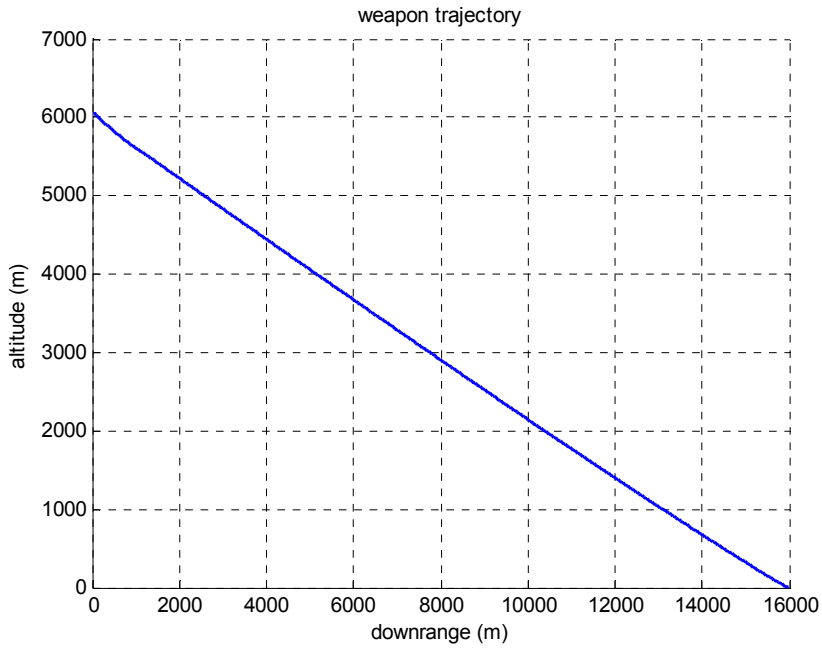

Figure 7-30 Weapon trajectory for a high altitude dive delivery with BTB control

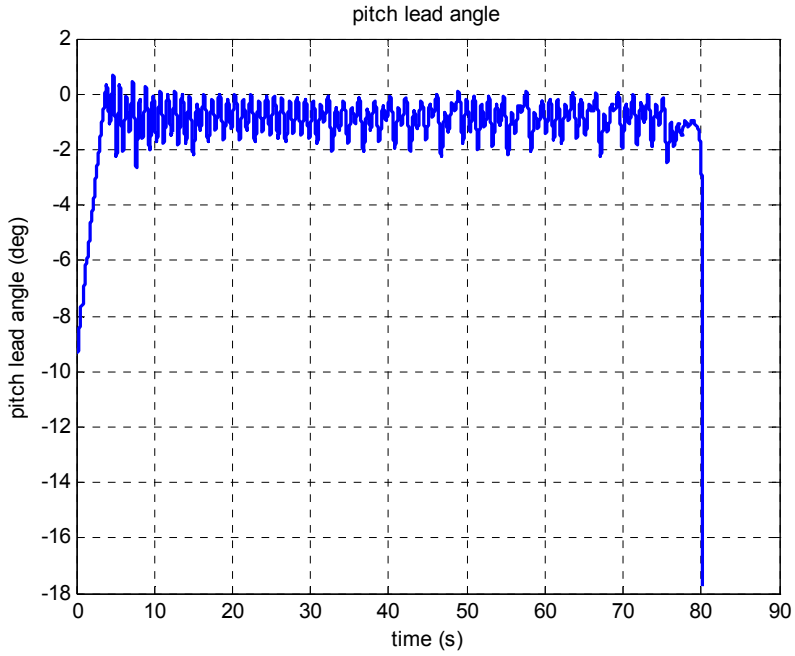

Figure 7-31 Pitch lead angle time history for a high altitude dive with BTB control

When the weapon is boresighted on the LOS, it assumes a combination of up and zero commands till impact on the target (Figure 7-32). The speed decrease and the oscillatory a.o.a behavior is like the BB cases (Figure 7-33). (Figure 7-34).

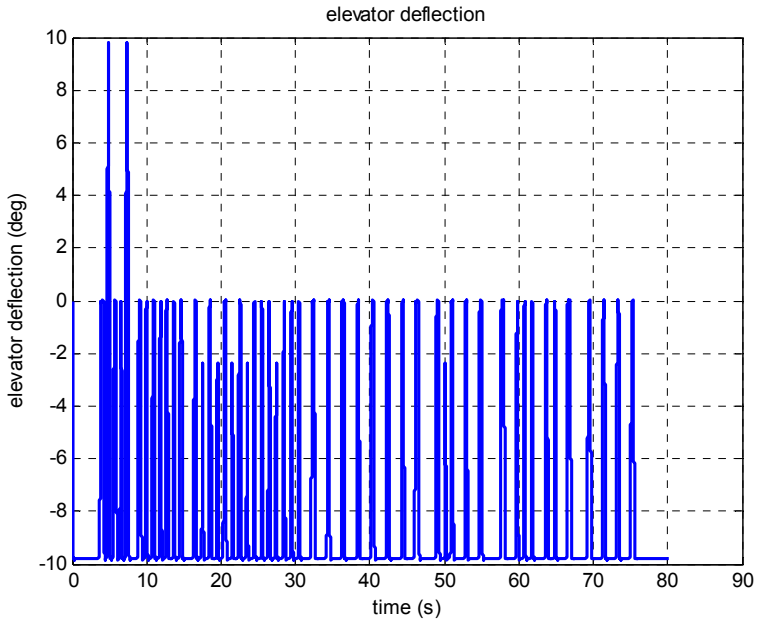

Figure 7-32 Elevator deflection time history for a high altitude dive with BTB control

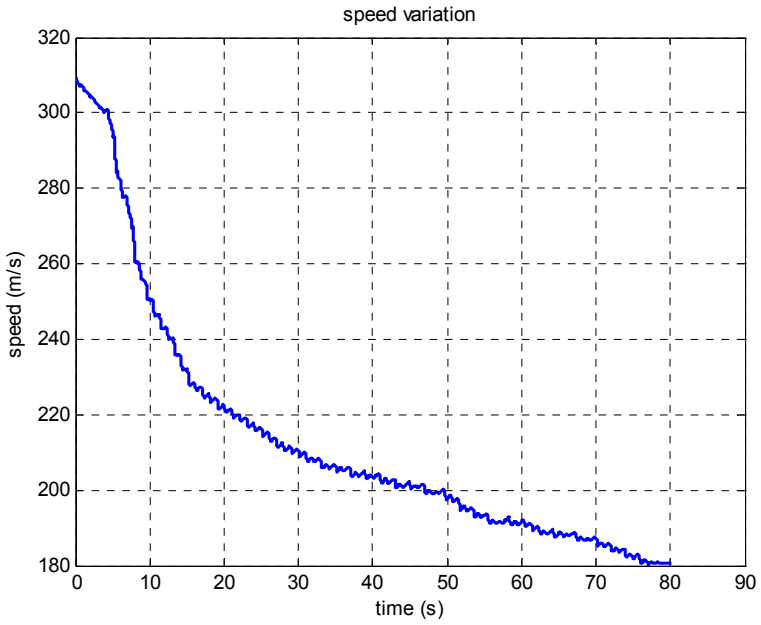

Figure 7-33 Total speed time history for a high altitude dive with BTB control

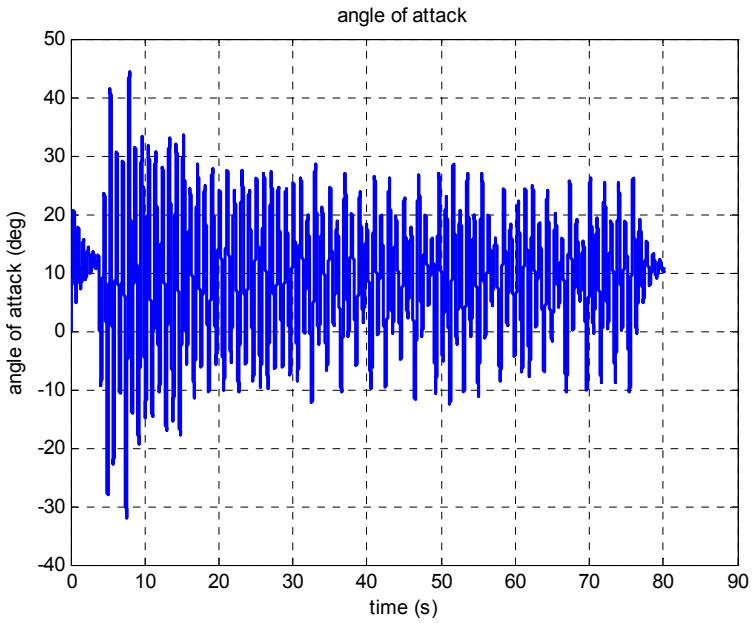

Figure 7-34 Angle of attack time history for a high altitude dive with BTB control

BTB Case-3: Primary parameters of the scenario are given in Table 7-7.

Table 7-7 Low altitude toss delivery parameters with BTB control

Launch Conditions		
Control scheme	Bang-trail-bang (3 position control)	
Deadzone width	0.1 Volts	
Delivery type	Low altitude toss	
Release speed	600 knots (308 m/s)	
Release altitude	20,000 ft (6,096 m)	
Initial attitude in fixed frame		
Heading (deg)	Pitch angle (deg)	Roll angle (deg)
0	10	0
Initial rotation rates		
p (deg/s)	q (deg/s)	r (deg/s)
0	0	0
Target variables		
Target type	stationary	
	Downrange (m)	Crossrange (m)
Initial target location	3,000	0
Final target location	3,000	0
Performance variables		
Miss distance (m)	Time of flight (s)	Impact speed (m/s)
23	12	196

This scenario is an example to the effects of deadzone in low altitude deliveries. The low altitude toss delivery characteristics resemble BB control. Results are given seen in Figure 7-35 and Figure 7-36.

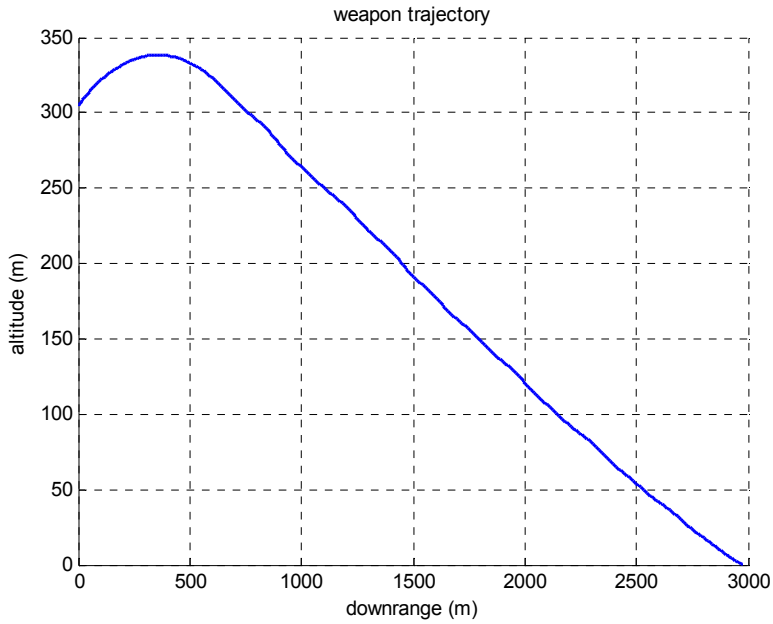

Figure 7-35 Weapon trajectory for a low altitude toss with BTB control

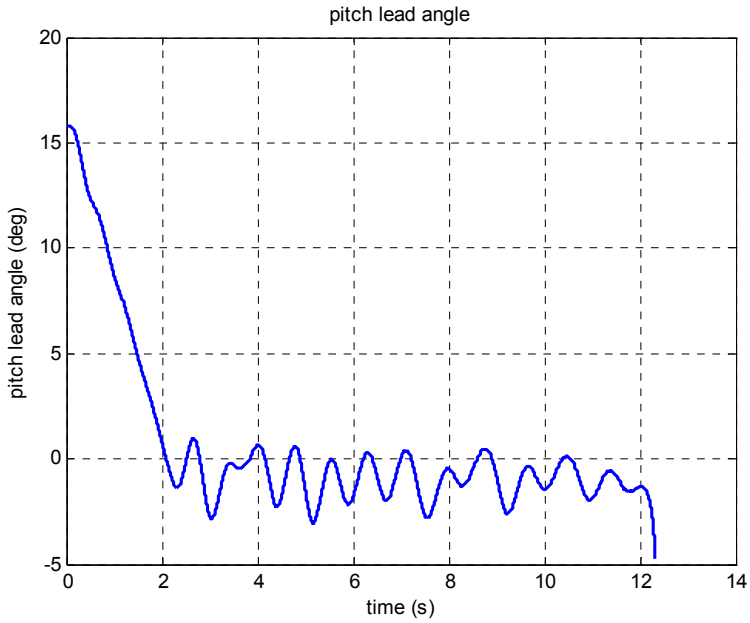

Figure 7-36 Pitch lead angle time history for a low altitude toss with BTB control

The elevator deflections show that (Figure 7-37) the weapon turns down with full deflections in the first seconds of flight, and tries to maintain itself around the LOS. A.o.a oscillations are experienced in this scenario, too (Figure 7-38).

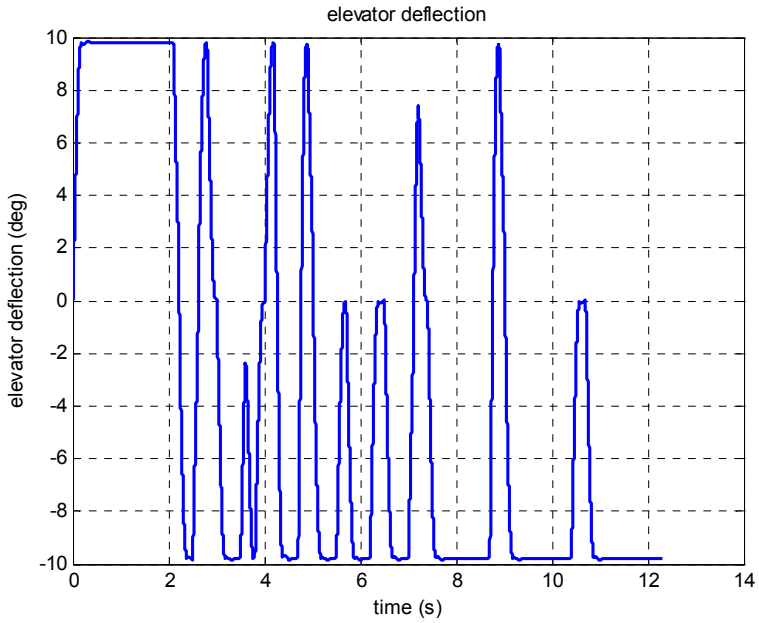

Figure 7-37 Elevator deflection time history for a low altitude toss with BTB control

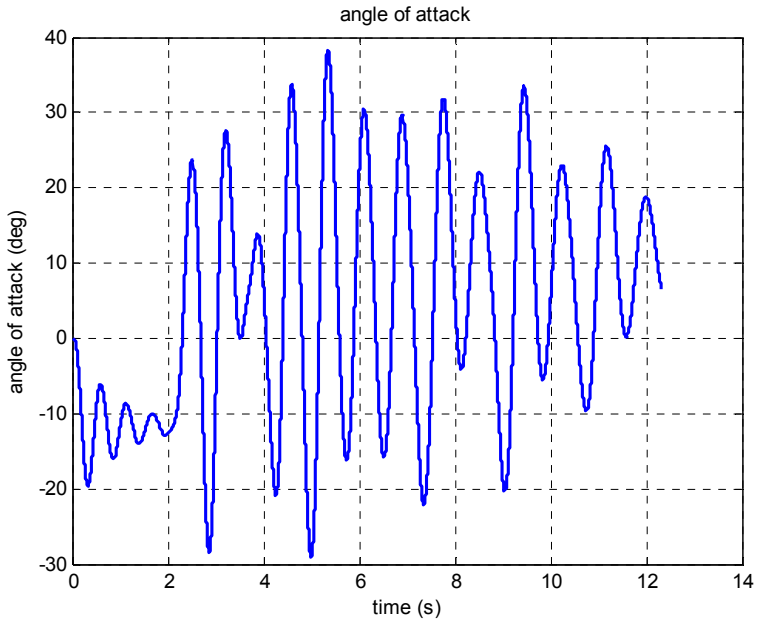

Figure 7-38 Angle of attack time history for a low altitude toss with BTB control

Simulation results show that the BTB control provides a range increase for high altitude level releases as shown in BTB Case-1. On the contrary, its performance is almost same with BB control at short range, low altitude scenarios (BTB case-3).

The deadzone decreases the number of canard deflections (therefore resulting in less energy dissipation) and the oscillations decrease slightly. However, these improvements are not significant. Oscillatory behavior in flight variables is still continuing in BTB scenarios as in BB cases.

As a conclusion, the behavior of BTB control is similar to BB control with some improvements in range.

7.4.3 EFFECT OF MAXIMUM CANARD DEFLECTON VALUE ON THE SYSTEM PERFORMANCE WITH BTB CONTROL SCHEME

From the simulation results regarding BB and BTB control schemes, it can be stated that a 10 degrees maximum canard deflection may introduce too large corrective actions for the weapon. Therefore, it is thought that the oscillation levels might be decreased if a smaller maximum canard deflection is chosen. With this idea in mind, it is decided to re-examine BB and BTB control schemes with smaller maximum canard deflection limits in order to investigate the feasibility of using smaller canard deflections.

For this purpose, 5 degrees maximum canard deflection limit is employed and the weapon performance is monitored for different launch scenarios. Since it is possible to correct small lead angle misalignments with small deflections, it is expected that 5 degrees BB and BTB schemes would perform better than 10 degree cases. The simulation results show that this hypothesis is true only for long range launches with a high speed, where smaller canard deflections provide less drag and make the weapon reach longer ranges with more impact speeds. However, the same does not seem to be true for low-medium altitude deliveries where release speed is low. For a sample low speed level delivery from 5,000 ft (1,524 m) altitude with 400 knots (206 m/s), the comparisons of BTB with 5 and 10 degrees deflection values can be seen in Table 7-8. 5 degrees deflections can

bring weapon to the LOS in a long time (Figure 7-39), and can not maintain its attitude. Continuous 5 degrees up deflections are seen in this phase until the impact (Figure 7-40).

The primary reason of this performance degradation in low-medium altitude deliveries can be summarized as follows. Since the weapon tries to maintain itself over the LOS, most of its canard deflections are full scale “up” deflections at the gliding phase of the flight. If these deflections are limited with a smaller value, the weapon will not be able to maintain its position around the LOS and will never reach above the apparent LOS. This can be seen from continuous 5 degrees up command during most of the flight time in Figure 7-40. The overall result is an increased miss distance due to shortfall.

Table 7-8 Performance comparison with BTB for 5 and 10 degrees deflections

	Low speed / low altitude delivery	
	BTB with δ=5°	BTB with δ=10°
miss distance (m)	651 lost acq	5.5
time of flight (s)	21	27
impact speed (m/s)	236	180

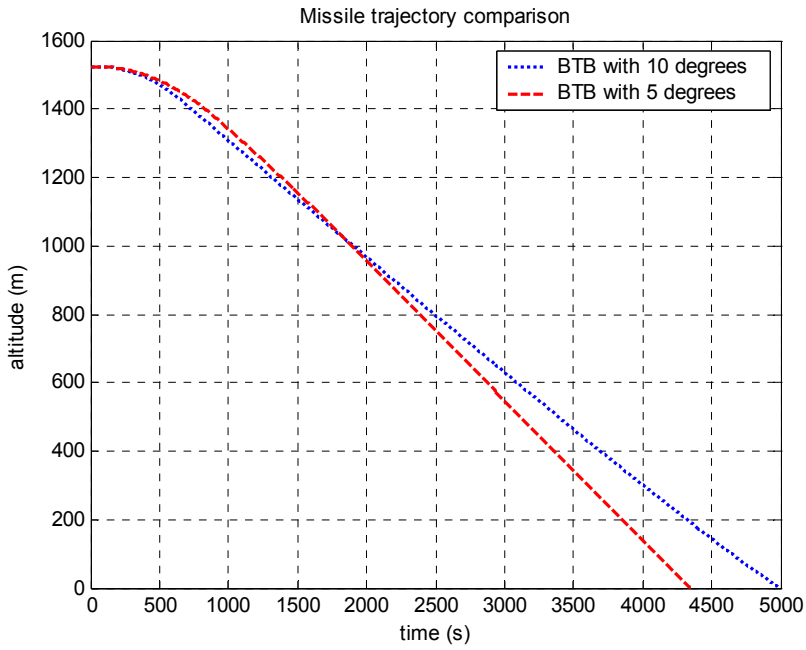

Figure 7-39 Weapon trajectory comparisons with BTB control for 5 and 10 degrees deflections

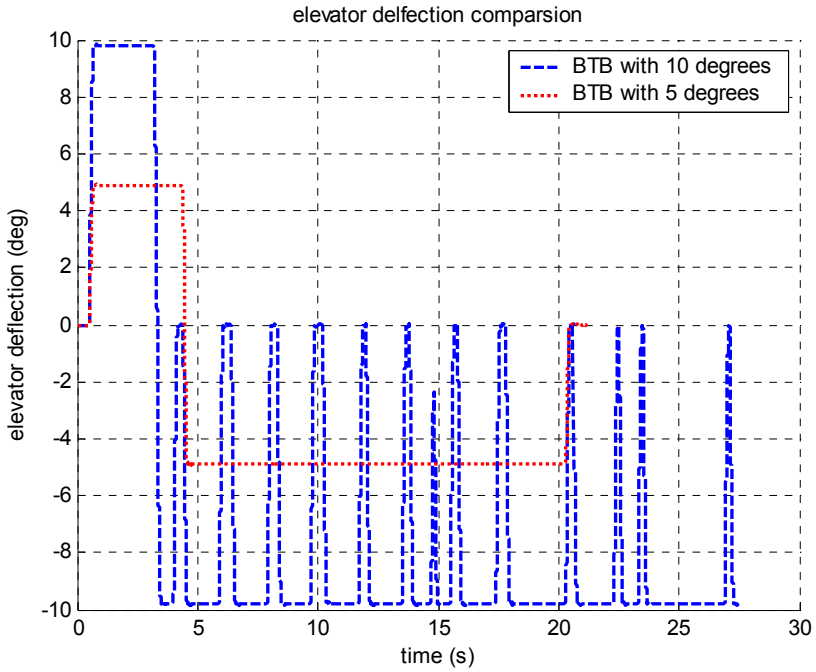

Figure 7-40 Elevator deflection comparison with BTB control for 5 and 10 degrees deflections

It is understood that decreasing the maximum canard deflection value can not be a general solution to cover all flight conditions; furthermore, it has adverse effects in low speed, low-medium altitude scenarios.

7.5 RESULTS FOR MULTIPOSITION (MP) CONTROL SCHEME

From the simulation results, it is seen that BB and BTB schemes are effective up to a limited range. It is also noted that the deadzone concept and smaller maximum canard deflection values can improve weapon's performance in some stages of flight. In the light of this information, a 5-position controller is constituted and examined in the simulations.

The multiposition control system is constituted with -10, -5, 0, +5, and +10 degrees canard deflection positions. 0 degrees deflections are applied with a 0.1 Volt deadzone value. The middle deflection value (5 degrees) is initiated when the

lead angle difference is between the deadzone limit and 1.5 degrees, which is half width of the detector's linear region.

The fine tuning of deadzone and middle deflection position requires some additional detailed research and may be subject to another study. But in this thesis, middle deflection values and lead angle decision criteria are selected using a trial and error method by employing several launch conditions in the nonlinear simulation. The middle deflection value is selected as 5 degrees since it can maintain the weapon around the LOS in gliding phase in most cases.

Since the performance of multiposition control is expected to be higher than BB and BTB schemes, only the most demanding cases such as target with cross-range component and moving target intercept scenario are covered in the following two cases.

Multiposition Case-1: This scenario shows a general system behavior for the multiposition control. Its parameters are shown in Table 7-9.

Table 7-9 High altitude level delivery parameters with multiposition control

Launch Conditions		
Control scheme	Multiposition (5 position control)	
Deadzone width	0.1 Volts	
Delivery type	High altitude level	
Release speed	600 knots (308 m/s)	
Release altitude	20,000 ft (6,096 m)	
Initial attitude in fixed frame		
Heading (deg)	Pitch angle (deg)	Roll angle (deg)
0	0	0
Initial rotation rates		
p (deg/s)	q (deg/s)	r (deg/s)
0	0	0
Target variables		
Target type	stationary	
	Downrange (m)	Crossrange (m)
Initial target location	15,000	500
Final target location	15,000	500
Performance variables		
Miss distance (m)	Time of flight (s)	Impact speed (m/s)
5	74	225

The miss distance value is decreased while time of flight and impact speed increases as compared to the results for BB and BTB control cases. Figure 7-41 shows the weapon's trajectory with a high altitude level delivery with MP control scheme. It can be seen that, even with the existence of cross-range component, lead angle values can be maintained at some small values as seen in Figure 7-42 and Figure 7-43.

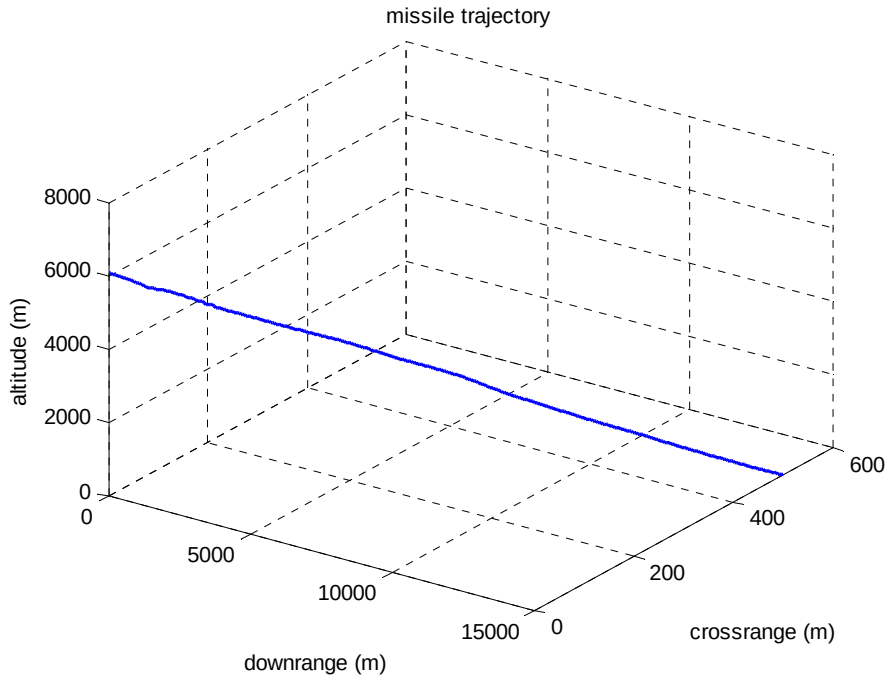

Figure 7-41 Weapon trajectory for a high altitude level delivery with MP control

The elevator and rudder deflections are shown in Figure 7-44 and Figure 7-45. It is seen that a 5 degrees elevator deflection is satisfactory to maintain attitude on the LOS in most phases of flight. 10 degrees deflection is required in the first seconds to pitch down and in cases where the lead angle can not be maintained by 5 degree deflections.

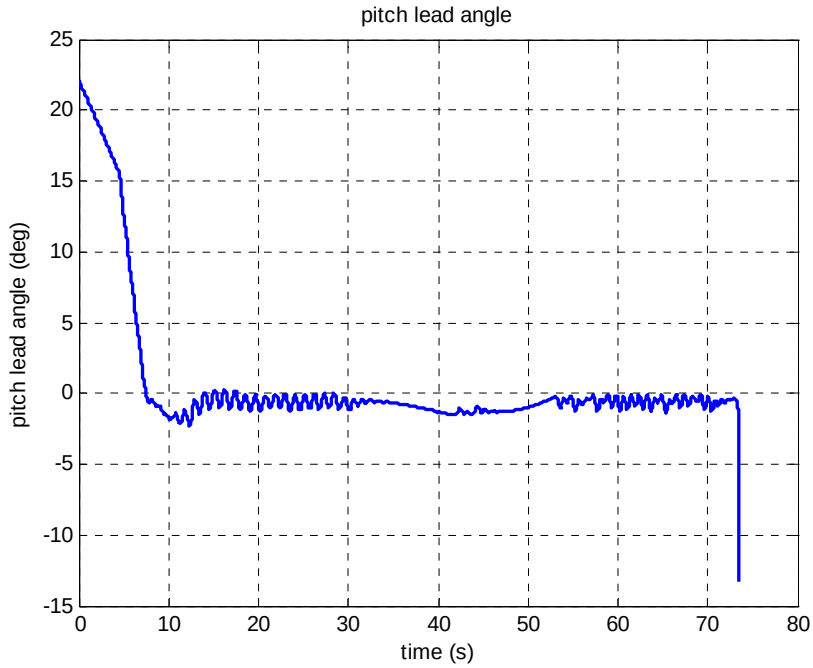

Figure 7-42 Pitch lead angle time history for a high altitude level delivery with MP control

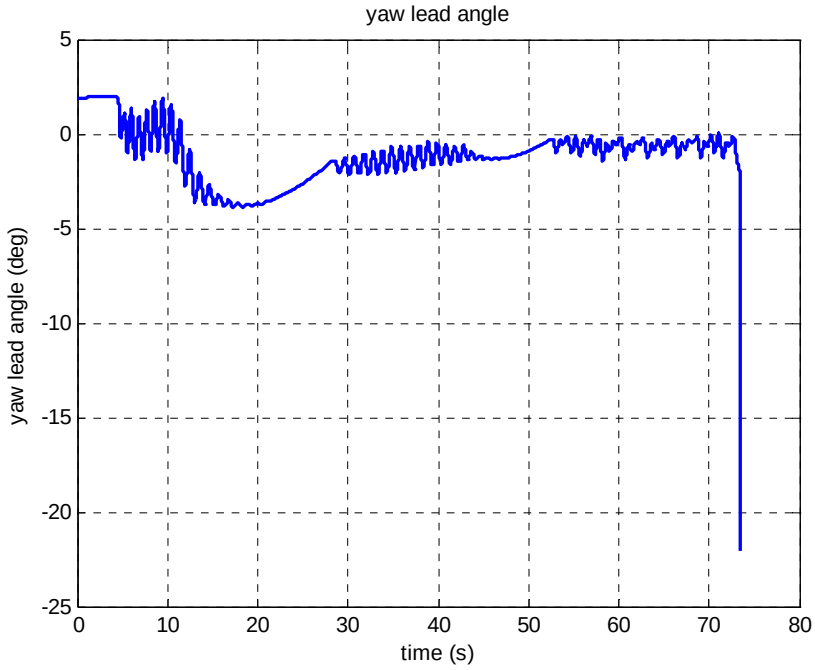

Figure 7-43 Yaw lead angle time history for a high altitude level delivery with MP control

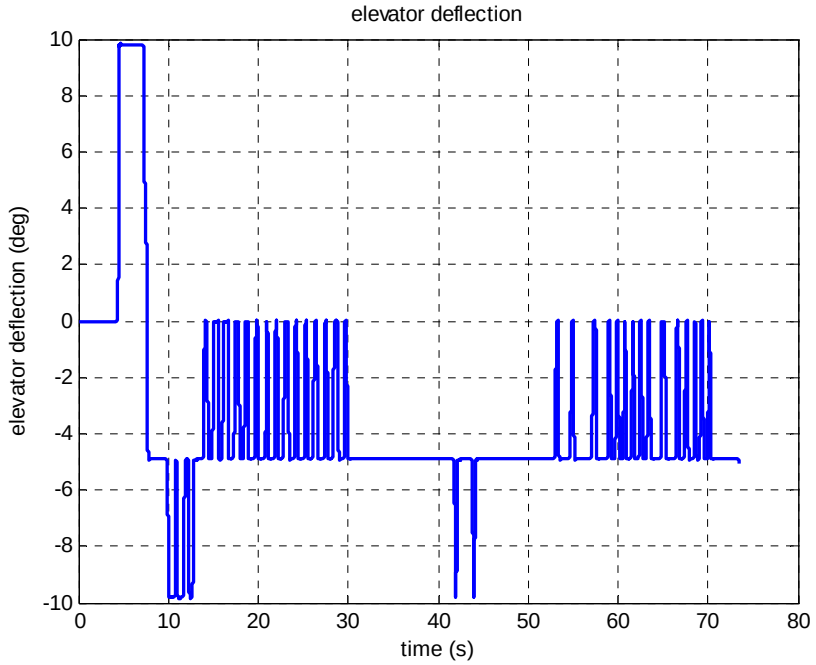

Figure 7-44 Elevator deflection time history for a high altitude level delivery with MP control

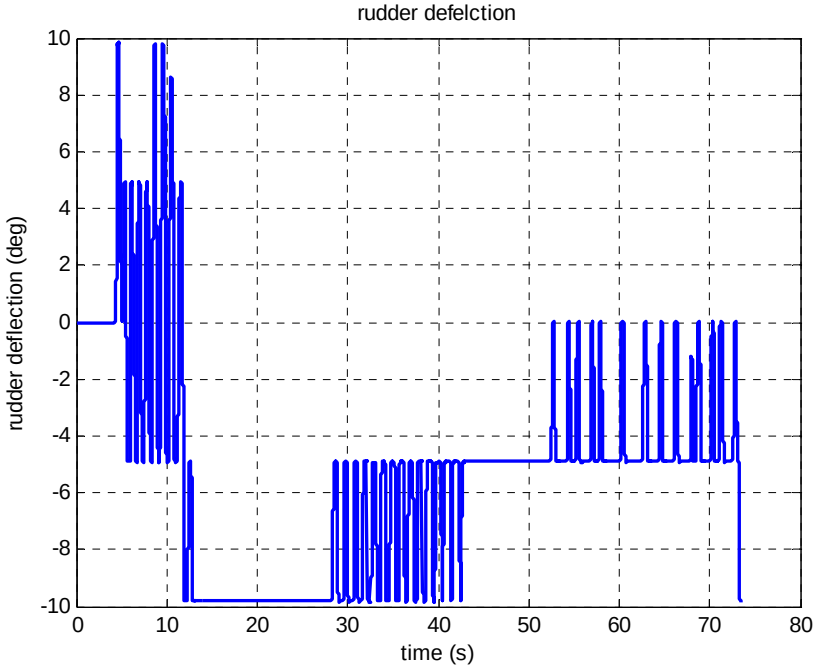

Figure 7-45 Rudder deflection time history for a high altitude level delivery with MP control

As seen in Figure 7-46, angle of attack values still show oscillations but their magnitudes are smaller than the ones observed with BB and BTB schemes.

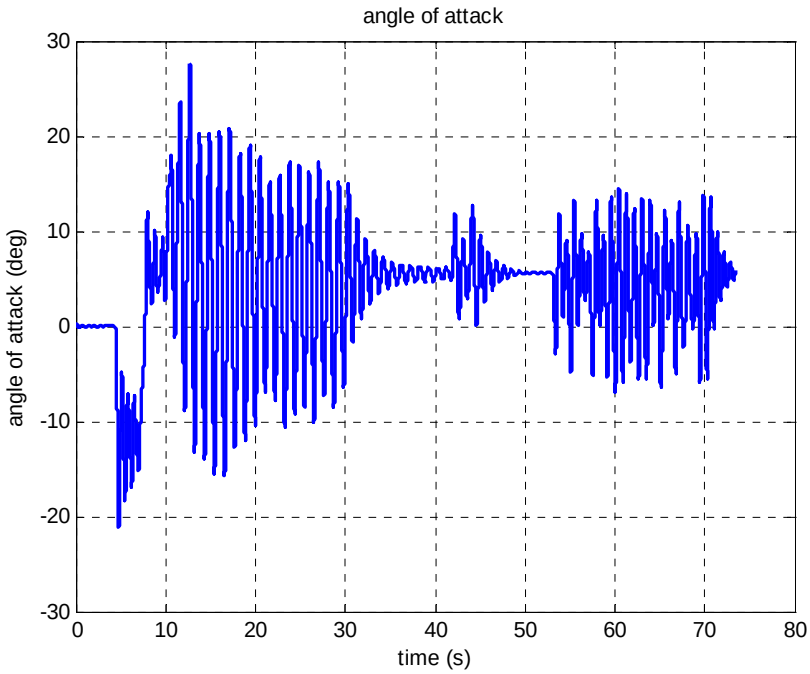

Figure 7-46 Angle of attack time history for a high altitude level delivery with MP control

Multiposition Case-2: The parameters of high altitude dive delivery against a moving target are given in Table 7-10. The moving target intercept capability of MP control is much higher than BB and BTB schemes, which is depicted in Table 7-10 and Figure 7-47.A 10 meters miss distance can be maintained while decreasing time of flight and increasing impact speed.

Lead angle values are maintained within ±1 degrees as depicted in Figure 7-48 and Figure 7-49.

Table 7-10 Dive delivery parameters against moving target with MP control

Launch Conditions		
Control scheme	Multiposition (5-position control)	
Deadzone width	0.1 Volts	
Delivery type	High altitude dive	
Release speed	600 knots (308 m/s)	
Release altitude	20,000 ft (6,096 m)	
Initial attitude in fixed frame		
Heading (deg)	Pitch angle (deg)	Roll angle (deg)
0	-30	0
Initial rotation rates		
p (deg/s)	q (deg/s)	r (deg/s)
0	0	0
Target variables		
Target type	sinusoidal evading	
	Downrange (m)	Crossrange (m)
Initial target location	9,000	0
Final target location	8,814.43	255.81
Performance variables		
Miss distance (m)	Time of flight (s)	Impact speed (m/s)
10	36	271

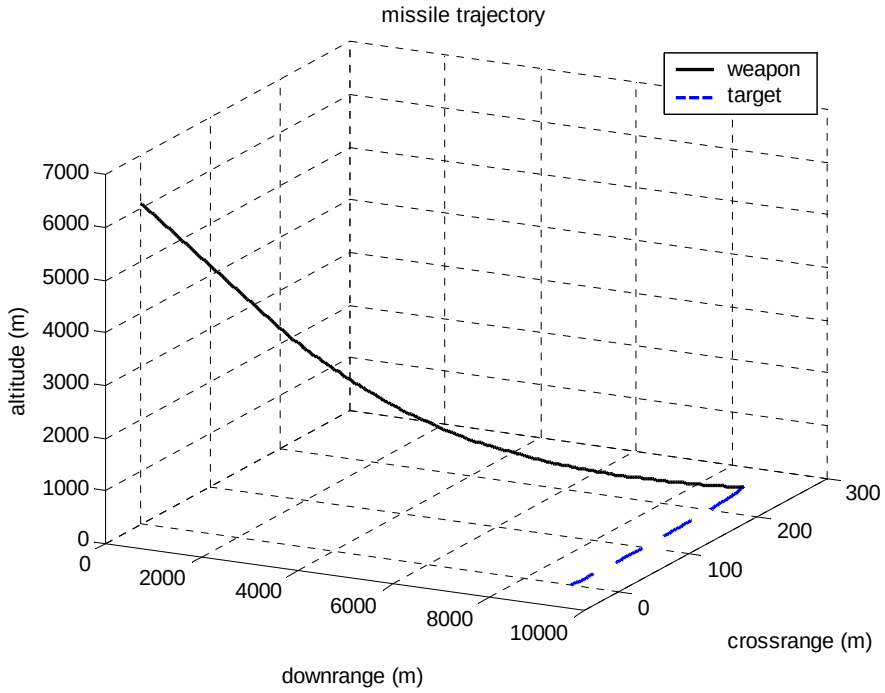

Figure 7-47 Weapon trajectory for high altitude dive against a moving target with MP control

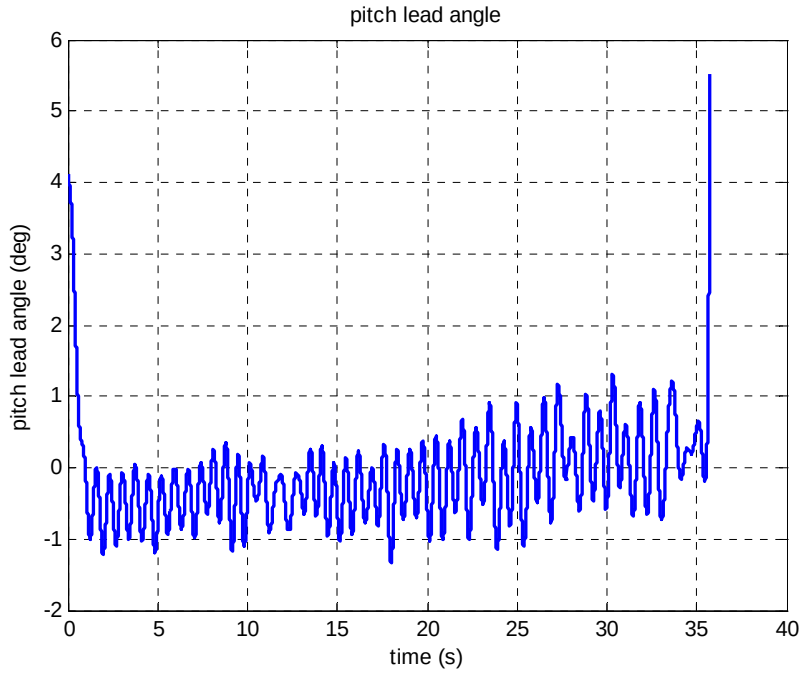

Figure 7-48 Pitch lead angle time history for high altitude dive against a moving target with MP control

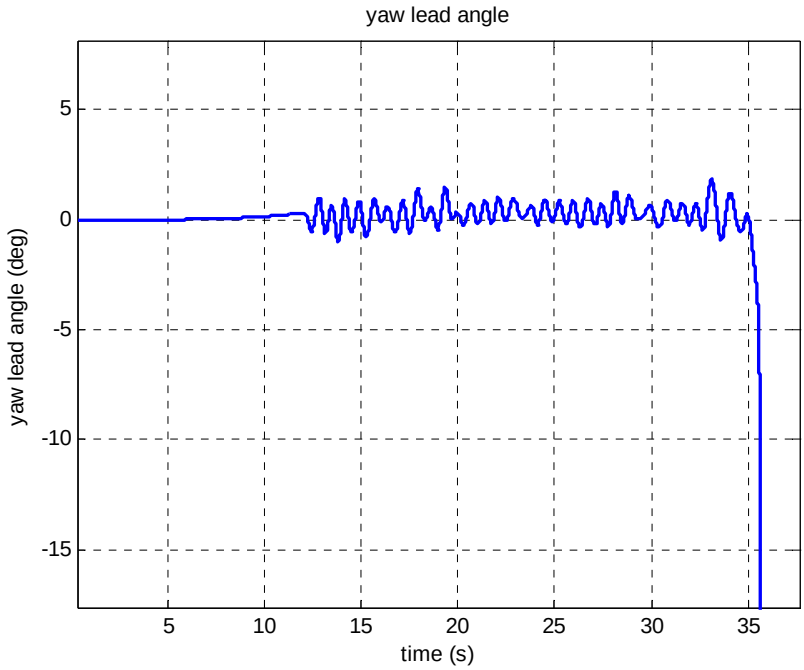

Figure 7-49 Yaw lead angle time history for high altitude dive against a moving target with MP control

The elevator and rudder deflections are shown in Figure 7-50 and Figure 7-51.

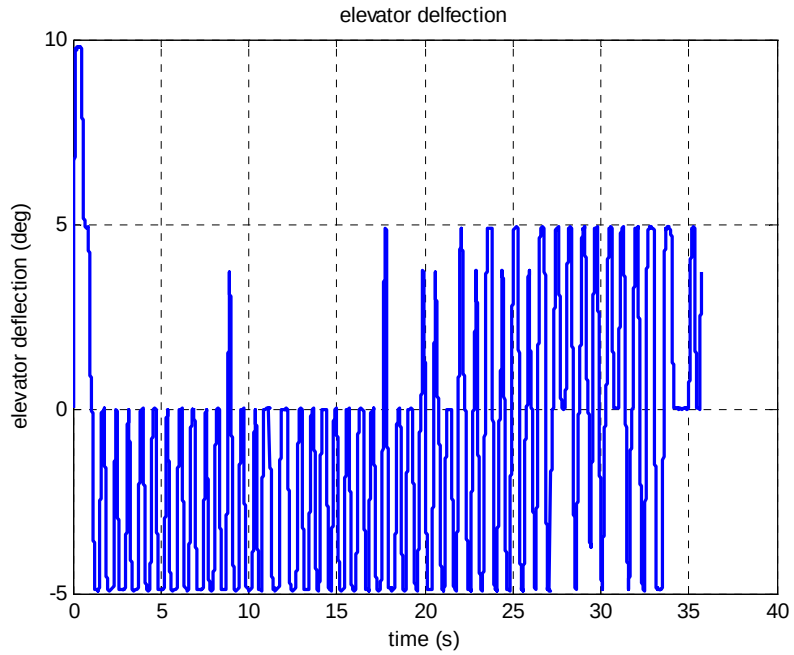

Figure 7-50 Elevator deflection time history for high altitude dive against a moving target with MP control

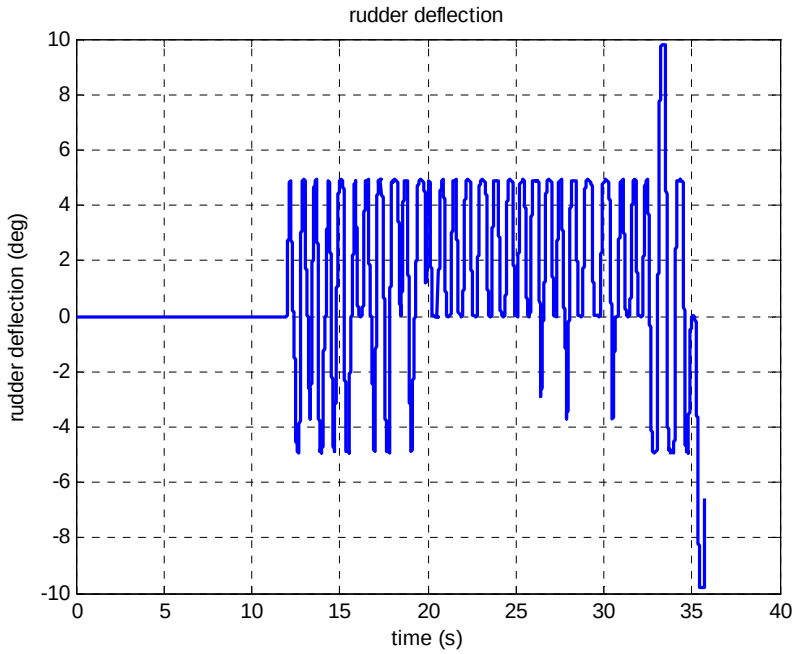

Figure 7-51 Rudder deflection time history for high altitude dive against a moving target with MP control

The angle of attack and sideslip angle show oscillatory behavior as expected (Figure 7-52 and Figure 7-53)

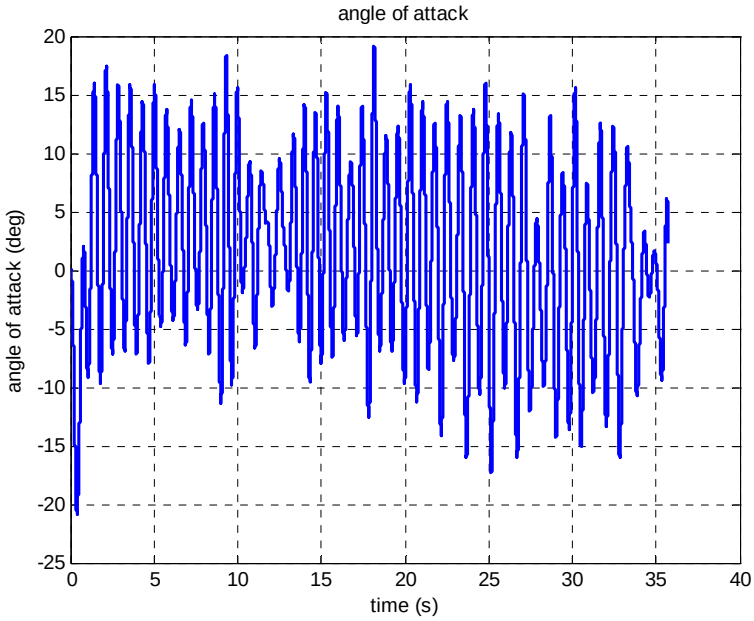

Figure 7-52 Angle of attack time history for high altitude dive against a moving target with MP control

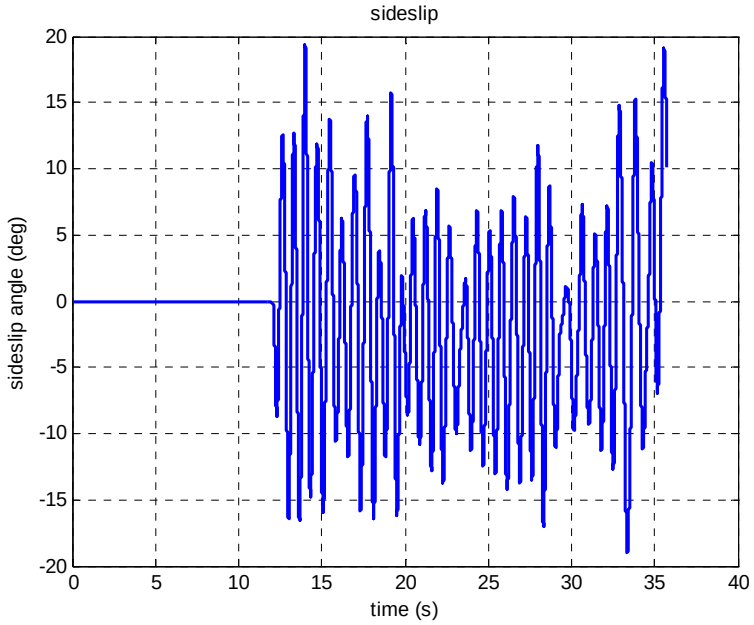

Figure 7-53 Sideslip angle time history for high altitude dive against a moving target with MP control

Multiposition control has the ability to combine half and full deflections whenever required and does not have the gaps of 5 degrees BTB control scheme. The simulation results show that the range can be increased significantly while preserving miss distance values (case-1 and case-2).

A 5 degrees up command seems to be adequate for maintaining course in most phases of flight. Since this deflection is a little bit higher than the required value to bring the weapon velocity on the LOS, the weapon sometimes goes over the LOS, which provides a slightly elevated trajectory and minimizes the miss distance by reducing effects of gravity.

The moving target intercept capability of multiposition control scheme is also high. All miss distance values are acceptable even for moving targets (case-2).

The impact speed, which is an important parameter when attacking hardened targets such as aircraft shelters, is much higher than BB and BTB control schemes.

The results of simulations show that the multiposition control has the following advantages over bang-bang and bang-trail-bang control schemes.

- Higher impact speed due to a lower drag
- Extended range with a better miss distance.
- Efficient moving target intercept capability in longer range deliveries.

7.6 RESULTS FOR CONTINUOUS (C) CONTROL SCHEME

The continuous control scheme directly uses the linear region of the detector to output proportional canard commands. Since the linear region is limited due to the nature of the seeker, these proportional commands can be generated when the lead angle difference is within the linear region limit. Beyond this limit, full canard deflections have to be employed.

The continuous control scheme is expected to give the best results for the system performance. Hence, it is included in the analysis for the purpose of determining the relative effectivenesses of other control schemes.

The following two scenarios are given as examples to demonstrate the behavior of flight variables and to show the performance of the weapon against moving targets.

Continuous Case-1: High altitude level delivery scenario parameters are given in Table 7-11. One distinctive characteristics of continuous control scheme is that, the impact speed is much higher than BB and BTB cases. As a result, the time of flight is shorter.

Table 7-11 High altitude level delivery parameters with continuous control

Launch Conditions		
Control scheme	Continuous	
Deadzone width	none	
Delivery type	High altitude level	
Release speed	600 knots (308 m/s)	
Release altitude	20,000 ft (6,096 m)	
Initial attitude in fixed frame		
Heading (deg)	Pitch angle (deg)	Roll angle (deg)
0	0	0
Initial rotation rates		
p (deg/s)	q (deg/s)	r (deg/s)
0	0	0
Target variables		
Target type	stationary	
	Downrange (m)	Crossrange (m)
Initial target location	21,000	0
Final target location	21,000	0
Performance variables		
Miss distance (m)	Time of flight (s)	Impact speed (m/s)
9.6	69	323

The range of the weapon is further increased with continuous control as shown in Figure 7-54. The lead angle variation shows a totally different character than BB, BTB, and multiposition cases (Figure 7-55).

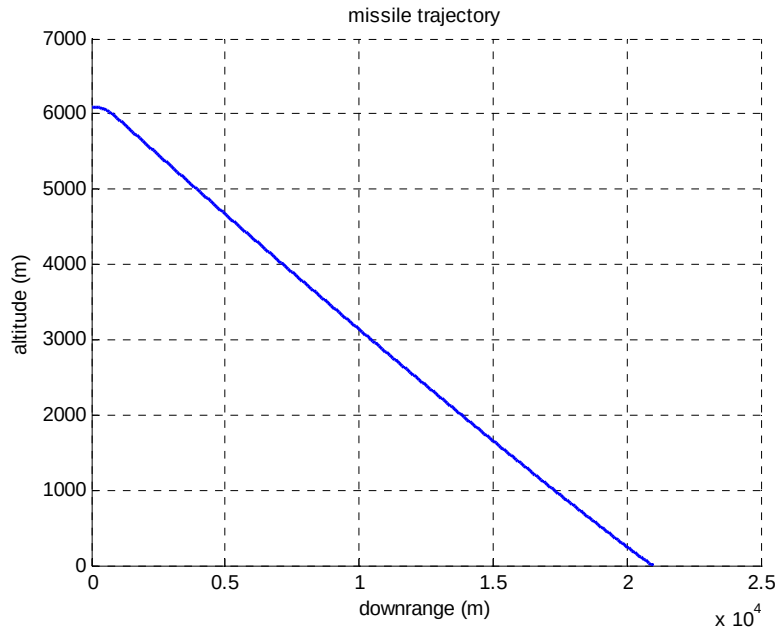

Figure 7-54 Weapon trajectory for a high altitude level delivery with continuous control

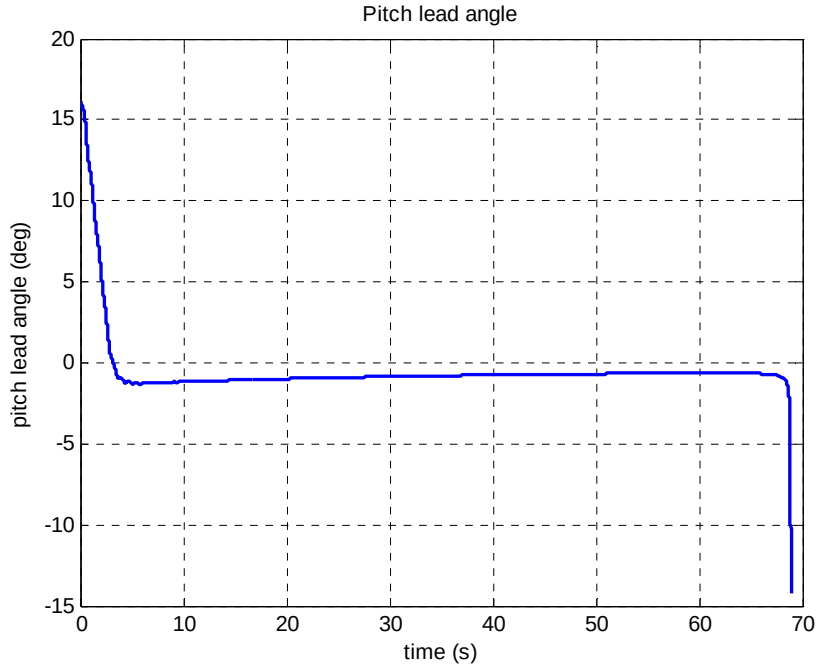

Figure 7-55 Pitch lead angle time history for a high altitude level delivery with continuous control

When the lead angle difference is brought to the linear region limit by full deflections in the first seconds of flight, small canard deflections are employed and the weapon is maintained at a very small lead angle difference by these small corrections in the gliding phase. The lead angle difference smoothly decreases but never becomes zero.

The elevator deflections are much smaller when compared with other schemes and a value between 1 and 4 degrees is satisfactory to maintain the altitude (Figure 7-56). The angle of attack behavior is shown in Figure 7-57.

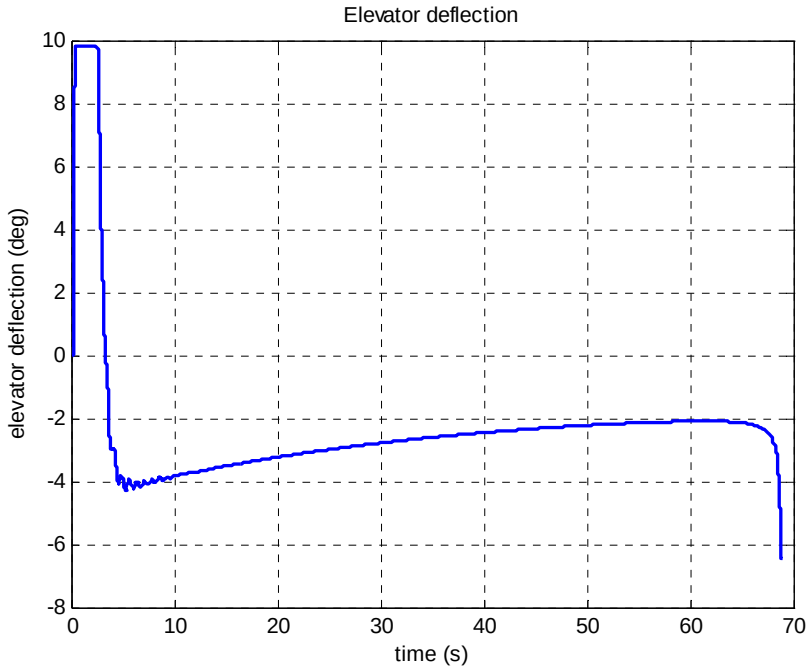

Figure 7-56 Elevator deflection time history for a high altitude level delivery with continuous control

Since the weapon flies with small canard deflections in most of the time, the oscillations in flight variables are minimized like angle of attack (Figure 7-57). With lower angle of attack values and a lower drag of slightly deflected canards, the system flies aligned with the streamline. The overall effect is the reduced drag and therefore less energy dissipation. As a direct consequence, the flight resembles the ballistic flight and the speed increases.

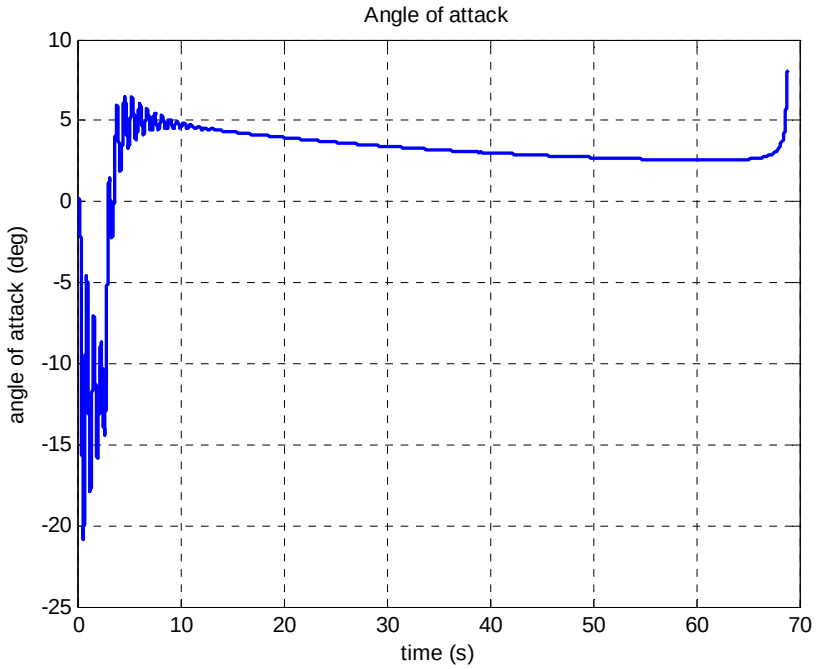

Figure 7-57 Angle of attack time history for a high altitude level delivery with continuous control

Continuous Case-2: This scenario depicts the moving target intercept capability of the weapon in a high altitude dive delivery. The miss distance can be maintained around 10 meters while the time of flight is short and impact speed characteristics are preserved as shown in Table 7-12.

Figure 7-58 and Figure 7-59 show the weapon and evading target trajectories. The weapon has to change its direction drastically in the last seconds to cope with the evasive maneuver of the target.

Pitch and yaw lead angle time histories are smooth (except in the last seconds) and no oscillations exist as a primary property of the continuous control scheme as observed in Figure 7-60 and Figure 7-61.

Table 7-12 High altitude dive delivery parameters against an evading target with continuous control

Launch Conditions		
Control scheme	Continuous	
Deadzone width	none	
Delivery type	High altitude dive	
Release speed	600 knots (308 m/s)	
Release altitude	20,000 ft (6,096 m)	
Initial attitude in fixed frame		
Heading (deg)	Pitch angle (deg)	Roll angle (deg)
0	-30	0
Initial rotation rates		
p (deg/s)	q (deg/s)	r (deg/s)
0	0	0
Target variables		
Target type	sinusoidal evading	
	Downrange (m)	Crossrange (m)
Initial target location	14,000	0
Final target location	13,627.25	175.2
Performance variables		
Miss distance (m)	Time of flight (s)	Impact speed (m/s)
11	44	353

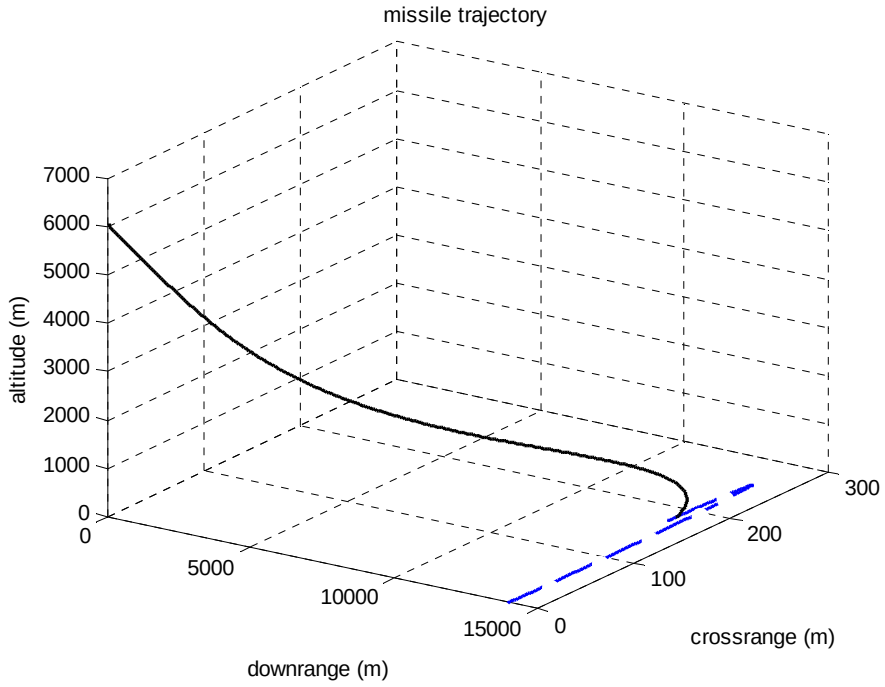

Figure 7-58 Weapon trajectory for a high altitude dive delivery against an evading target with continuous control

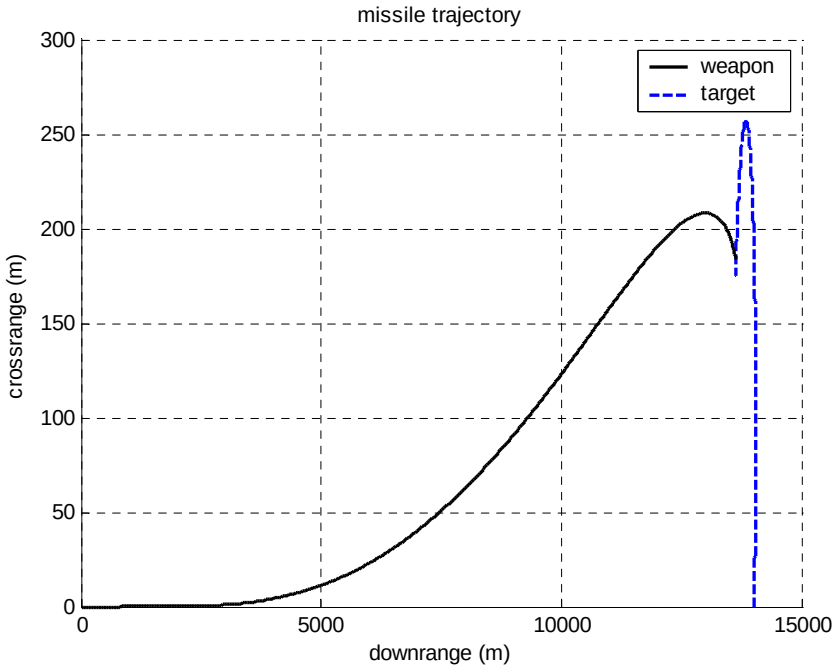

Figure 7-59 Weapon trajectory for a high altitude dive delivery against an evading target with continuous control (top view)

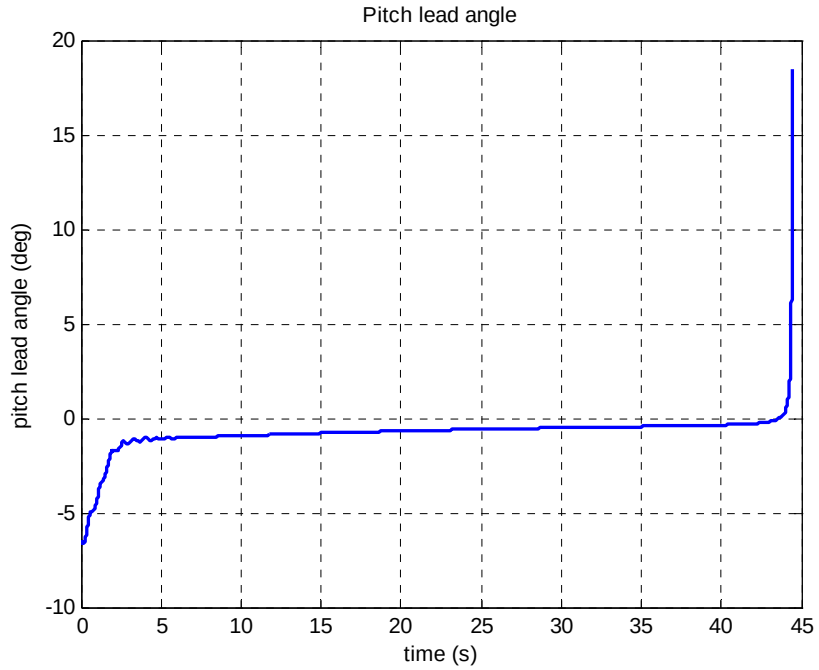

Figure 7-60 Pitch lead angle time history for a high altitude dive delivery against an evading target with continuous control

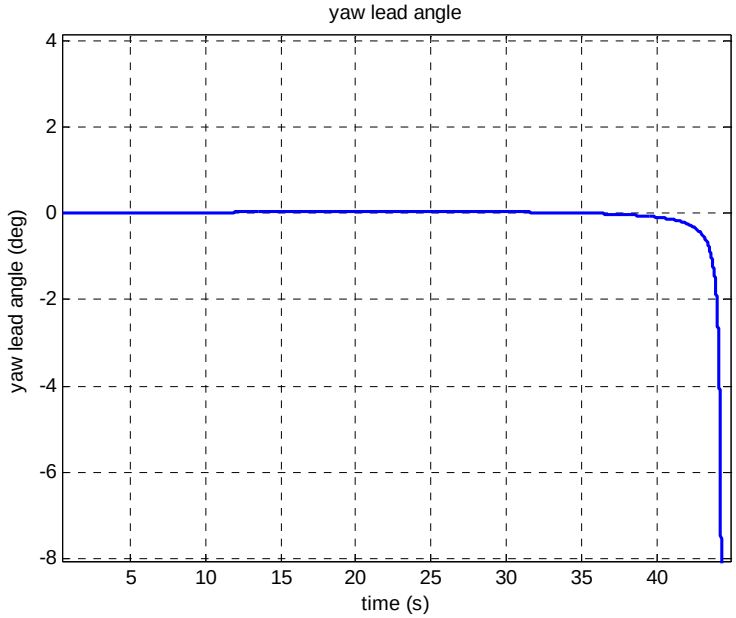

Figure 7-61 Yaw lead angle time history for a high altitude dive delivery against an evading target with continuous control

In order to compensate the evasive maneuver; the weapon has to employ full canard deflections in the terminal phase as seen in Figure 7-62 and Figure 7-63.

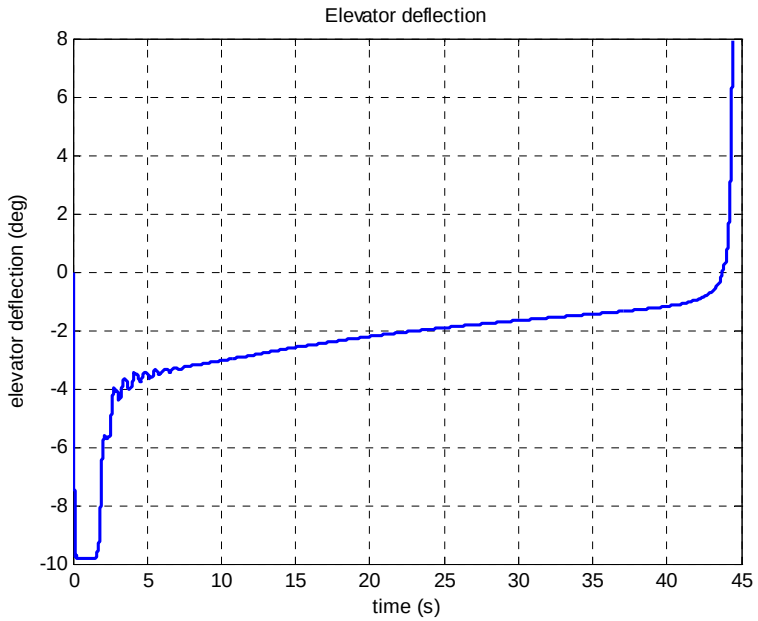

Figure 7-62 Elevator deflection time history for a high altitude dive delivery against an evading target with continuous control

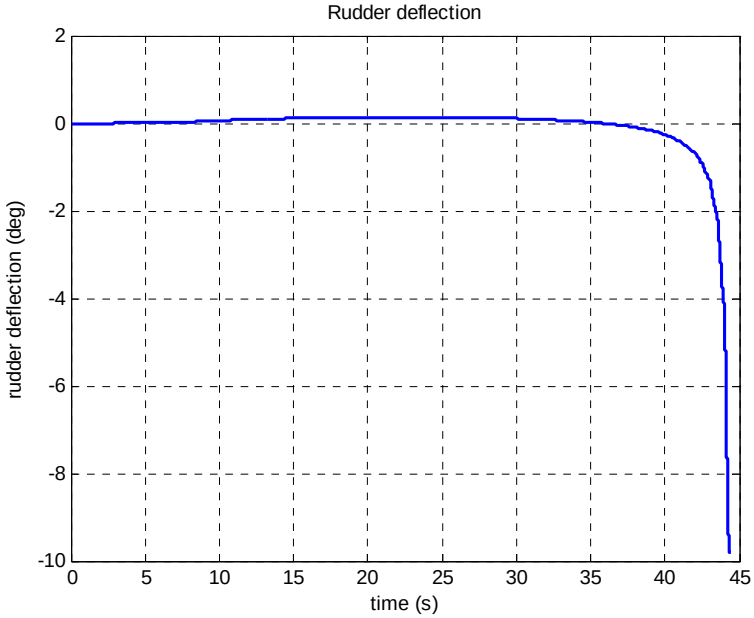

Figure 7-63 Rudder deflection time history for a high altitude dive delivery against an evading target with continuous control

The angle of attack and sideslip angle behaviors are much smoother when compared with other control schemes as seen in Figure 7-72 and Figure 7-65.

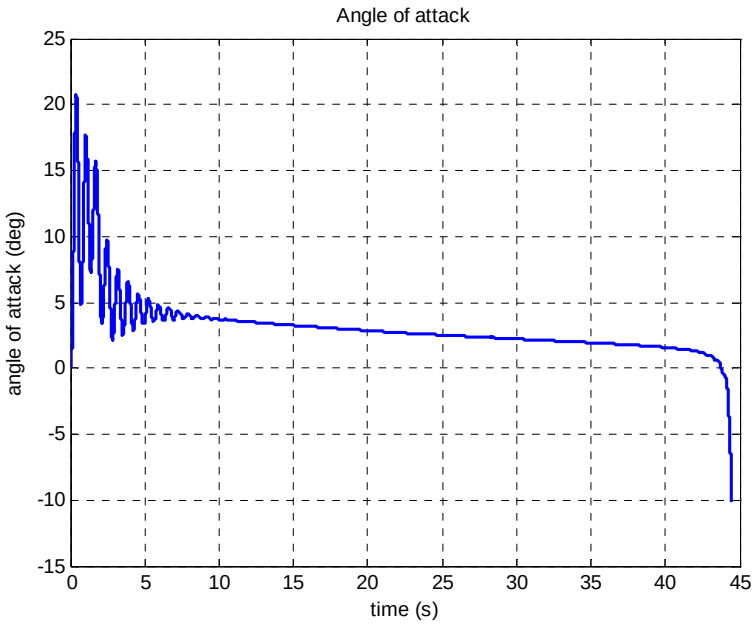

Figure 7-64 Angle of attack time history for a high altitude dive delivery against an evading target with continuous control

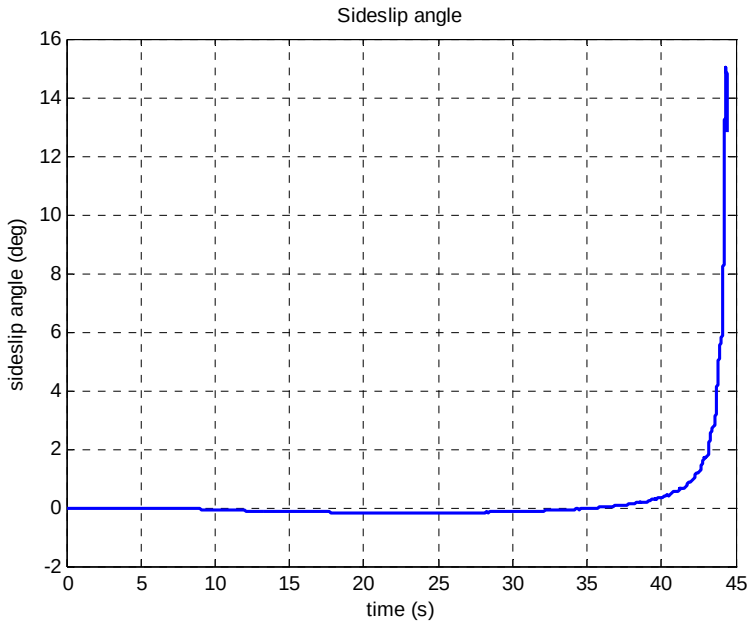

Figure 7-65 Sideslip angle time history for a high altitude dive delivery against an evading target with continuous control

The speed variation of the weapon is seen in Figure 7-66.

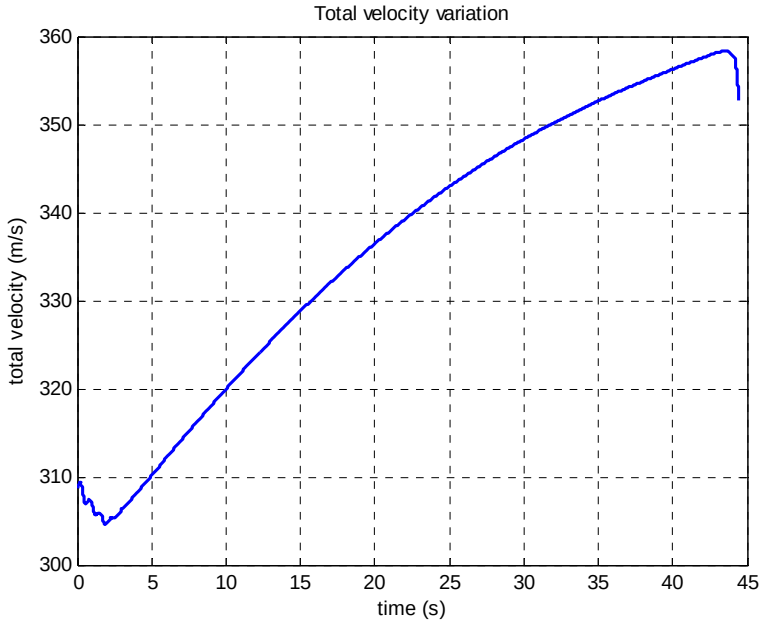

Figure 7-66 Speed time history for a high altitude dive delivery against an evading target with continuous control

The speed increases since the canard deflections are small and the weapon is aligned with the streamline. It decreases in the terminal phase near impact due to full deflections

In the light of simulation studies as demonstrated in continuous case-1 and case-2, the following conclusions about the weapon's flight characteristics are obtained.

Important flight variables show smooth behavior and oscillations are minimized. The primary reason is the small canard deflections which do not make the weapon fly with high angles of attack and sideslips. Small deflections along with reduced exposure area of the weapon to the wind direction let the weapon to experience lesser drag than other schemes. The flight pattern becomes similar to ballistic flight and weapon's speed increases.

An important observation is the gravity effect on the weapon. Once the weapon falls below the LOS by down commands, canard deflections to eliminate the lead angle are given. But, since the existence of gravity effect is not taken into account, the weapon is always pulled down by the gravity and the trajectory never goes above the instantaneous LOS again. This effect is mostly seen in long range scenarios where the weapon flies with an almost constant angle of attack path like a water ski sliding on sea surface. This phenomenon can be clearly seen in lead angle and elevator deflection time histories of case-1.

Due to the gravity effect, the weapon always falls a few meters short of target. This is expected since the weapon is pulled down by the gravity. The multiposition control can achieve better miss distance values than the continuous scheme due to its slightly elevated trajectory, which lets the weapon to go above the LOS, whereas the continuous control always stays beyond the LOS and falls shorter in the order of a few meters. As an example, for a high altitude level launch scenario from 10,000 ft altitude with 500 knots speed against a stationary target at 9,000 meters range, the miss distance of continuous control is around 11 meters while the multiposition control gives less than 6 meters.

The range increase achieved by the continuous control is not as large as expected. The reason for this is the miss distance constraint. If some gravity compensation logic can be implemented to the system, it is expected that the results may change.

7.6.1 DOWN SENSOR AND ITS EFFECT ON PERFORMANCE

The miss distance values that are experienced for continuous control scheme has shown that, for long range performance where both the range and miss distance are important factors, it is necessary to employ a down sensor so that the weapon can take some precautions to minimize the effect of gravity on the guidance system.

Therefore, the effect of a theoretical down sensor on the weapon's performance is investigated for the purpose of developing a guide for the implementation of such a sensor without dealing with its mechanical properties. It is shown by a preliminary study about the nature of the sensor that tilt sensors and inclinometers are possible candidates for a down sensor. Magnetometers incorporating flux sensors backed by accelerometers appear to be alternative candidates.

7.6.1.1 Weapon's Maneuverability

The weapon's maneuverability (and the g levels it is subjected to) is investigated in order to analyze the possibility of employing an electrolytic tilt or a pendulum type sensor.

If the weapon is subjected to 1g or a fraction of the gravity vector with no external forces during gliding phase, it may be possible to determine the gravity (thus down) direction by such kind of sensors. If the g levels become higher than 1g, it becomes hard or even impossible to use these types of sensors.

Figure 7-67 shows the acceleration of the weapon in the direction of gravity for a sample high altitude level delivery scenario against a stationary target at 15,000 m range. The weapon is subjected to 1g gravitational acceleration during the ballistic phase in the first 5 seconds of flight and there are oscillations in the order of 4 to 5g's in the first stages of guided flight where full canard deflections are employed.

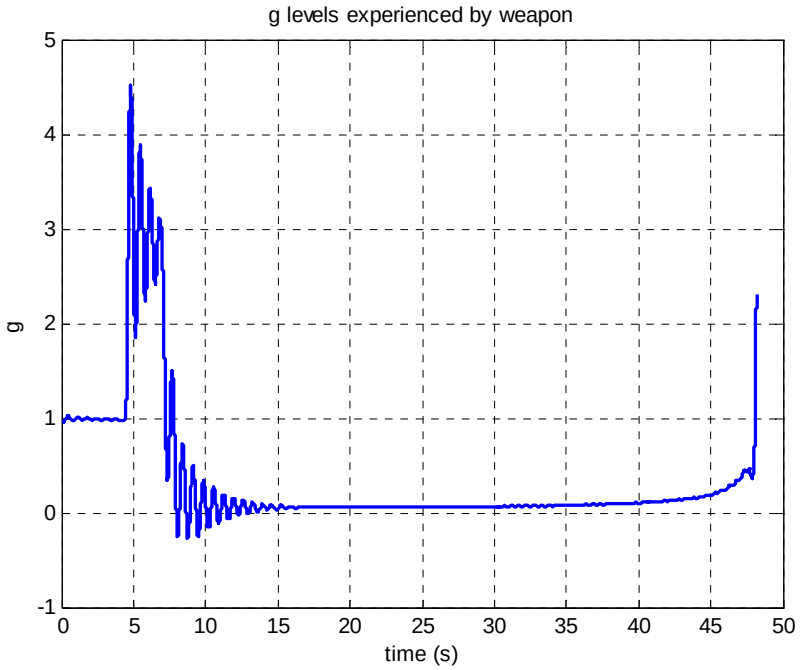

Figure 7-67 g levels experienced during the flight with continuous control for a high altitude level delivery against a stationary target at 15,000 m range

If the weapon is fired at a distant stationary target, it may only be possible to extract an accurate data from the down sensor at the gliding phase after some time. It is not possible to use such a sensor while employing BB, BTB or multiposition control schemes due to high g values experienced during full scale deflections. It can only be used for a limited time even in continuous scheme in the gliding phase where the lift is almost equal to the weight of the weapon.

Regarding the g levels that the weapon experiences, it is concluded that the down sensor to be used must not rely on the measurement of the magnitude of gravity vector since some additional accelerations are introduced during maneuvers.

7.6.1.2 Results

The effect of a down sensor is modeled basically in order to see the amount of possible improvement in the weapon's performance. The continuous control scheme produces canard deflection commands that try to eliminate the lead angle error without taking the gravity into account. The down sensor provides the

direction of gravity and all up commands are generated with a bias to produce additional deflections to elevate the weapon above the instantaneous LOS.

The results of simulations show that this approach has a significant positive effect on the weapon's miss distance. This also leads to a range increase where miss distance values are decreased from 30 meters to within 10 meters at the edge of flight envelope. Figure 7-68 shows the zoomed view of a portion of the weapon's trajectory. The elevated trajectory can be seen clearly which provides a better miss distance.

Improving the miss distance leads to a range increase, where the 10 meters miss distance constraint can be met within longer ranges as seen in Figure 7-69. For a high altitude level delivery from 20,000 ft (6,096 m) altitude, the effective range exceeds 20,000 meters by an additional 25% by just giving an offset to the up commands. It is expected that enhanced algorithms may provide even further improvements in range.

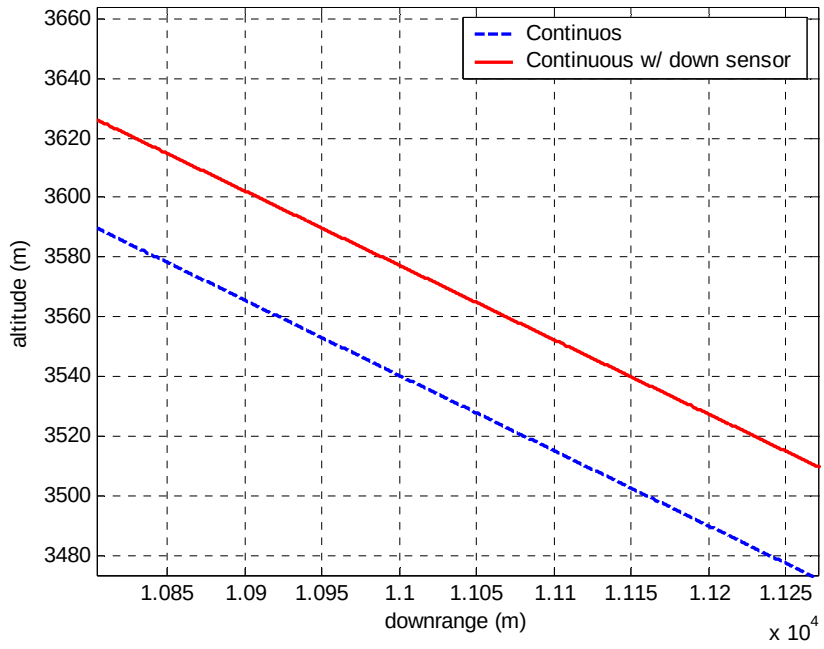

Figure 7-68 Elevated trajectory with down sensor

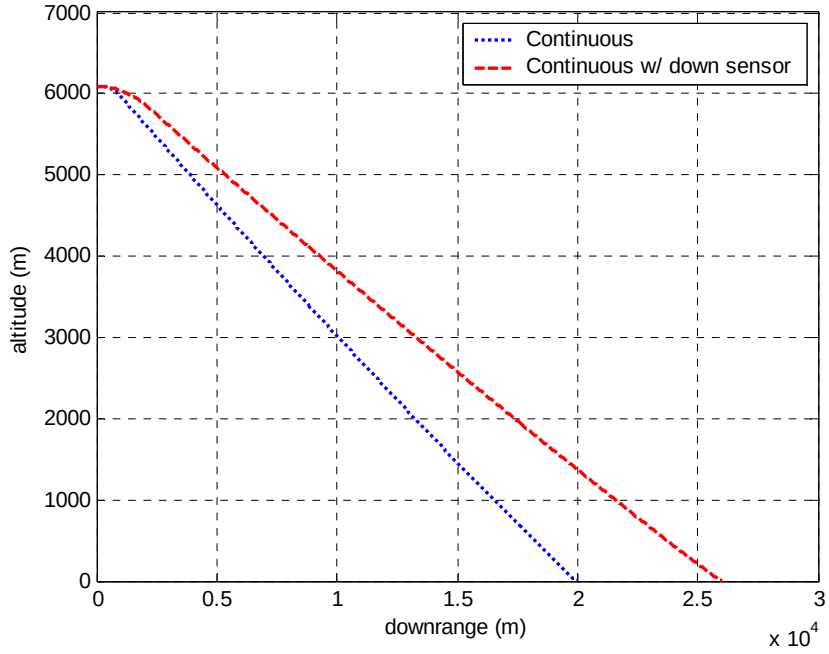

Figure 7-69 Effect of down sensor on range for 8 meter miss distance criterion

7.7 EFFECT OF NOISE ON THE PERFORMANCE

The term “noise” stands for the variance of seeker output when subjected to laser beam with the same angle of arrival in this thesis. Since there are no other sensors on board, only sensor subjected to noise is the seeker. During seeker tests, it is noticed that the uncertainty region could not be eliminated after some limit and different readings at the same input conditions is possible. The width of the uncertainty region in output voltage is determined, and a noise in the form of Gaussian random distribution with the specified variance is added to the simulation to see its effects on weapon’s behavior.

The seeker noise has a negative effect on the weapon’s performance starting from BTB control scheme. The deadzone widths used in the ideal case had to be revised to eliminate the effects of noise. While an increase in deadzone width can not thoroughly eliminate noise effects, some range decreases in BTB, multiposition and continuous control schemes are observed.

The effects of noise on the range of multiple schemes are shown in Figure 7-70. The existence of noise makes the BTB control scheme similar to the BB control scheme and degrades its performance. The noise effect on the multiposition control scheme can be summarized as a slight decrease in the maximum range. Continuous control canard deflections show an oscillatory behavior around the ideal case and a more drag is experienced with respect to the ideal case. Flight variables show oscillatory behaviors (Figure 7-71 and Figure 7-72). However, the weapon's performance is not heavily affected. Only the range is decreased slightly.

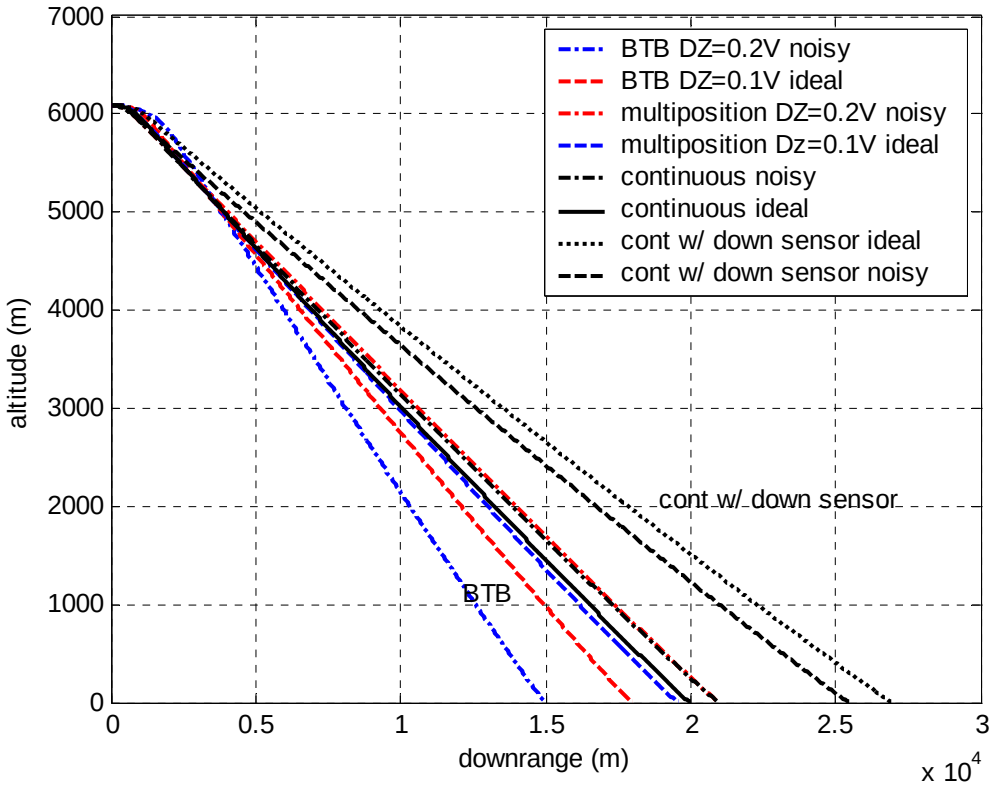

Figure 7-70 Effect of seeker noise on multiple control schemes

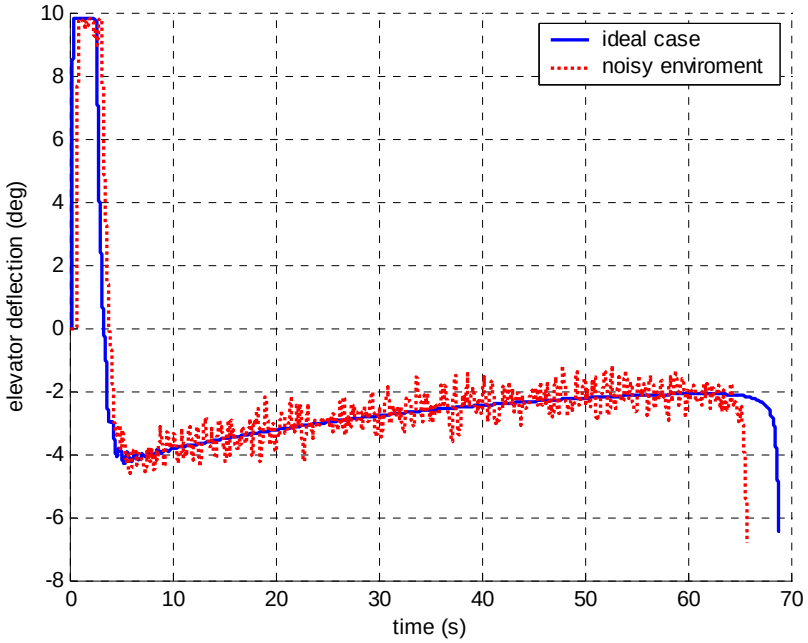

Figure 7-71 Elevator deflection behavior with continuous control in ideal and noisy environments

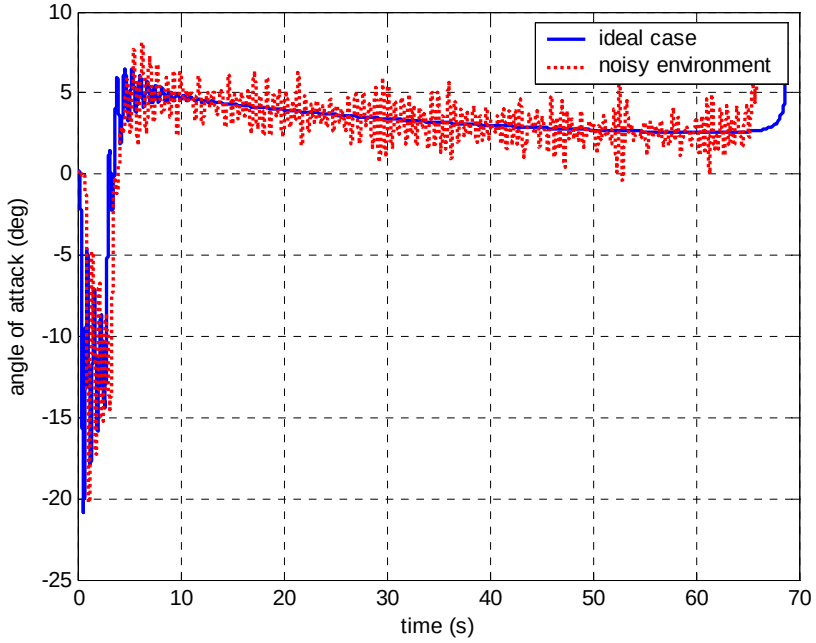

Figure 7-72 Angle of attack behavior with continuous control in ideal and noisy environments

Summarizing, the effect of noise on all control surface deflections are similar. Only BTB control scheme is affected more since it resembles BB control under noisy effects. The range decrease is seen in all control schemes and the general behavior of results obtained in ideal case runs is not affected.

7.8 EXTENSIVE SIMULATION RESULTS FOR COMPARISON OF CONTROL SCHEMES AND SOME REMARKS

In order to compare the performances of various control schemes and to constitute a flight envelope for each scheme (i.e, BB, BTB, multiposition, continuous, continuous with a down sensor), an extensive set of simulations are run covering altitudes from 1,000 ft (305 m) to 20,000 ft (6,096 m) with 5,000 ft intervals with release speeds between 400 (206 m/s) and 700 knots (360 m/s) with 100 knot increments.

In these runs, the effectiveness of the weapon's performance is investigated in terms of the total energy required initially. The total energy which is the combination of kinetic and potential energies unites the effects of release speed and altitude as one parameter.

The hit criterion is assumed to be 10 meters as the maximum miss distance. Several trials are run at different target ranges to achieve this 10 meters limit. The results of 400 and 700 knot cases are shown in Figure 7-73.

The minimum ranges for 700 knots case are smaller than the 400 knots case which is an indication that the launch altitude has a slightly more effect on the weapon's performance than the release speed.

The release envelope of the BB control scheme is limited when compared with other schemes. The range can not be further increased even with increasing total energy after a limit, and the slopes of the range curves are steeper than other schemes.

The BB control cases show that both the moving target intercept effectiveness and impact speeds are low. The BB control scheme causes a lot of energy loss with full scale deflections and this limits the range due to resulting high drag.

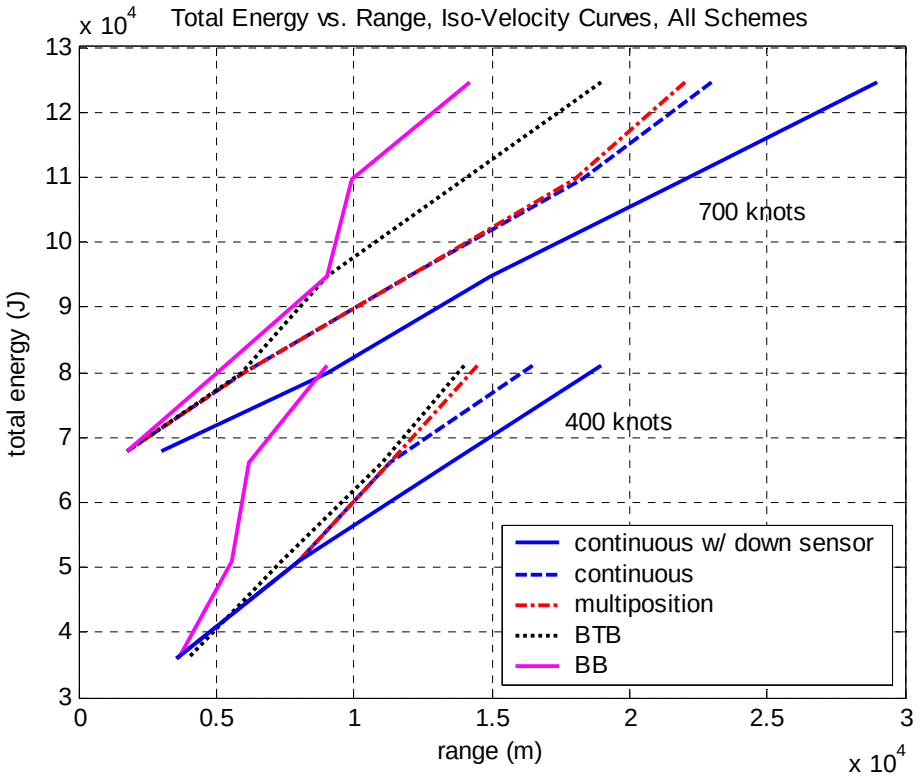

Figure 7-73 Sample flight envelope comparison of control schemes with 10 m miss distance criterion

The BTB scheme introduces some improvements in terms of range to the system. The existence of a deadzone prevents canard deflections for small lead angle errors. However the speed of the weapon still decreases drastically. This control system is effective within its range envelope only for stationary targets as bang-bang control scheme.

One interesting result of these simulations is that, the impact speeds are around 180 m/s for both BB and BTB schemes when the 10 meter miss distance is achieved.

The simulations show that multiposition control scheme gives satisfactory results except the longest range scenarios in terms of range, miss distance, and moving target intercept capability. The miss distance values are slightly better than the continuous scheme thanks to the 5 degrees mid-deflection which provides an elevation to the weapon above the LOS.

The performance of the multiposition control scheme seems to be same as the continuous scheme except at high energy levels. The multiposition control scheme works better than expected and can be a reasonable candidate for a performance improvement attempt.

The continuous control scheme provides a better range increase than BB and BTB control schemes. However, due to gravity effects, its miss distance becomes a constraint in long range intercepts and therefore limits the range. The range improvement introduced by the continuous control scheme does not differ from the multiposition control scheme much. One positive effect of the continuous control scheme is that it can maintain the moving target intercept capability within its entire flight envelope which is depicted in continuous case-2.

For the cases where a theoretical down sensor is added to the continuous control scheme, it is seen that the miss distance performance is increased. As a result, the effective range of the system can be increased significantly as seen in Figure 7-73. The down sensor provides a slightly elevated trajectory with the ability to go above instantaneous LOS. It is concluded that if the continuous control scheme is to be used, it must be backed up with a down sensor.

Table 7-13 summarizes the characteristics of various control schemes.

Table 7-13 Comparison of control schemes

Control scheme	BB	BTB with δ=10°	BTB with δ=5°	Multiposition	Continuous	Continuous w/ down sensor
Flight Behaviour	oscillatory	oscillatory	less oscillatory	less oscillatory	smooth	smooth
Oscillation around LOS	yes	yes	yes	yes	no	yes
Seeker noise effect on performance	none	medium	light	light	light	light
Impact speed	low	low	medium	medium	high	high
Long range capability	none	limited	limited	good	good	best
Drag	high	high	moderate	moderate	low	low
Moving target intercept efficiency	low	low	moderate	good	good	good
CEP within envelope	fair	fair	fair	good	fair	good
Time of flight	long	long	medium	medium	short	short

BB and BTB control schemes suffer from a high energy loss and speed decrease. Their flights are oscillatory. Impact speeds are low. Moving target intercept capabilities are limited within their range envelope.

The multiposition control scheme increases the range and provides good miss distance values within this range. Its moving target intercept effectiveness is higher than BTB and BB schemes. It can be used at most situations where the continuous scheme is employed.

The effects of continuous and multiposition schemes on the weapon's performance can be distinguished at medium to long range intercepts and for moving targets. For short range releases, BB and BTB schemes are also effective. There is no improvement in the weapon's performance at short ranges with the continuous or multiposition control scheme. High energy releases provide longer ranges for both multiposition and continuous schemes. Both of these schemes can be used to increase the range and impact speed of the weapon.

CHAPTER VIII

SUMMARY AND CONCLUSIONS

8.1 SUMMARY

This thesis aims to develop a base for the modeling and analysis of laser guided weapons, and in particular investigates the effects of several control schemes on the performance of a generic laser guided weapon system in which the velocity pursuit guidance is employed using the data collected by a velocity aligning seeker without any additional sensors onboard.

In the modeling and simulation of a generic laser guided weapon system, the following tasks are performed.

- The laser seeker is modeled experimentally.
- Aerodynamic coefficients of a generic geometry are found using a readily available Missile Datcom computer package.
- A nonlinear 6-DOF simulation is formed in Matlab Simulink environment, utilizing velocity pursuit guidance.
- Multiple modules of control schemes, utilizing bang-bang, bang-trail-bang, multiposition and continuous control surface deflections are created.
- The simulation environment developed is used to implement several improvement methods and analyze their effects on the weapon's performance

In modeling the laser seeker, its behavior in various atmospheric conditions and possible reflection characteristics from various target surfaces are investigated. Laser designator characteristics, reflection patterns are shown and a laser model

based on the detection range is constructed. It is seen that the reflected energy from a target is heavily affected by the designator's output power, atmospheric visibility and reflectivity of the target surface.

In order to obtain a realistic model and to determine the possibility of using several control schemes, a series of tests are conducted on a 4-quadrant laser detector. In these tests, a collimated laser beam is sent to the detector at various arrival angles and voltages generated by the detector are recorded. Test results are used to determine the relationship between the lead angle and the voltage generated.

The results obtained by these tests have constituted a valuable source of laser detector behavior to be used in nonlinear simulations. It is seen that the laser seeker may be modeled as a combination of a linear region where accurate voltage-lead angle relationship can be obtained, and a saturated region which provides only the directional information. The width of this linear region is determined. The maximum possible noise levels that can be experienced during an actual operation are also determined by these tests.

The aerodynamic coefficients of a generic geometry are determined by a readily available software package called "Missile Datcom" version 6/93. It is understood that Datcom revision number is effective on the results.

An overall nonlinear 6-DOF simulation is created in the Matlab Simulink environment by using the dynamic equations of motion, data generated for aerodynamic coefficients, velocity pursuit guidance, seeker model developed, noise effects, and various control schemes.

A set of typical launch scenarios are created and the performance of a generic weapon is analyzed for each scenario using various control schemes by a series of runs while monitoring performance parameters like the range, miss distance, impact speed, time of flight, etc.

The canard deflection schemes as control schemes used in this analysis are,

- bang-bang scheme

- bang-trail bang scheme with multiple deadzones and canard deflection values
- multiposition scheme
- continuous scheme
- continuous scheme with theoretical down sensor

The targets are selected to be stationary and moving for all cases. Weapon envelopes are also created for a given miss distance value. Effects of each canard deflection scheme are determined and compared.

For a possible implementation in the gravity compensation logic, the effect of adding a down sensor on the weapon's performance is investigated. The maneuverability of the weapon is investigated for using as a reference for the selection of a down sensor.

The simulation studies are evaluated in the light of results. Some guidelines for several improvement attempts are presented with a set of comments and remarks.

8.2 CONCLUSIONS

One of the important results of this study is the knowledge gained about the characteristics of laser seekers. The results of the seeker tests reveal that the output range of the laser seeker is composed of a linear region and a saturated region. The width of the linear region is found to be ±3 degrees which is small but adequate to implement proportional control types. Therefore, it is shown that the existing seeker can be used to generate the lead angle data for various control schemes.

The nonlinear simulations performed with several altitude/speed release combinations for both stationary and moving targets, using velocity pursuit guidance with bang-bang, bang-trail-bang, multiposition and continuous control schemes.

In bang-bang (BB) control scheme, the weapon performs cyclic full deflections throughout the flight no matter how small the lead angle between the weapon and target is. It is seen that the weapon flight characteristics is oscillatory. The speed decreases heavily due to a high drag caused by full canard deflections and high angle of attack. It is seen that the weapons performance is satisfactory in high altitude, high speed releases within its flight envelope. However, due to a high energy dissipation and drag, the range is found to be limited. As a consequence, the moving target intercept efficiency is found to be low with BB control. The miss distance is found to be heavily dependent on the release speed with BB control. There are incidents observed in which some out of FOV movements occur causing loss of data acquisition.

In the Bang-Trail-Bang (BTB) control case, results resemble BB results. It is observed that the use of a deadzone prevents cyclic deflections up to an extent, where no canard deflection is produced for a lead angle error limit. However, important flight parameters and weapon behavior are found to be similar to the BB control in terms of high oscillations experienced. It is seen that the BTB control provides a range increase by decreasing number of deflections and increasing speed slightly. The velocity of the weapon decreases with time due to full canard movements. The flight envelope is slightly enlarged but there are still problems with acquisition losses and moving target intercepts.

An important phenomenon observed is the gravity effect on the weapon's performance. Since it is not possible to determine the true down direction in actual applications, all commands are given without taking the gravity pull into account. This feature becomes important in scenarios incorporating long range glides and low speed deliveries. In these type of deliveries gravity pulls the weapon beyond the LOS and since no counter action can be taken on time, impact points are short of target.

In order to decrease oscillations and reduce drag, a 5 degrees full canard deflection value is also tried for the BTB scheme. The results for long range deliveries are found satisfactory in which the speed decreases and the drag is reduced. However

this control scheme produce high miss distances when released from medium altitudes with low release speeds. The primary factor is the gravity effect where, even continuous 5 degrees up commands can not maintain weapon on the LOS.

In order to combine the positive sides of BTB with 5 and 10 degrees deflections, a 5-position control scheme is constructed and several simulations are performed. In this multiposition control, two main design criteria used are the value of mid-deflection and the decision of when to use this deflection. After several runs with various values, it is decided that (0/5/10) degrees canard positions with 1.5 degree lead angle criteria is found to be the most successful considering range improvement. 5 degrees deflection provides slightly more energy to go above the instantaneous LOS to the weapon and maintains acceptable miss distance values within its envelope. Thanks to the mid-deflections, drag and oscillations are decreased by appreciably. The impact speed which is an important parameter when attacking hard targets is also maintained higher than BB and BTB schemes. Both the moving target intercept capability and the range are increased significantly by the multiposition control.

The continuous control, which produces proportional canard deflections within the linear region of seeker, is another scheme used and is expected to give the best results. The continuous control is shown to provide very high impact speeds thanks to small canard deflections and less drag. The weapon flies in a streamlined attitude in a gliding phase. Range and moving target intercept capabilities are found to be high with respect to BB and BTB schemes as expected. However, the improvement in range is observed to be less than expected as compared to the multiposition control case. One main reason for this is probably the miss distances going out of limits at long range deliveries. Commands to make lead angle zero are not enough to compensate gravitational pull-down and the weapon impacts short of target.

A theoretical down sensor is added to the system which provides the down direction to the control system. As a result, biased “up” commands are generated

to overcome gravity effects, leading to some improvements in the miss distance and some significant increases in the range.

A maneuverability analysis is performed to provide guidelines for the down sensor selection. The analysis showed that, the weapon experiences high g loads during flight. It is concluded that, pendulum or electrolytic tilt sensors which rely on measurement of gravitational acceleration can not be used to determine down direction.

From the analysis of multiple control schemes, it is concluded that the multiposition scheme can provide significant improvement on weapon's performance and can be used instead of continuous scheme in most cases. The key factor in this decision is the cost of building a multiposition control system when compared with the continuous scheme. If there is a way to implement the multiposition control with small cost when compared with fully proportional controller, multiposition scheme may be feasible.

Another important conclusion obtained from the studies is that, the continuous scheme must be backed up with a down sensor to maintain accuracy and long range capability.

8.3 RECOMMENDATIONS FOR FUTURE WORK

Further research in this area can be done in the following themes.

Fine tuning of multiposition control system may be focused on. Effects of the mid-deflection location and the lead angle value used as a decision criterion in canard deflections may be investigated by considering all launch scenarios that the weapon may face.

One possible further study on the multiposition control case can be the mechanical construction details of implementing such a system. If the multiposition system can be implemented in a control actuation system with a lower cost than

constructing a fully continuous controller, it may be feasible to use it instead of continuous control scheme.

The down sensor is assumed to be a theoretical one in this thesis. One step forward may be to search for physical sensors with fast response times in estimating the down direction. If a down sensor with minimal cost can be implemented in the system, the results may be cost effective in improving the miss distance and providing significant increases in the range.

Further studies may be involved with decreasing weapon's susceptibility against weather conditions and design of a recovery algorithm, which will be helpful in re-acquiring laser reflection after an acquisition loss. This algorithm can be constituted by tracking the time history of laser spot position and considering the attitude of seeker at each time by the help of a down sensor.

REFERENCES

[1] Redstone Arsenal website, www.redstone.army.mil/history/chron4/LASER2, 2003.

[2] Dornheim, M., "Improved Air Defenses Driving Upgrades in Tactical Weapons", Aviation Week and Space Technology, March 1985.

[3] "Operation Desert Storm, Evaluation of the Air Campaign, Report to the Ranking Minority Member, Committee on Commerce, House of Representatives", U.S. General Accounting Office, June 1997.

[4] Cordesman, A., "Kosovo, The Statistics of Other Recent Air Campaigns", Center for Strategic and International Studies, April 6, 1999.

[5] Moseley, M. (T. Lt. Gen.), "Operation Iraqi Freedom-By the Numbers" USCENTAF, Assessment and Analysis Division, April 30, 2003.

[6] Federation of American Scientists website, www.fas.org, 2004.

[7] "JP 3-09.1 Joint Tactics, Techniques and Procedures for Laser Designation Operations" May 28, 1999.

[8] "JP 3-09.1 Joint Laser Designation Procedures", June 01, 1991.

[9] Czech Defense Site, www.military.cz, 2004.

[10] Perkgöz, C., "A Guidance and Control Method for a Tail Controlled Bomb", M.S Thesis, Electrical and Electronics Engineering Dept., METU, Ankara, 2002.

[11] Akkal, E., "Control Actuation Systems and Seeker Units of an ASGM", M.S. Thesis, Electrical and Electronics Engineering Dept., METU, Ankara, December 2003.

[12] Ralph, J.F.,and Edwards, K.L., "The Effect of Aircraft Biases on the Delivery of an Enhanced Laser Guided Weapon", presented at ICAS 2002, Southwest Research Institute website, www.tss.swri.edu./pub/pdf/1994ITSEC, 2004.

[13] Baba, M., Narita, D., and Ohtani, K., "360 Degrees Shape Measurement System for Objects Having from Lambertian to Specular Reflectance Properties Utilizing a Novel Rangefinder", Institute of Physics website, www.iop.org/EJ/article/1464-4258/4/6/372/oa2672.pdf, 2002.

[14] Kim, I., McArthur, B., and Korevaar, E., "Comparison of Laser Beam Propagation at 785 nm and 1550 nm in Fog and Haze for Optical Wireless Communication", Proceedings of SPIE, Vol. 4214, January 2000.

[15] Akbulut, A. and Efe M. "An Experimental Hybrid FSO/RF Communication System," www.electra.science.ankara.edu.tr/akif/siu/FSO_Paper, 2004.

[16] Lecture Notes, Martin Marietta Co., "Laser Seeker System Workshop", Orlando Florida, 1993.

[17] LEOT Laser Tutorials, "Laser Distance Measurement", Module-6 www.cord.org/cm/leot , 2001.

[18] MIL-HDBK-828, "Laser Safety on Ranges and in Other Indoor Areas", 1993.

[19] Weichel, H., "Laser Beam Propagation in the Atmosphere", SPIE Optical Engineering Press, 1990.

[20] LEOT Laser Tutorials, "Laser Trackers and Alignment Systems", Module-7, www.cord.org/cm/leot , 2001.

[21] Kelly, E. and Jones, G., "The Three Components of Reflection", Information Display, SID,Vol. 14, No. 10, pp 24-29, October 1998.

[22] Nayar, S.K., Ikeuchi, K. and Kanade, T., "Surface Reflection Physical and Geometrical Perspectives", IEEE Trans. Pattern Analysis and Machine. Intelligence, Vol. 13, No. 7, July 1991.

[23] Army Technology website, www.army-technology.com, 2002.

[24] Fox, C., "The Infrared and Electro-Optical Systems Handbook", Volume 6, "Active Electro-Optical Systems", 1996.

[25] Lecture Notes, Martin Marietta Co., "Electrical Power and Optical Systems and Interfaces", Orlando, Florida, 1993.

[26] Lecture Notes, Martin Marietta Co., "System Engineering, Laser Seeker Requirements" Orlando, Florida, 1993.

[27] Matlab Curve Fitting Toolbox User's Guide, Version 1, 2001.

[28] Titterton, D.H. and Weston, J.L., "Strapdown Inertial Navigation Technology" Peter Peregrinus Ltd., London, 1997.

[29] Blakelock, J.H., "Automatic Control of Aircraft and Missiles", John Wiley & Sons Inc., 1991.

[30] Ateşoğlu, Ö., "Different Autopilot Designs And Their Performance Comparison For Guided Missiles", M.S. Thesis, Aeronautical Engineering Dept., METU Ankara, December 1996.

[31] Mahmutyazıcıoğlu, G., "Aerodynamic Parameter Estimation Using Aeroballistic Data", Ph.D. Thesis, Mechanical Engineering Dept., METU, Ankara, 2000.

[32] Blake, W.B., "Missile Datcom User's Manual, 1997 Fortran 90 revision", February 1998.

[33] Marsaglia, G. and Tsang, W.W., "The Ziggurat Method for Generating Random Variables", Journal of Statistical Software website, www.jstatsoft.org/V05/i08/ziggurat.pdf., 2004.

[34] "Arena Active Protection System", www.armor.ua/fotonov/Tanks/EQP, 2004.

[35] Bias, E. and Richardson D., "Time for Shifting Gears?", Armada International, July 2003.